AFRL-HE-WP-TR-2006-0147

Human Neck Response during Vertical Impact with Variable Weighted Helmets

Erica J. Doczy
Joseph A. Pellettiere

Air Force Research Laboratory

Hilary L. Gallagher

ORISE
P.O. Box 117
Oak Ridge, TN 37831-0117

September 2006
Interim Report for August 2004 to August 2005

Air Force Research Laboratory
Human Effectiveness Directorate
Biosciences and Protection Division
Biomechanics Branch
Wright-Patterson AFB OH 45433-7947

NOTICE AND SIGNATURE PAGE

Using Government drawings, specifications, or other data included in this document for any purpose other than Government procurement does not in any way obligate the U.S. Government. The fact that the Government formulated or supplied the drawings, specifications, or other data does not license the holder or any other person or corporation; or convey any rights or permission to manufacture, use, or sell any patented invention that may relate to them.

This report was cleared for public release by the Air Force Research Laboratory, Wright-Patterson Air Force Base, Public Affairs Office and is available to the general public, including foreign nationals. Copies may be obtained from the Defense Technical Information Center (DTIC) (http://www.dtic.mil).

The voluntary informed consent of the subjects used in this research was obtained as required by Air Force Instruction 40-402.

AFRL-HE-WP-TR-2006-0147 HAS BEEN REVIEWED AND IS APPROVED FOR PUBLICATION IN ACCORDANCE WITH ASSIGNED DISTRIBUTION STATEMENT.

FOR THE DIRECTOR

//SIGNED//

MARK M. HOFFMAN
Deputy Chief, Biosciences and Protection Division
Air Force Research Laboratory

This report is published in the interest of scientific and technical information exchange, and its publication does not constitute the Government's approval or disapproval of its ideas or findings.

REPORT DOCUMENTATION PAGE

Form Approved
OMB No. 074-0188

PLEASE DO NOT RETURN YOUR FORM TO THE ABOVE ADDRESS.

1. REPORT DATE (DD-MMM-YYYY)	2. REPORT TYPE	3. DATES COVERED (From – To)
SEP 2006	Interim Report	August 04 - August 05

4. TITLE AND SUBTITLE

Human Neck Response during Vertical Impact with Variable Weighted Helmets

5a. CONTRACT NUMBER
N/A

5b. GRANT NUMBER

5c. PROGRAM ELEMENT NUMBER
62202F

6. AUTHOR(S)

Erica J. Dozcy*
Joseph Pellettiere*
Hilary Gallagher**

5d. PROJECT NUMBER
7184

5e. TASK NUMBER
02

5f. WORKUNIT NUMBER
12

7. PERFORMING ORGANIZATION NAME(S) AND ADDRESS(ES)

*Air Force Materiel Command
Air Force Research Laboratory, Human Effectiveness Directorate
Biosciences & Protection Division
Biomechanics Branch
Wright-Patterson AFB OH 45433-7947

**ORISE
PO Box 117
Oak Ridge TN 37831-0117

8. PERFORMING ORGANIZATION REPORT NUMBER
AFRL-HE-WP-TR-2006-0147

9. SPONSORING / MONITORING AGENCY NAME(S) AND ADDRESS(ES)

10. SPONSOR / MONITOR'S ACRONYM
AFRL/HEPA

11. SPONSOR/MONITOR'S REPORT NUMBER(S)

12. DISTRIBUTION / AVAILABILITY STATEMENT
Approved for public release; distribution is unlimited

13. SUPPLEMENTARY NOTES
AFRL/PA Cleared 28 Dec 2006, AFRL/WS-06-2920.

14. ABSTRACT

Helmet-mounted systems, such as night vision goggles and helmet-mounted displays, are designed to enhance pilot performance; however, they may also affect pilot safety during ejection due to the change in helmet inertial properties. The weight of a helmet, along with a pilot's bracing ability, can affect the human response and potential for neck injury during impact. A useful tool for investigating the mechanics of bracing and the relationships to helmet weight and impact acceleration is electromyography (EMG). Twenty-four male and female volunteer subjects participated in this study on the Vertical Deceleration Tower (VDT), located at WPAFB. The VDT produced a vertical acceleration with a half sine wave pulse of 150ms duration; peak accelerations ranged from 6 to 10 G. Helmet weights were 3.0, 4.0 and 5.0 lbs. Surface EMG was collected on the left and right sternocleidomastoid (SCM) and trapezius using DelSys surface EMG sensors. Neck loads were calculated using measured head accelerations and inertial property data. Neck load significantly increased with an increase in helmet weight. Neck muscle activity was reported in %MVC (maximum voluntary contraction). A method of collecting neck muscle activity data from the trapezius and SCM during short-duration impact experiments was successfully developed. A better understanding of the relationship between bracing and injury potential can be used to develop detailed instructions for pilots during their training to reduce their injury potential through proper positioning and bracing in the event of an ejection.

15. SUBJECT TERMS
Helmet Weight, Neck Loading, EMG

16. SECURITY CLASSIFICATION OF:			17. LIMITATION OF ABSTRACT	18. NUMBER OF PAGES	19a. NAME OF RESPONSIBLE PERSON:
a. REPORT	b. ABSTRACT	c. THIS PAGE			Erica Doczy
U	U	U	SAR	83	19b. TELEPHONE NUMBER *(Include area code)*

Standard Form 298 (Rev. 8/98)
Prescribed by ANSI Std. Z39-18

THIS PAGE IS INTENTIONALLY LEFT BLANK

TABLE OF CONTENTS

LIST OF FIGURES

LIST OF TABLES

THIS PAGE IS INTENTIONALLY LEFT BLANK

PREFACE

The impact tests and data analysis described in this report were accomplished by the Biomechanics Branch, Human Effectiveness Directorate of the Air Force Research Laboratory (AFRL/HEPA) at Wright-Patterson Air Force Base, Ohio. The test facility for this study was the Vertical Deceleration Tower (VDT). Engineering support at AFRL/HEPA was provided by General Dynamics under contract FA8650-04-D-6472.

ACKNOWLEDGMENT

The technical assistance of Mr. Chuck Goodyear and Mr. Steve Mosher of General Dynamics and Mr. Gianluca De Luca of Delsys Incorporated is greatly acknowledged. A special thank you goes out to the volunteer subjects who made this study possible.

INTRODUCTION

Helmet-mounted systems (HMS), such as night vision goggles and helmet-mounted displays, are designed to enhance pilot performance through improvements in situational awareness, target acquisition, and weapon delivery. However, using HMS may also affect pilot safety by increasing the potential for neck injury during all phases of ejection (catapult stroke, windblast, seat stabilization, and parachute opening shock). This increase in neck injury potential is due to the increase in dynamic forces generated in the cervical spine as a result of the change in helmet inertial properties including weight and center-of-gravity (Cg). The effects of helmet weight as well as bracing ability on subject response during impact are unknown. Electromyography (EMG) is a useful tool to investigate the mechanics of bracing and its relationships to helmet weight and impact acceleration. In addition, EMG could be used to estimate the force produced by the muscles in a dynamic environment and to help establish the relationship between that force and the potential for neck injury. A series of tests were conducted by the Air Force Research Laboratory's Biomechanics Branch (AFRL/HEPA) using male and female volunteers to investigate the effects of helmet weight on human response and neck muscle activity during short-duration vertical impacts of variable magnitude, simulating the dynamic conditions similar to the catapult stroke phase of ejection.

BACKGROUND

Tests by Buhrman and Perry at the Air Force Research Lab's Biomechanics Branch have evaluated the effects of variable helmet inertial properties on the biodynamic response of human volunteers exposed to frontal (-Gx) and lateral (+Gy) impact accelerations [1, 2]. The objective of this study was to provide additional human dynamic data from a vertical (+Gz) impact environment with a variable weighted helmet. These data are required to complete the development of multi-axial cervical injury criteria for the three coordinate axes, to continue the development of head/neck biodynamic models, and to continue the development of the biodynamic response database. The results of this research program will contribute to the development of design guidelines for the safe use of helmet systems that include devices that increase the weight and distribution of head-supported mass.

The effects of subject bracing on human neck response have not been defined in the past, but it has been observed that the active neck musculature plays a significant role in reducing head/neck motion during impact [3-5]. Active musculature also affects the load-carrying capacity of the neck and therefore risk of neck injury. If the relationship between bracing and potential of injury were better understood, detailed instructions could be provided to pilots during training so that in the event of an ejection they could lower their chances of injury with their position and brace. Mertz *et al.* investigated the effect of muscle tone on neck injury risk and provided estimates of the maximum forces and moments that individuals of various sizes can resist with tensed muscles [5]. Based on static neck muscle strength data, Mertz *et al.* estimated maximum passive neck forces and developed a risk curve that quantified the chance of serious neck injury for tension and extension moments [4]. These risk curves were designed to account for an estimated muscle tone, since tone during impact has not previously been quantified. The addition of these data would aid in the further development and validation of these valuable risk curves.

Recently, modeling and simulation have become viable methods to investigate the safety potential of different equipment and environments without putting actual people at risk. Previously, due to computational limitations, the majority of human models was passive in nature and modeled only the involuntary response. This method proves quite reasonable to determine only the kinematics of the occupant or the overall global force response. However, in order to investigate deeper into the types of injuries, a more realistic model is needed. An ideal model would incorporate the active muscle response of the particular crewmember, since the neck's load-carrying capacity increases with muscle tensing [4]. This muscle response would include any voluntary bracing as well as muscle activation that occurs as a result of the impact-induced stress. It should be noted that, although the computational models can simulate the active muscle response of the human, little data exist to validate these models so that they can be applied to real-world problems. In the past, active musculature neck models have been validated with kinematic response data from human impact testing, but experimental neck muscle EMG data are necessary to provide accurate muscle activation signals for different impact simulations [3]. EMG signals can be collected during bracing and impact of human volunteers who are subjected to a variety of dynamic events. These data can then form the baseline from which several groups of muscles can be incorporated into previously passive models.

Neck muscle EMG data are a useful tool to investigate the mechanics of bracing and its relationships to helmet weight and impact acceleration. In the past EMG has been successfully used for gait and posture analysis, physical therapy, risk prevention, ergonomic design, movement analysis, and athletic strength training. EMG recordings have not typically been utilized during dynamic tests due to the limitations of the EMG hardware and the ability to conduct dynamic tests using live human subjects. This study expanded on the use of EMG by using it to investigate muscle activity during a dynamic impact event.

Before using EMG in a dynamic environment, a thorough understanding of the electromyographic recording methods and signals is required. When a muscle is activated, action potentials from the brain travel to motor neurons which branch out to the muscle fibers. EMG sensors record the action potentials of the motor unit, comprised of several activated muscle fibers. An "EMG signal directly reflects the recruitment and firing characteristics of the detected motor units within the measured muscle" [6]. The amplitude of an EMG signal is stochastic, but correlates well to the force produced by the observed muscle. As the firing rates of the motor units increase, the amplitude of the EMG signal also increases [7].

There are two major types of EMG instrumentation to choose from: indwelling and surface EMG (sEMG). Indwelling uses fine wires inserted directly into the muscle, while sEMG detects action potentials through the skin. Not only are there obvious differences in the measurement methodologies between the two types, there are also differences in the signals they collect. Indwelling EMG picks up higher frequency contents of the EMG signal and is not affected by artifacts such as the impedance of the skin and adipose tissue [8]. The use of indwelling EMG is crucial for the collection of deep muscle activation data. Surface EMG, however, can provide useful information when applied to superior muscles. Although sEMG reads from the surface of the skin rather than the muscle tissue itself, sEMG has demonstrated a low variance ratio [9] and high correlation with indwelling EMG for amplitude and frequency recordings [10]. During dynamic studies, an indwelling EMG signal may suffer from wire movement artifacts, whereas

the sEMG method is not as susceptible to this interference [6]. Due to its reliability, combined with its ease of use, sEMG is recommended for use on day-to-day investigations, dynamic experiments, and analysis of fatigue [11, 12]. This study employed sEMG.

The raw and processed EMG data provide valuable information about the muscle activity. Raw EMG data can be used to determine the activation timing of the muscle, correlated with the contraction stimulus. The root mean square (RMS) of the EMG signal is used to smooth the signal and represents the mean power of the signal [6]. A Fast Fourier Transform (FFT) can be performed to analyze the frequency content of the signal and evaluate muscular fatigue. Muscle fatigue indicates an impairment of performance that leads to the inability of a muscle to produce the desired force [13]. As a muscle fatigues, the firing rates of the motor units decrease, but the output amplitude of the motor units increases in an attempt to compensate for the fatiguing process and produce the same total force output for the muscle [14, 15]. This phenomenon results in a decrease in higher frequency components and an increase in amplitude [7, 14].

This study evaluates the activity of the upper trapezius and sternocleidomastoid (SCM) muscles during short-duration vertical impacts. In the past, the role of upper trapezius and SCM during long-duration head and neck loading situations has been studied. The SCM controls the rotation and tilt of the head. Hodgdon et al. found that the SCM also plays a stabilizing role during vibrations [16]. The upper trapezius muscles aid in extension of the neck. Causes of fatigue in both the trapezius and SCM muscles have been successfully investigated using EMG in past research efforts [15, 17-19]. Phillips and Petrofsky examined the characteristic changes in EMG data from the upper trapezius and SCM associated with isometric muscle contractions. They thoroughly investigated the mechanics of muscle fatigue during helmet loading and verified the SCM's role in the forward contraction mode [17]. Phillips and Petrofsky concluded that weight and Cg of a flight helmet affect the neck muscle fatigue during sustained contraction [18].

The high instance of reported neck pain in fighter pilots prompted an EMG investigation by Hamalainen, who examined the activation of the cervical erector spinae muscles during head movements and sustained acceleration using surface-integrated EMG. This study concluded that during sustained accelerations neck muscular strain is significantly increased with flexion and extension motions of the neck [20].

Although the activity of the neck muscles and its relationship to neck injury, pain and fatigue have been of interest for several years, past research does not quantify the level of muscular activation during short-duration impact events, such as an ejection. In 1989 researchers at the Armstrong Laboratory (now AFRL) attempted to collect EMG signals during vertical impact study with human volunteers [21]. Difficulties with the instrumentation and restrictions within the test design limited the conclusions drawn about neck muscle activity during impact. However, promising observations on the ability to collect EMG were made. Years later, in 2003, a dynamic EMG pilot study was conducted by the AFRL Biomechanics Branch to refine EMG data collection procedures and develop a reliable method of collecting meaningful EMG data of the neck during short-duration frontal impacts [22]. During this type of impact, the trapezius exhibited a higher amplitude output than the sternocleidomastoid.

METHODS

A series of short-duration +Gz (vertical) impact acceleration tests were conducted using human volunteer subjects. The impact levels ranged from 6 to 10 G and the total helmet weight worn by the subjects ranged from 3.0 to 5.0 lbs (Table 1). Subjects completed the test cells up to three times each, the first time in order of severity (alphabetical order by cell name) for safety reasons, followed by randomized exposures.

Table 1. +Gz impact test matrix

IMPACT LEVEL (Carriage Accel)	**TOTAL HEAD SUPPORTED WEIGHT**		
	3.0 lbs	**4.0 lbs**	**5.0 lbs**
6 G	A		
8 G	B		
10 G	C	D	E

Facility and Equipment

The vertical impact acceleration tests were conducted using the Vertical Deceleration Tower (VDT), located at Wright Patterson AFB, OH. The VDT facility is composed of two vertical rails and a drop carriage. The carriage is allowed to enter a free-fall state (guided by the rails) from a predetermined drop height. A plunger mounted on the rear of the carriage is guided into a cylinder filled with water located at the base of and between the vertical rails. A +Gz acceleration pulse is produced when water is displaced from the cylinder by the carriage-mounted plunger and the carriage decelerates (Figure 1). The acceleration pulse is controlled by varying the drop height, which determines the peak G level, and by varying the shape of the plunger, which determines the rise time of the pulse. This study used an acceleration profile generated by the VDT that approximated a half-sine wave pulse with a rise-time of approximately 85 ms and pulse duration of 170 ms. Prior to human testing, tests were conducted with an instrumented large Advanced Dynamic Anthropomorphic Manikin (ADAM) to ensure that testing conditions were within acceptable safety ranges. All tests were conducted using a modified ACES II ejection seat affixed to the carriage assembly. The seat back and pan were not reclined. A PCU-15 or -16/P harness and lap belt were used to restrain the subjects, and all shoulder strap and lab belt attachment points were preloaded to 20 ± 5 lbs.

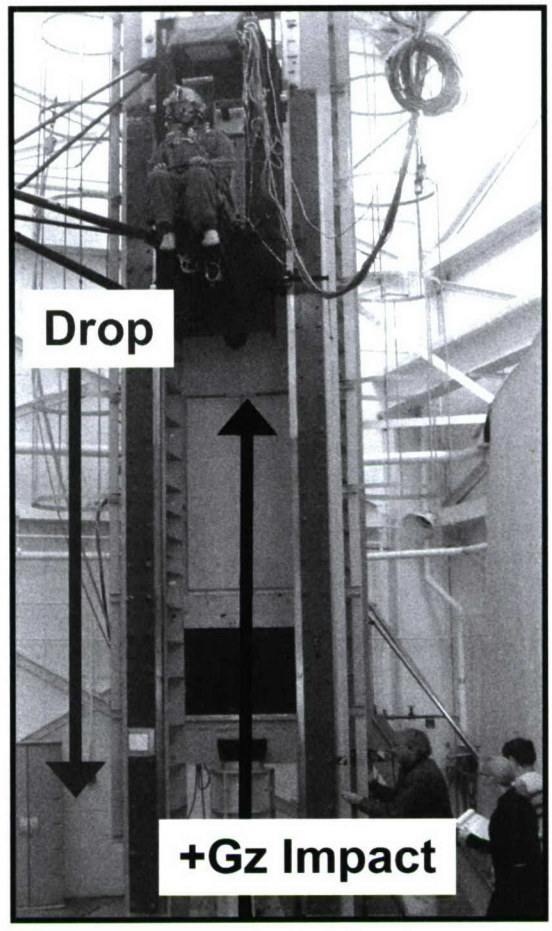

Figure 1. Vertical Deceleration Tower (VDT)

A Variable Weighted Impact (VWI) helmet was used to achieve the range in helmet weight. The VWI helmet consists of a modified standard HGU-55/P flight helmet that can support variable weights along a halo for adjustable Cg (Figure 2). The VWI helmet was set up to represent inertial properties of typical Air Force helmet-mounted systems, with the weight frontally loaded. A larger moment arm is created with the added mass placed in front of the helmet, as opposed to the mass added closer to the natural Cg of the head which is closer to the ears. A modified MBU-12/P oxygen mask and integrated chin nape strap were used in conjunction with the VWI helmet for stability. The mask was cut to allow instrumentation cables from the mouth accelerometer package to pass through. Subjects were fitted with the VWI helmet in sizes medium, large, or extra large, depending on head size. Precise measurements of the helmet mass properties were collected for each helmet variation and size to ensure that the Cg of the helmet remained within designated safe limits [2] (Appendix B).

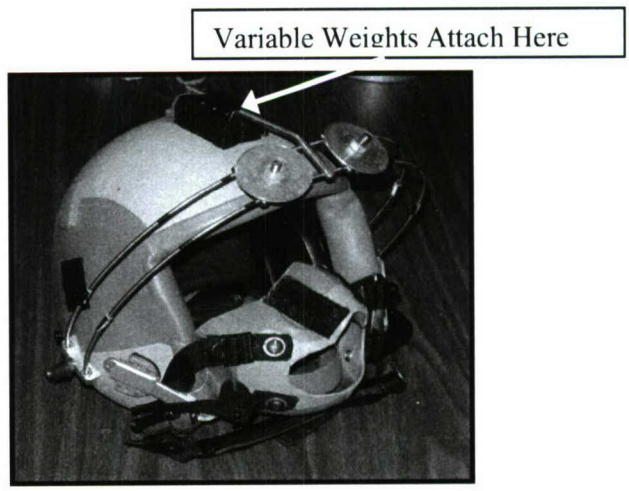

Figure 2. Variable Weighted Impact (VWI) helmet

Subjects

Fifteen male and nine female volunteer subjects were tested with approval obtained from the Wright Site Institutional Review Board. All subjects were active duty military personnel. They ranged in age from 20 to 43 years and in weight from 104 to 291 lbs (Table 2). Anthropometric measurements were taken from each subject for inclusion in the AFRL Biodynamics Database (www.biodyn.wpafb.af.mil). Included in those measurements was the neck circumference, measured at the base of the neck (Figure 3). Six of the 24 subjects were unable to attend the measurement session and therefore were not included in the database and any subsequent anthropometric analysis.

Table 2. Human subjects

	Male (n=15)	Female (n=9)
Age (yrs)		
Range	21-43	20-32
Mean	32 +/- 6	25 +/- 4
Weight (lbs)		
Range	142-291	104-189
Mean	200 +/- 41	147 +/- 25
Height (in.)		
Range	69-77	62-70
Mean	72 +/- 2	66 +/- 3

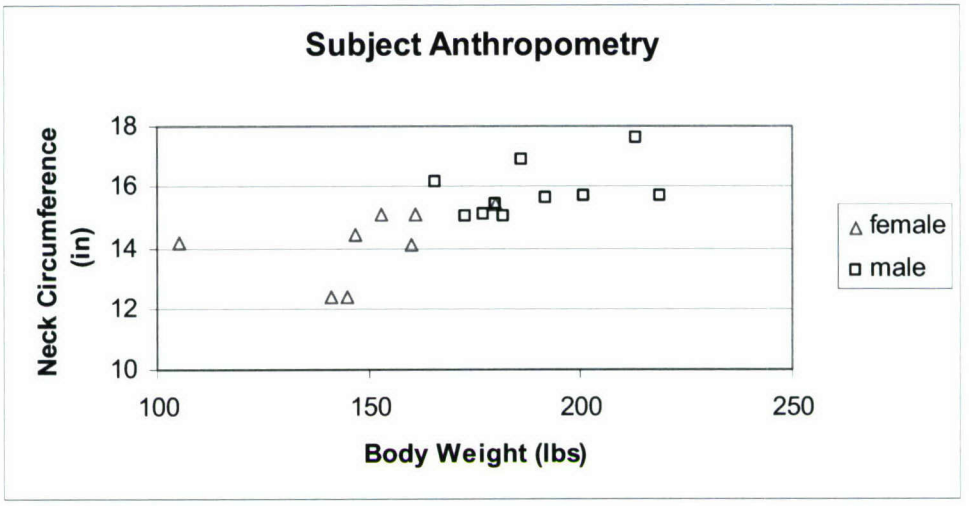

Figure 3. Subject neck circumference vs. body weight.

All tests were conducted with the subjects in the same position, with special attention given to the initial position of the head and neck. The subjects were restrained such that their backs were straight and against the seat back. They were also instructed to keep their heads up and against the headrest. It was especially important to maintain this position during impact as position of the head during +Gz acceleration affects the internal neck forces and therefore injury mechanism [20]. The subjects were informed that after being raised to a predetermined height they would hear a count-down from 'T10' to 'T0'. At 'T2' the subjects were instructed to brace their helmet against the headrest and hold the brace throughout the drop and on impact. The main mechanism of the brace was neck extension.

Instrumentation

Measurements were taken during the impact events that included carriage accelerations and velocity, seat accelerations, subject head linear and angular accelerations, chest accelerations and displacements, neck EMG, and forces developed in the seat and the restraint system. Subject head accelerations were collected using a piezoresistive accelerometer package connected to individually formed mouth packs. The electronic data channel assignments and additional details are specified in Appendix C. All channels were sampled at 1,000 samples per second. A head anatomical axis system was used as a reference for the electronic data (Figure 4). Two Weinberger high-speed (500 frames per second) video cameras were secured to the carriage camera mounts and used for visual documentation of the impact event (one lateral and one oblique). Eleven circular displacement markers were placed on the seat and on the subject's torso, shoulder, and helmet. Motion analysis data were collected using the two Weinberger cameras recording at 500 frames per second.

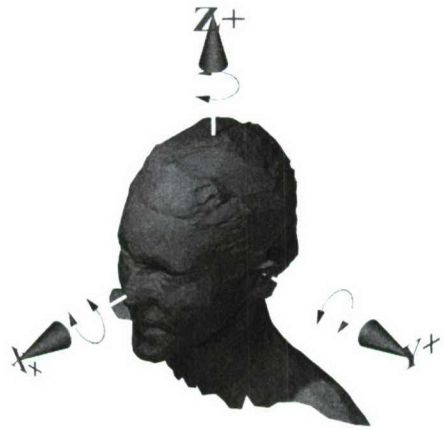

Figure 4. Anatomical axis system of the human head

Acceleration and Neck Force Analysis

An in-house program, Neckload3, used the measured linear and angular head accelerations (collected with the mouth pack instrumentation) and the inertial properties of the head/helmet to approximate the resultant forces and moments seen at the occipital condyle (head-neck joint or OC). The measured head accelerations and therefore calculated neck forces and moments were reported in the head coordinate system (Figure 4). The neck forces and moments were calculated using the equations of motion for a rigid body. The equation for calculating the resultant force is:

(1) $\vec{F} = m(\vec{a}_{cm} - \vec{g})$

where $\vec{F}$ is the force, m is the total mass of the combined helmet/head, $\vec{a}_{cm}$ is the acceleration at the center of mass, and $\vec{g}$ is a vector in the direction of the acceleration of gravity.

The linear acceleration at the center of mass of the combined head/helmet system was computed from the measured linear and angular accelerations at the mouth pack. The equation for the acceleration at the center of mass is:

(2) $\vec{a}_{cm} = \vec{a} + \dot{\vec{\omega}} \times \vec{r} + \vec{\omega} \times (\vec{\omega} \times \vec{r})$

where $\vec{a}$ is the actual acceleration at the mouth pack, $\vec{\omega}$ is the angular velocity, $\dot{\vec{\omega}}$ is the angular acceleration, and $\vec{r}$ is a vector from the bite bar accelerometer location to the center of mass. The angular velocity can be calculated by integrating the angular acceleration. However, the piezoresistive accelerometers measure a combination of the actual acceleration and the acceleration of gravity:

(3) $\vec{a} = \vec{a}_M - \vec{g}_0 + \vec{g}$

where $\vec{a}_M$ is the measured acceleration at the mouth pack as measured by the piezoresistive accelerometers, $\vec{a}$ is the actual acceleration at the mouth pack and $\vec{g}_0$ is the initial acceleration of gravity vector at the time before the impact when the accelerometer is zeroed. Since the calculations were done in the head anatomical coordinate system, the direction of the acceleration of gravity changes and must be calculated for each time step based on the change in angles. The input mouth pack acceleration that was read by the Neckload3 program was assumed to be $\vec{a}_M - \vec{g}_0$.

So,

(4) $\vec{a}_{cm} - \vec{g} = \vec{a}_M - \vec{g}_0 + \dot{\vec{\omega}} \times \vec{r} + \vec{\omega} \times (\vec{\omega} \times \vec{r})$

The resultant moment is calculated using:

(5) $\vec{\tau} = \vec{R} \times m(\vec{a}_{cm} - \vec{g}) + I \cdot \dot{\vec{\omega}} + \vec{\omega} \times (I \cdot \vec{\omega})$

where $\vec{\tau}$ is the moment, $\vec{R}$ is a vector from the point at which the moment is calculated to the center of mass and I is the inertial tensor for the moments of inertia in the head anatomical coordinate system.

The inertial properties were approximated by a sub-routine of Neckload3 called Combine. Combine approximated the properties such as Cg and moment of inertia of the subject's head with helmet using the subject's total body weight, head circumference, and previously measured helmet inertial properties (Appendix B). The inertial tensor of the combined system was calculated from the principal moments of inertia of the helmet and head by finding the inertial tensors of the individual components using:

(6) $I = AI_pA^T$

where A is the direction cosine matrix, I is the inertial tensor in the anatomical coordinate system and I_p is the inertial tensor in the principal axis coordinate system. The inertial tensors of the individual components were then combined using the parallel-axis theorem.

Because Neckload3 did not take into account external forces on the head, the program output represented the forces and moments after the head has separated from the headrest. For the peak value analysis, a cut-off time of 250 ms was used during the evaluations to omit from the evaluation the peaks due to headrest strikes following any rebound effects. The in-house program NeckloadDb used the summary sheets of each test to create a neck force database for maximum and minimum values within each cell.

Visual inspection of data plots was used to identify data points that were inconsistent from the majority and well beyond what a reasonable value should be. Outlier parameters were removed from 12 tests prior to statistical analysis. A confidence level of 95% was used for all statistical analyses. The accelerations and forces were examined for significant differences among varying

test parameters, including vertical acceleration levels, helmet weights, and gender. Due to the nature of the impact, of particular interest were the linear Z and angular Y accelerations and corresponding force parameters.

EMG

Delsys DE 2.3 sensors were used to record muscle activity of the SCM and upper trapezius. These sensors contain surface electrodes which are housed in an enclosure, keeping the distance between the two detection points consistent and ensuring that the filter effect of the sensors remain constant [7]. The inter-electrode distance of the sensors was fixed at 10mm; a small distance is beneficial in reducing signal contaminants such as Electrocardiogram (ECG) signals [23].

After the harness was donned by the subject, the skin over the left and right SCM and upper trapezium was shaved (if hair was present) and cleaned twice with alcohol swabs to prepare the areas for EMG sensor placement. This was done to minimize skin impedance and ensure stable contact of the sensor to the skin [6, 7, 19, 24]. A conductive gel was applied to the sensors, which were then fixed to the subjects using a double-sided adhesive and covered with medical tape. Special care was given to adhering the sensors to the subject to ensure that the contact points did not move, as this artifact during dynamic conditions may complicate the signal [25].

In order to increase the degree of accuracy and precision of EMG data collection, a few basic procedures were adopted. A consistent sensor placement methodology was used to keep sensor placement symmetric between right and left trapezius and SCM. This methodology was also used to keep the day-to-day placement of the sensors upon a single subject more precise, and the subject-to-subject placement of the sensors within an acceptable realm of comparability with respect to their differing anthropometry. Boney processes were used as anatomical landmarks to aid in measurement repeatability from subject to subject. To place the SCM sensors, a measurement was taken from the mastoid process (insertion) toward the clavicular head (origin) while the subject was instructed to sit upright and turn his or her head as far as possible in the opposite direction as the instrumented side [26] (Figure 5). The sensor was placed in the midpoint of this measurement. The upper trapezium sensors were placed in parallel with the muscle fiber direction at the base of the neck. Distance from the spinous process of C7 was kept constant for both left and right sensors to ensure symmetry. In general, the sensors were placed on the belly of the muscle, along the longitudinal mid-point of the muscle, avoiding the tendon and motor point. This general placement methodology is recommended in the literature [7, 15, 17, 24]. The reference sensor was placed on the spinous process of C7, since it is an electrically neutral location and mechanically stable [7, 24, 27].

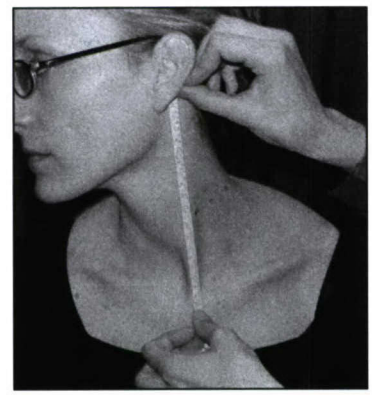

Figure 5. Method for finding the center of the SCM muscle

The thickness of adipose and skin tissue is indirectly proportional to the recorded EMG amplitude. The EMG amplitude should therefore be normalized when comparing the same muscle across different subjects [7]. To do this, a Maximum Voluntary Contraction (MVC) was recorded before each test. This MVC collection process consisted of three isometric contractions, five seconds in duration, two to three minutes apart. The strongest contraction (maximum peak amplitude) was considered the reference contraction or MVC. This method has been successfully utilized by several researchers in the past and is recommended as the standard MVC normalization method [6, 15, 17, 19]. The contraction consisted of the subject, wearing a helmet, in a 0-0 (neither seat pan nor back was reclined) generic seat, bracing head against the headrest, a static resistance. A load cell was placed in line with the headrest and displayed the force in pounds on a monitor in front of the subject (Figure 6). The subject was encouraged to produce the highest force value they could. The subject was also instructed to brace with only the head and neck. The subject's feet were placed on a wheeled platform to ensure that it was not possible to use the lower body to brace.

Figure 6. Seat and monitor used to collect MVC

The EMG signal was sampled at 2 KHz in order to avoid aliasing effects [6]. The cutoff frequency was supplied by a 450 Hz filter, built into the sensor. Before any EMG analysis, the DC offset was removed. To smooth the data and examine the EMG amplitude, RMS was calculated using a 125-point moving window.

Subject Reproducibility

Many studies have been conducted to collect and analyze the biodynamic response during vertical impact acceleration. There is little data, however, describing the effects of subject training on human response during dynamic tests. The effect of subject reproducibility and how it might affect data variability are also in question. To address this issue, additional tests were conducted within this study. Subjects completed each test configuration up to three times (Table 1). The tests were first conducted in a sequential manner as previously described (A,B,C,D,E), with the order of severity increasing for subject accommodation and safety. The last two replications were randomized so that the biodynamic response was not dependent on the last test configuration.

RESULTS

One hundred and forty-three human tests were completed on the VDT: 91 male and 52 female. Due to subject preference, medical recommendations, and scheduling conflicts, no female subjects completed cell E (10 G, 5.0 lb helmet weight).

Acceleration Responses

Of interest were the seat, chest and head acceleration (accel) responses in the direction of impact. From the time histories of each test, peak values were taken and then averaged across all tests within a particular cell (Figures 7-8 and Table 3). The averages were based on all subjects, all repetitions. The ratio of chest acceleration to input (seat accel) increased with carriage G level; however, the average chest acceleration measurement was approximately 50% greater than the seat acceleration. In all test conditions the average head Z acceleration was lower than the average chest Z acceleration.

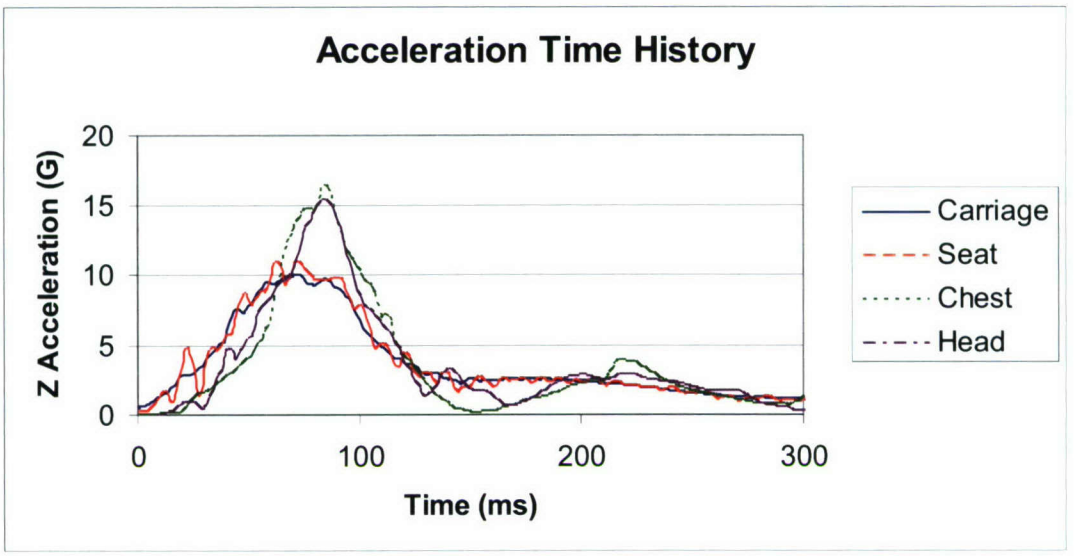

Figure 7. Example time history acceleration data from a 10 G test

Table 3. General acceleration summary

Test Cell	Nominal Carriage Accel (G)	Seat Z Accel (G)	Chest Z Accel (G)	Head Z Accel (G)
A	6	6.45	8.68	8.25
B	8	8.61	13.02	12.20
C	10	11.17	17.61	15.79
D	10	10.97	17.36	15.72
E	10	10.98	18.33	16.21

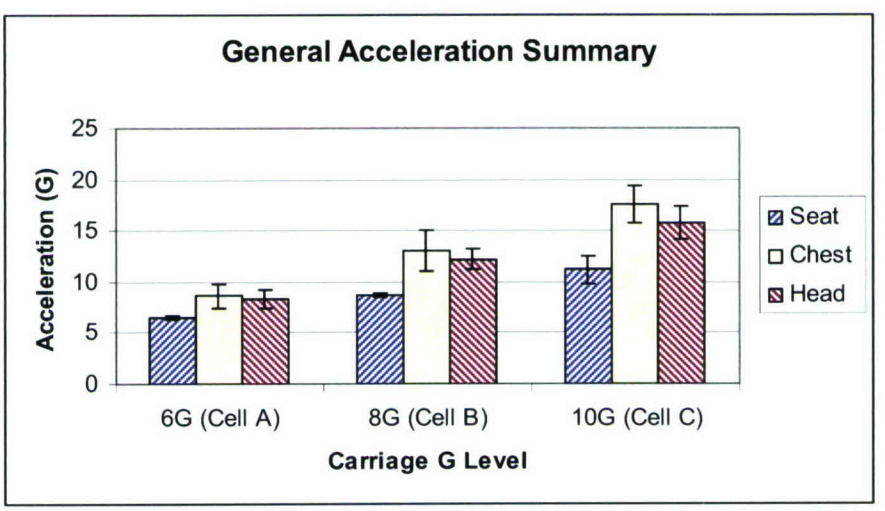

Figure 8. General acceleration summary as a function of carriage acceleration

To evaluate the effect of vertical acceleration level on head and neck response, cells A, B, and C were investigated. Nineteen subjects were included in this evaluation (nine female and ten male). One female and two male subjects in this evaluation completed cells A and B, but not C; therefore three separate analyses of variance (ANOVA) were used to manage the missing data. The average peak head Z acceleration ranged from 8.24 to 15.53 G for both male and female subjects across 6 and 10 G carriage accelerations (Table 4). The angular acceleration ranged from 159.39 to 498.91 rad/s^2. A mixed design model was used: gender was considered a between factor, cell a within factor, and subject considered random. The reported means are least-squares means which use parameter estimates to estimate missing data, then calculate the means using standard methods. The peak Z acceleration was in the direction of impact: upward. The prominent Y angular acceleration (pitch) of the head occurred in flexion. These accelerations increased with increasing carriage acceleration level (Figures 9-10). The error bars for the male and female data points represent the standard deviations. The error bars shown for the values of both genders are standard deviations pooled across gender. The mean peak head Z and Ry acceleration for both males and females increased linearly as the carriage acceleration increased. A statistical analysis was conducted on the resulting head accelerations using a 95% confidence interval (Table 5). There was not a significant gender effect for head X or head Ry acceleration; however, gender effect was significant for head Z acceleration. Post-hoc paired comparisons of cells used two-tailed t-tests with pooled error and a per-comparison error level of 0.05/3 = 0.0167 (i.e., Bonferroni procedure). Cell A had a statistically significant head X acceleration compared to cells B and C; however, B and C were not significantly different from each other. For head Z and Ry accelerations, cells A, B and C were all significantly different from each other.

Table 4. Head acceleration response summary for varying acceleration level

Accel Level (G)	Head Z Accel (G)			Head X Accel (G)			Head Ry Accel (rad/sec^2)		
	Male	Both	Fem	Male	Both	Fem	Male	Both	Fem
6 (Cell A)	7.79	8.24	8.69	0.66	0.69	0.72	144.25	159.39	174.53
8 (Cell B)	11.88	12.10	12.32	1.72	1.71	1.70	280.62	338.51	396.40
10 (Cell C)	15.28	15.53	15.78	2.11	2.09	2.07	480.25	498.91	517.57

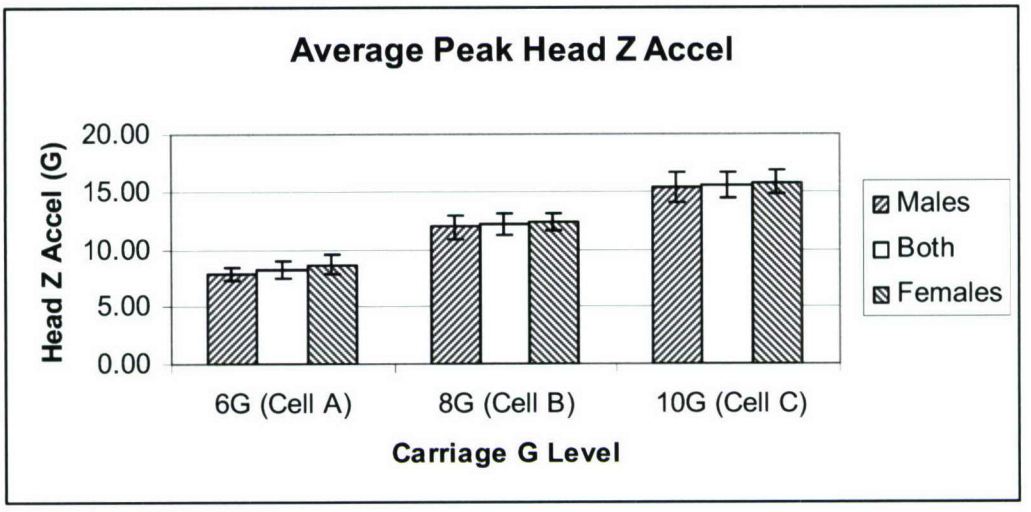

Figure 9. Head Z linear acceleration response summary as a function of increasing carriage acceleration

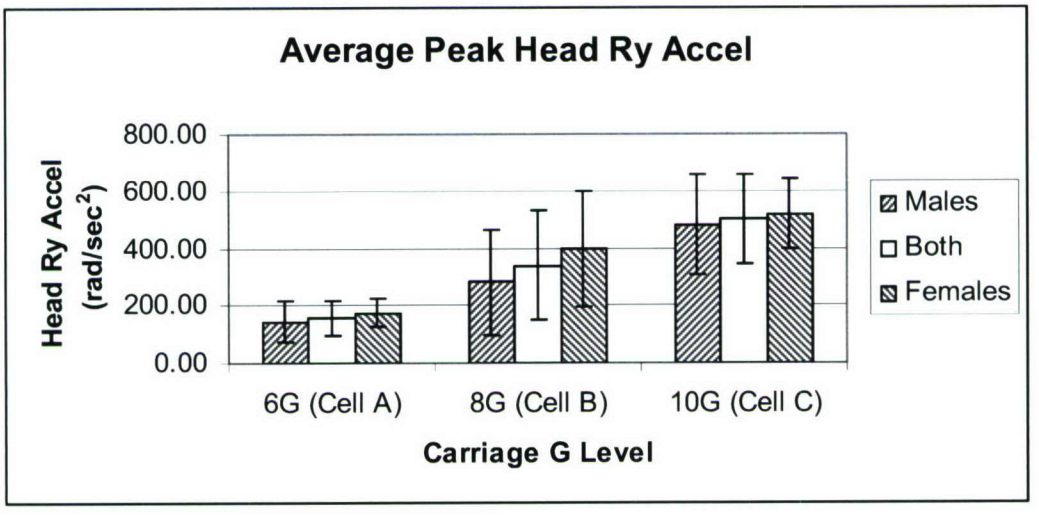

Figure 10. Head Ry angular acceleration response summary as a function of increasing carriage acceleration

Table 5. Statistical analysis of head acceleration response for varying acceleration level

Parameter	*p* Value		
	Main Effect of G Level	Main Effect of Gender	Interaction Between G Level and Gender
Head Z Accel	0.0001	0.0337	0.7259
Head X Accel	0.0001	0.9895	0.9769
Head Ry Accel	0.0001	0.2602	0.5153

To evaluate the effect of helmet weight on head acceleration response, cells C, D, and E were investigated. Only five subjects were able to complete cell E (all males); therefore, two different analyses were performed to evaluate helmet weight effects. The first evaluation included only the five male subjects who completed all three cells. The second evaluation was aimed at making use of more valuable data from cells C and D and therefore utilized the eleven subjects who completed cells C and D, estimating missing values for cell E using the same method as described above for estimating cell C. A design model was used with cell as a within factor and subject considered random. The eleven subjects consisted of seven male and four female subjects; however, due to the cell E estimations for all female subjects, gender was not used as a factor in the model. The average peak values from the pertinent head accelerations for both evaluation methods differed slightly (Table 6). The head Z accelerations increased slightly with increasing helmet weight, while the head Ry accelerations showed a slight decrease (Figures 11-12). The error bars for the data points in the 5-subject evaluation represent the standard deviations. Since the 11-subject evaluation contained over 50 percent estimated cell E data points, standard deviations would be uninformative and were therefore omitted from the plots. There is no significant effect of helmet weight on Z or Ry head acceleration for both evaluation methods (Table 7).

Table 6. Head acceleration response summary for varying helmet weight

Helmet Weight (lbs)	Head Z Accel (G)		Head X Accel (G)		Head Ry Accel (rad/s^2)	
	5-subject	11-subject	5-subject	11-subject	5-subject	11-subject
3.0 (Cell C)	15.62	15.51	2.73	2.40	478.37	501.25
4.0 (Cell D)	16.11	15.60	1.96	2.18	413.50	514.00
5.0 (Cell E)	16.18	15.87	1.78	1.72	347.57	409.26

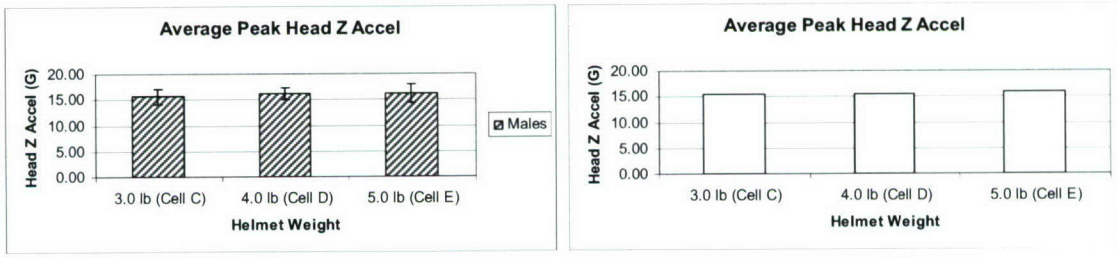

(a) (b)

Figure 11. Head Z linear acceleration response summary as a function of increasing helmet weight for (a) 5-subject and (b) 11-subject evaluation

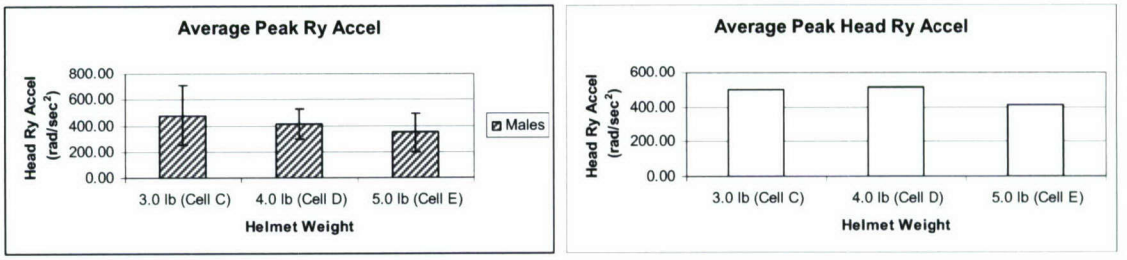

(a) (b)

Figure 12. Head Ry angular acceleration response summary as a function of increasing helmet weight for (a) 5-subject and (b) 11-subject evaluation

Table 7. Statistical analysis of head acceleration response for varying helmet weight

Parameter	*p* Value for Main Effect of Helmet Weight	
	5-subject	11-subject
Head Z Accel	0.7682	0.8574
Head X Accel	0.0417	0.1444
Head Ry Accel	0.1334	0.2395

Neck Forces and Moments

The neck force and moment analysis was completed using similar methods to the head acceleration analysis. The peak Z force ranged from 103.30 to 176.43 lbs compression for both males and females across carriage acceleration level, and the peak Y moment ranged from 189.41 to 459.23 in-lbs flexion (Table 8). The neck forces and moments increased with increasing G level for both males and females (Figures 13-14). Again, the error bars for the male and female data points represent the standard deviations. The error bars indicated for the values of both genders are standard deviations pooled across gender. There was not a significant gender effect for neck X force, or Y moment; however, gender effect was significant for neck Z force (Table 9). The Bonferroni procedure was used to complete the post-hoc paired comparison. For all three dependent force and moment variables, cells A, B and C were statistically different from each other.

Table 8. Resultant neck force and moment response summary for varying acceleration level

Accel Level (G)	Head Z Force (lbs)			Head X Force (lbs)			Head Y Moment (in-lbs)		
	Male	Both	Fem	Male	Both	Fem	Male	Both	Fem
6 (Cell A)	106.18	103.30	100.42	25.48	28.96	32.44	171.86	189.41	206.97
8 (Cell B)	151.05	146.39	141.73	39.97	47.63	55.30	250.54	310.79	371.04
10 (Cell C)	187.27	176.43	165.59	60.01	70.81	81.61	455.84	459.23	462.61

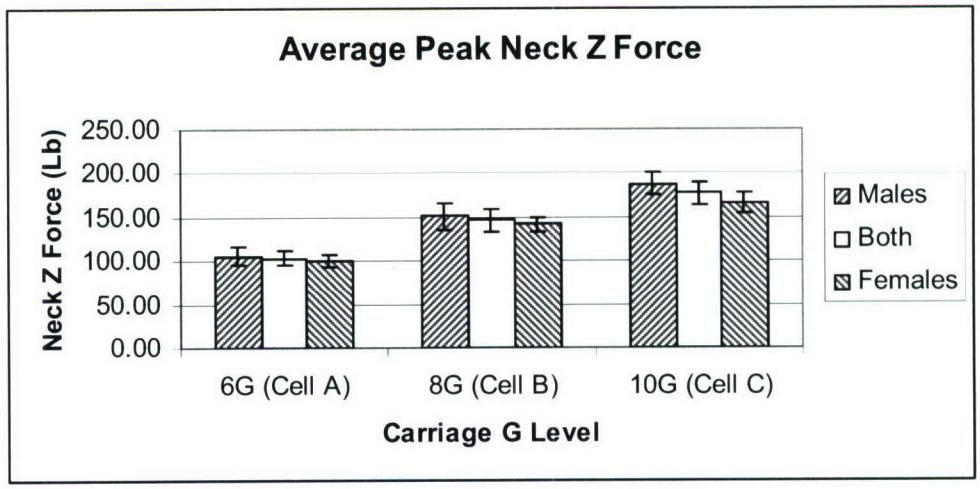

Figure 13. Neck Z resultant force response summary as a function of increasing carriage acceleration

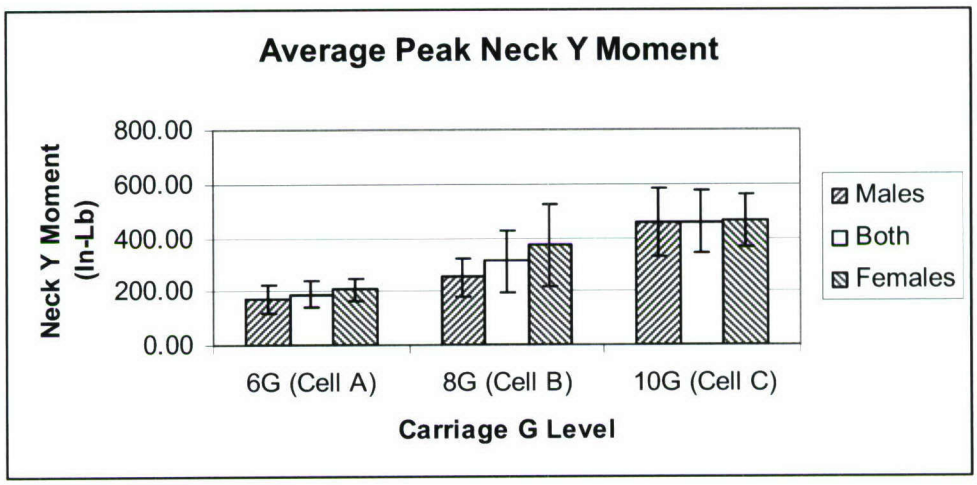

Figure 14. Neck Y resultant moment response summary as a function of increasing carriage acceleration

Table 9. Statistical analysis of neck force response for varying acceleration level

Parameter	*p* Value		
	Main Effect of G Level	Main Effect of Gender	Interaction between G Level and Gender
Neck Z Force	0.0001	0.0088	0.0629
Neck X Force	0.0001	0.1375	0.4272
Neck Y Moment	0.0001	0.1962	0.0760

To evaluate the effect of helmet weight on neck forces and moments, cells C, D, and E were investigated. Two different analyses were performed to evaluate helmet weight effects on neck forces, as performed with the acceleration analysis. The average peak values from the pertinent neck forces and moments for both evaluation methods differed slightly (Table 10). The average neck Z force and Y moment increased with increasing helmet weight (Figures 15-16). The error bars for the data points in the 5-subject evaluation represent the standard deviations, while no error bars are listed for the 11-subject evaluation. Using the approximations for eleven subjects, all cells (C, D and E) had statistically different neck Z force means (Table 11). Using only five subjects in the post-hoc Bonferroni analysis revealed no difference between C and D. Using the approximations for eleven subjects, cell C had a statistically significant neck Y moment compared with both cells D and E, however using only five subjects revealed only a difference between cells C and E.

Table 10. Resultant neck force and moment response summary for varying helmet weight

Helmet Weight (lb)	Head Z Force (lbs)		Head X Force (lbs)		Head Y Moment (in-lbs)	
	5-subject	11-subject	5-subject	11-subject	5-subject	11-subject
3.0 (Cell C)	189.64	180.34	58.38	75.78	473.28	479.84
4.0 (Cell D)	204.10	191.55	64.98	85.08	580.12	610.40
5.0 (Cell E)	222.53	211.61	62.30	81.05	604.30	622.72

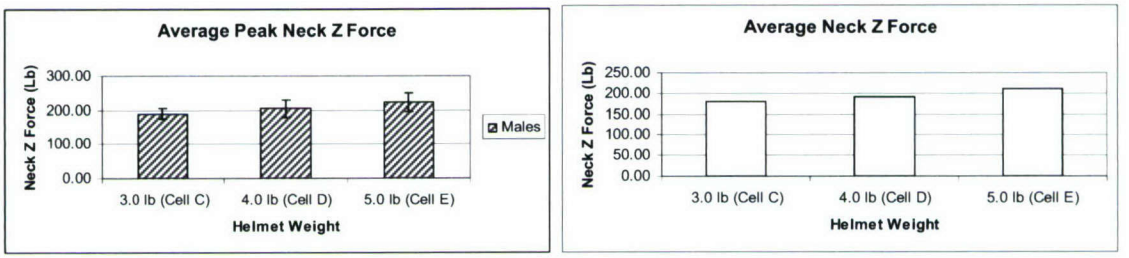

(a) (b)

Figure 15. Neck resultant Z force response summary as a function of helmet weight for (a) 5-subject and (b) 11-subject evaluation

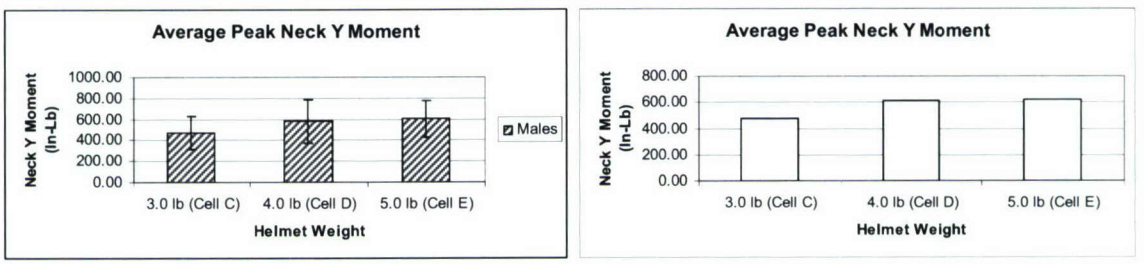

(a) (b)

Figure 16. Neck resultant Y moment response summary as a function of helmet weight for (a) 5-subject and (b) 11-subject evaluation

Table 11. Statistical analysis of neck force response for varying helmet weight

Parameter	*p* Value for Main Effect of Helmet Weight	
	5-subject	11-subject
Neck Z Force	0.0011	0.0001
Neck X Force	0.6855	0.4992
Neck Y Moment	0.0196	0.0010

The preceding force and moment data were calculated using the in-house program Neckload3. As described in Methods, this program does not take into account the external forces on the head resulting from the headrest.

In addition to the head acceleration and neck force analysis, all test videos were reviewed for visual analysis of head and neck kinematics. Any test in which the subject failed to keep his or her head against the headrest was noted as having flexion or extension. From this information the percentage of tests within each cell in which noticeable neck flexion or extension occurred was calculated (Figure 17). All of the female subjects who completed cell D exhibited neck flexion or extension. The highest percentage of male flexion or extension occurred in cell E. Several subjects did not complete the test matrix; therefore, the number of subjects within each cell was not consistent. The population of female subjects for cells A-E was 9, 9, 7, 4, and 0, respectively. The population of male subjects was 15, 11, 9, 7, and 5.

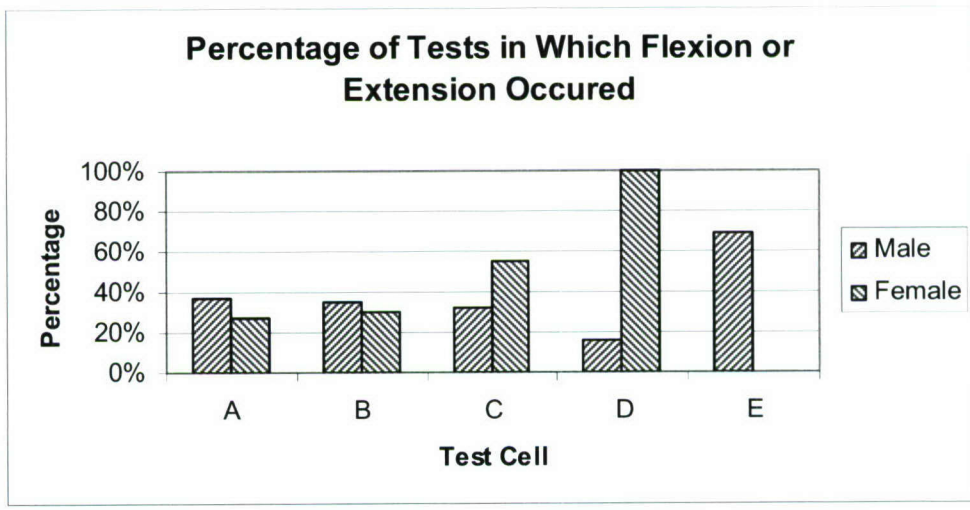

Figure 17. Prevalence of neck flexion or extension across all test conditions for male and female subjects

EMG

EMG data were reported in peak RMS amplitude (mV) and %MVC. As previously described, the %MVC was calculated using the dynamic test data divided by the static MVC (Figure 18). When analyzing EMG data, the test sequence was divided into two different time frames: 1) before carriage drop, or bracing period, and 2) free fall and impact. The distribution of the EMG data was skewed; therefore, before statistical analysis the data were converted to a logarithmic scale so that the assumptions of normality and equal variance were met (referred to as logged data).

Not all tests produced usable EMG data sets in every channel. Factors that led to this missing data included problems maintaining adequate sensor contact, ECG signal contamination, and electrical interference from the VDT and data acquisition system. These types of difficulties with EMG recordings are not uncommon and have been reported by other investigators [20, 23, 28]. Most of these problems occurred early in the test program and through troubleshooting were solved by implementing more appropriate data acquisition and sensor placement techniques.

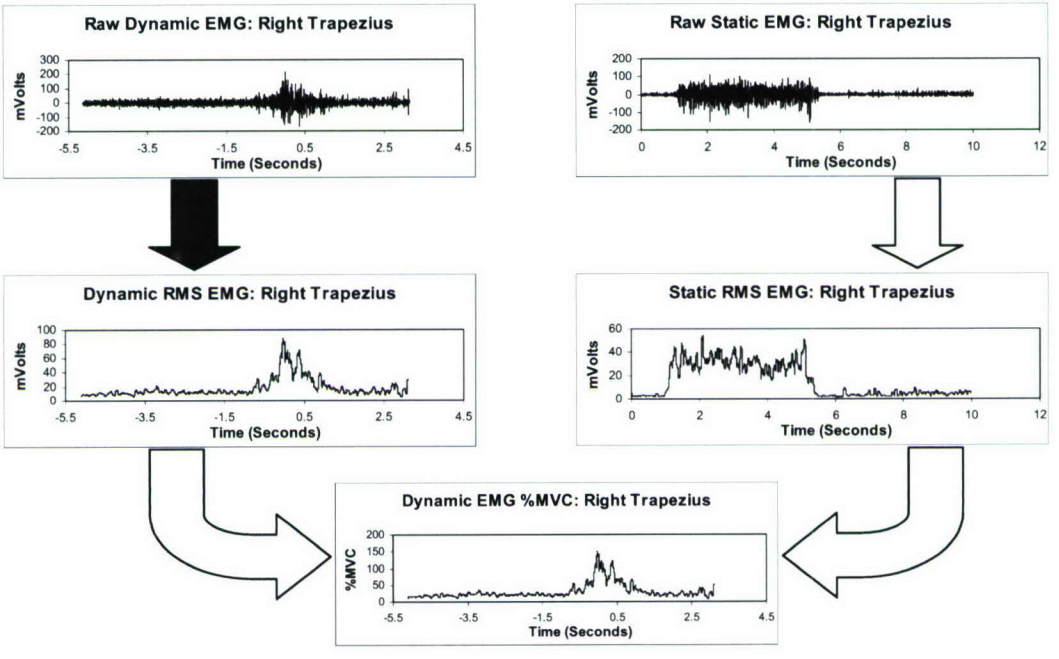

Figure 18. Example of EMG data analysis from raw to %MVC.

To investigate the effect of carriage G level on neck muscle activity, cells A, B and C were analyzed. To analyze cells for each EMG variable, only subjects who had usable EMG data from two of the three tests were utilized. Separate ANOVAs were used to manage the missing data. The logged means were transformed back to the original units, and the averages of the peak values were reviewed during both the bracing and impact periods of each test condition (Tables 12-13). Although both left and right SCM and upper trapezius were recorded, for each test the greater value of the two sides was used for statistical analysis. A mixed design model was used: gender was considered a between factor, cell a within factor, and subject considered random. From this statistical analysis, the only significant difference based on varying G level

occurred in the trapezius (traps) %MVC for both bracing and impact (Tables 14-15). During the bracing period, cells A and C were different, while during the impact period cells A and B were different. There were no gender effects on any of the EMG parameters. Summary plots were generated for all of the neck EMG data (Appendix A).

Table 12. Neck EMG response summary for varying acceleration level: bracing period

Logged Units												
	SCM RMS (mV)			SCM %MVC			Traps RMS (mV)			Traps %MVC		
Accel Level (G)	Male	Both	Fem	Male	Both	Fem	Male	Both	Fem	Male	Both	Fem
6 (Cell A)	3.3	3.4	3.5	2.8	3.3	3.7	3.7	3.8	3.8	3.7	3.7	3.6
8 (Cell B)	3.3	3.1	2.9	3.3	3.2	3.1	3.6	3.6	3.7	4.3	4.2	4.2
10 (Cell C)	3.2	3.1	3.0	3.3	3.2	3.2	3.8	3.8	3.8	4.2	4.4	4.6
Actual Units												
	SCM RMS (mV)			SCM %MVC			Traps RMS (mV)			Traps %MVC		
Accel Level (G)	Male	Both	Fem	Male	Both	Fem	Male	Both	Fem	Male	Both	Fem
6 (Cell A)	26.9	29.4	32.2	16.6	26.4	42.1	40.6	42.3	44.1	40.6	39.0	37.4
8 (Cell B)	26.8	22.4	18.8	25.9	23.5	21.4	37.2	38.0	38.9	71.3	67.7	64.4
10 (Cell C)	24.7	22.7	21.0	26.1	24.8	23.6	44.3	43.4	42.5	64.9	80.3	99.5

Table 13. Neck EMG response summary for varying acceleration level: impact period

Logged Units												
	SCM RMS (mV)			SCM %MVC			Traps RMS (mV)			Traps %MVC		
Accel Level (G)	Male	Both	Fem	Male	Both	Fem	Male	Both	Fem	Male	Both	Fem
6 (Cell A)	5.2	5.1	5.0	5.0	5.3	5.5	4.6	4.6	4.6	4.9	4.9	5.0
8 (Cell B)	5.4	5.2	5.0	5.9	5.5	5.1	4.8	4.8	4.8	5.4	5.5	5.5
10 (Cell C)	5.5	5.3	5.2	5.7	5.6	5.5	4.5	4.8	5.0	5.1	5.4	5.7
Actual Units												
	SCM RMS (mV)			SCM %MVC			Traps RMS (mV)			Traps %MVC		
Accel Level (G)	Male	Both	Fem	Male	Both	Fem	Male	Both	Fem	Male	Both	Fem
6 (Cell A)	182.0	163.2	146.3	71.8	94.4	126.7	97.3	100.2	103.2	128.3	137.3	146.9
8 (Cell B)	228.7	183.4	147.1	100.9	78.8	65.7	127.0	124.2	121.4	228.3	232.1	236.0
10 (Cell C)	239.5	209.1	182.5	120.3	123.7	133.3	92.6	115.4	143.8	166.8	218.2	285.2

Table 14. Statistical analysis of neck EMG for varying acceleration level: bracing period

Parameter	*p* Value		
	Main Effect of G Level	Main Effect of Gender	Interaction Between G Level and Gender
SCM %MVC	0.9499	0.6209	0.2619
SCM RMS	0.2176	0.7121	0.2982
Trap %MVC	0.0439	0.7955	0.4135
Trap RMS	0.6727	0.8900	0.9309

Table 15. Statistical analysis of neck EMG for varying acceleration level: impact period

Parameter	*p* Value		
	Main Effect of G Level	Main Effect of Gender	Interaction Between G Level and Gender
SCM %MVC	0.6673	0.6864	0.2379
SCM RMS	0.0837	0.1887	0.5203
Trap %MVC	0.0211	0.3453	0.2256
Trap RMS	0.1187	0.4080	0.0626

To examine the difference between voluntary neck muscle contraction while bracing and involuntary contraction during impact, summary EMG data for both male and female subjects from the two different time periods were examined (Figures 19-20). The SCM showed a greater difference than the trapezius in amplitude between the bracing and impact periods.

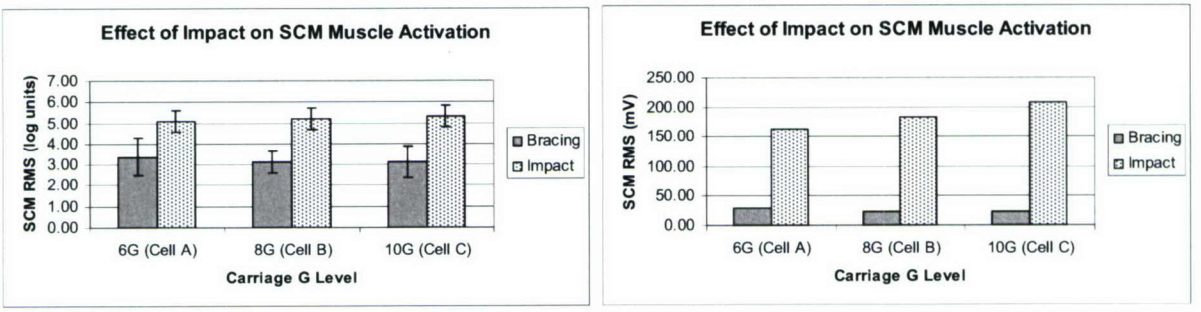

Figure 19. Effect of bracing on SCM as a function of varying acceleration level

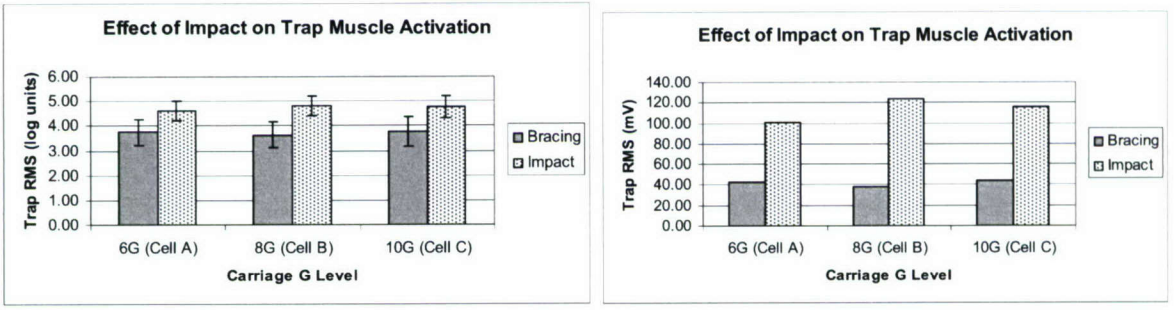

Figure 20. Effect of bracing on trapezius as a function of varying acceleration level

To evaluate the effect of helmet weight on neck muscle activity, cells C, D, and E were investigated. As with the acceleration and force data evaluation, two different statistical evaluation methods were used: a 5-subject evaluation using the five male subjects that completed all three cells, and an evaluation using subjects that completed cells C and D and approximating the cell E value. In this case, 9 to 11 subjects were used in the analysis, depending on the availability of useful EMG data in each parameter. For ease of discussion this evaluation method will still be referred to as the 11-subject technique. The design model consisted of cell as a within factor and subject considered random. The subjects in the 11-subject evaluation consisted of female subjects; however, due to the cell E estimations for all female subjects, gender was not used as a factor in the model. Summary tables of neck EMG data for the bracing and impact periods within each test condition were generated (Tables 16-17). From the corresponding statistical data, there was no main effect from helmet weight on any of the neck EMG measurements before or during impact (Tables 18-19).

Table 16. Neck EMG response summary for varying helmet weight: bracing period

Logged Units								
Helmet Weight (lbs)	SCM RMS (mV)		SCM %MVC		Traps RMS (mV)		Traps %MVC	
	5-sub	11-sub	5-sub	11-sub	5-sub	11-sub	5-sub	11-sub
3.0 (Cell C)	3.0	3.1	3.2	3.2	3.4	3.7	3.9	4.2
4.0 (Cell D)	3.2	3.1	3.7	3.6	3.3	3.5	4.2	4.2
5.0 (Cell E)	2.9	2.9	2.9	2.8	3.4	3.6	4.2	4.4
Actual Units								
Helmet Weight (lbs)	SCM RMS (mV)		SCM %MVC		Traps RMS (mV)		Traps %MVC	
	5-sub	11-sub	5-sub	11-sub	5-sub	11-sub	5-sub	11-sub
3.0 (Cell C)	20.8	22.4	25.2	25.2	31.0	38.6	47.9	65.7
4.0 (Cell D)	24.4	22.3	41.3	36.5	28.1	31.6	63.2	67.6
5.0 (Cell E)	17.6	17.4	17.6	16.6	29.5	34.9	65.6	79.5

Table 17. Neck EMG response summary for varying helmet weight: impact period

Logged Units								
Helmet Weight (lbs)	SCM RMS (mV)		SCM %MVC		Traps RMS (mV)		Traps %MVC	
	5-sub	11-sub	5-sub	11-sub	5-sub	11-sub	5-sub	11-sub
3.0 (Cell C)	5.6	5.3	6.1	5.7	4.7	4.7	5.4	5.4
4.0 (Cell D)	5.5	5.3	6.0	5.5	4.6	4.7	5.2	5.5
5.0 (Cell E)	5.5	5.3	5.6	5.1	4.5	4.6	5.4	5.5
Actual Units								
Helmet Weight (lbs)	SCM RMS (mV)		SCM %MVC		Traps RMS (mV)		Traps %MVC	
	5-sub	11-sub	5-sub	11-sub	5-sub	11-sub	5-sub	11-sub
3.0 (Cell C)	263.8	207.7	431.3	309.0	108.6	110.2	219.7	211.8
4.0 (Cell D)	233.5	209.1	395.0	234.6	98.1	105.0	175.1	232.2
5.0 (Cell E)	249.0	209.1	259.6	169.3	90.9	94.7	215.6	243.8

Table 18. Statistical analysis of neck EMG for varying helmet weight: bracing period

Parameter	*p* Value	
	Main Effect of Helmet Weight	
	5-subject	11-subject
SCM %MVC	0.0971	0.1402
SCM RMS	0.5683	0.5874
Trap %MVC	0.4867	0.7793
Trap RMS	0.9292	0.6258

Table 19. Statistical analysis of neck EMG for varying helmet weight: impact period

Parameter	*p* Value	
	Main Effect of Helmet Weight	
	5-subject	11-subject
SCM %MVC	0.1058	0.5464
SCM RMS	0.6219	0.9977
Trap %MVC	0.6992	0.8585
Trap RMS	0.2453	0.6761

Again, the activity of the trapezius and SCM were plotted over varying helmet weight for both bracing and impact period (Figures 21-22). The same phenomenon is noted in cells C, D and E: the SCM had a greater difference than the trapezius in amplitude between the bracing and impact periods

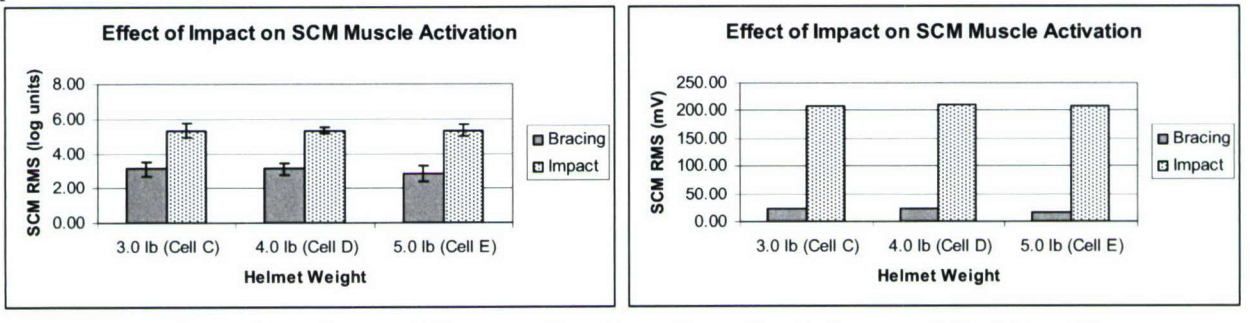

Figure 21. Effect of bracing on SCM as a function of varying helmet weight (11-subject analysis)

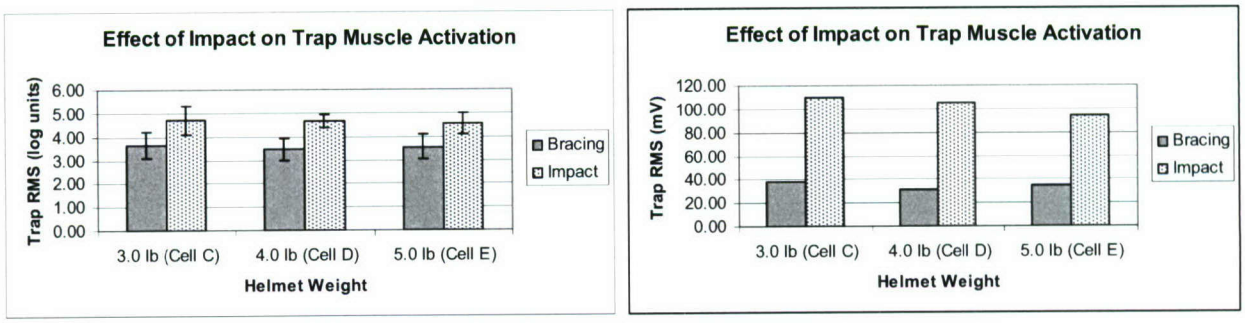

Figure 22. Effect of bracing on trapezius as a function of varying helmet weight (11-subject analysis)

Subject Reproducibility

To analyze subject reproducibility, data were used from 17 subjects who completed a significant number of repetitions for each cell. A total of 128 tests were included in the evaluation. Ten of the subjects (5 male, 5 female) had no impact acceleration test experience, while 7 subjects (5 male, 2 female) had some prior experience as an impact test subject. Parameters investigated include head and chest Z accelerations, as well as neck Z force (Table 20).

Table 20. +Gz, helmet weight, and descriptive statistics for each cell for all subjects and replications

Cell	G Level	Helmet Weight (lb)	n	Chest Z Accel (G)			Head Z Accel (G)			Neck Z Force (lb)		
				Min	Median	Max	Min	Median	Max	Min	Median	Max
A	6	3.0	23	6.8	8.5	11.7	7.0	8.3	14.0	87.1	101.8	120.7
B	8	3.0	36	10.6	12.6	20.3	10.4	12.2	17.9	120.5	143.3	217.3
C	10	3.0	30	15.1	16.8	23.5	11.4	16.1	20.6	121.1	180.5	234.2
D	10	4.0	26	13.6	17.8	20.3	12.0	15.3	19.8	160.9	190.2	248.2
E	10	5.0	13	14.8	17.8	26.1	13.0	15.5	20.5	183.7	212.9	285.7

The subjects were sorted by experience and then again by gender. The replications are labeled 1, 2, and 3 and the circled replications distinguish those subjects who had a flexion or extension of the neck upon impact. The figures below show the neck Z force data variability of each subject for cell C (10G, 3.0-lb helmet, Figure 23) and D (10G, 4.0-lb helmet, Figure 24).

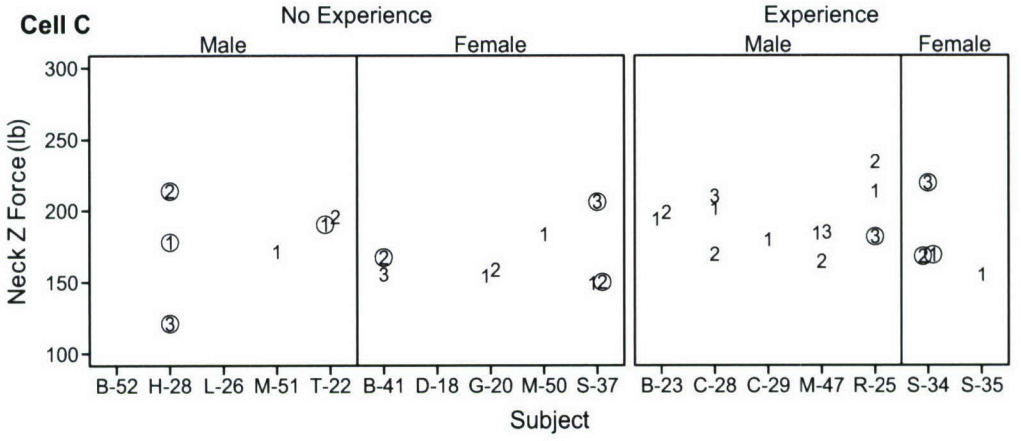

Figure 23. Neck force for each subject testing cell C

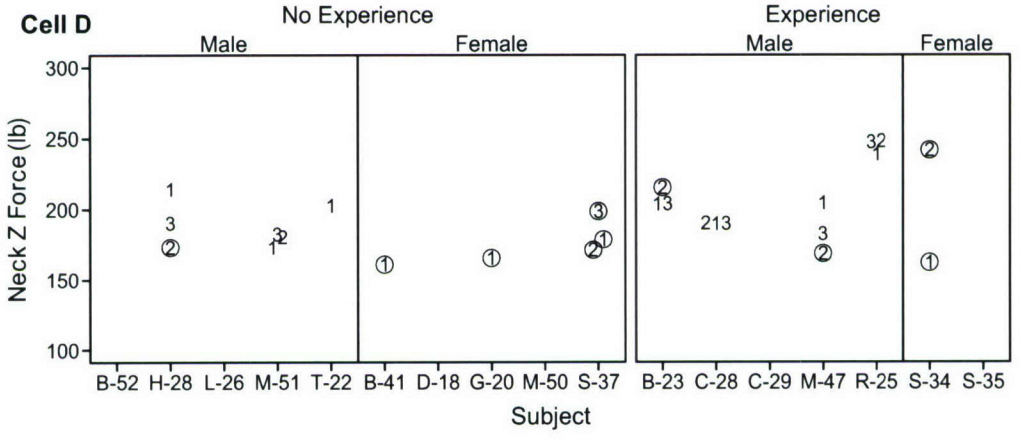

Figure 24. Neck force for each subject testing cell D

Factors of interest in analyzing the acceleration and force data (dependent variables) include replication (i.e., order effect), flexion/extension, cell, experience, and gender. As seen in the figures above, there were many instances where a subject was missing an entire cell or did not have three replications per cell. Also, there were instances where a subject had neck flexion/extension for all of the replications or none of the replications for a particular cell, indicating that some subjects may be more prone to neck motion than others. Visual inspection of plots indicated no meaningful relationship between flexion/extension and any of the dependent variables; therefore, this factor was not considered further.

There were two models used in analyses of variance (ANOVA). The first model determined whether replication had an effect and if a replication effect varies with experience. The second model determined whether cell, experience, or gender had an effect. There were a low number of subjects and most subjects had missing data; therefore it was decided to treat subject as a fixed factor. These analyses should be interpreted cautiously; conclusions should not be generalized to a subject population, but should be considered as a "best guess" for these subjects only.

The first ANOVA model included all combinations of subject and cell where the subject had three replications. Dependent variables were then averaged across cells for each combination of subject and replication. There were six subjects with experience and five subjects with no

experience. Experience, replication, and subject with subject nested in experience were the factors in the analysis. The error term used for all F-tests was the replication*subject (experience) interaction. For all three dependent variables there was not a replication main effect ($p > 0.1781$) or a replication*experience interaction ($p > 0.7373$).

The second ANOVA model used the following factors: cell, experience, gender, and subject with subject nested in experience and gender. Cell E was not included in the analyses due to the fact that only five males were able to complete this cell (one male with no experience and four males with experience). Also due to missing data in at least two cells from B, C, and D, three subjects were not used. Only main effects and two-way interactions were included in the model as a result of the low number of subjects for each combination of experience and gender (Table 21).

Table 21. Results from analyses of variance

Dependent Variable	Source	df	SS	F	*p*
Chest Z Accel (G)	Cell	3	923.38	133.93	0.0001
	Experience	1	9.97	4.34	0.0403
	Gender	1	14.92	6.49	0.0126
	Subject (Experience*Gender)	10	113.73	4.95	0.0001
	Cell*Experience	3	0.63	0.09	0.9642
	Cell*Gender	3	2.24	0.32	0.8075
	Experience*Gender	1	4.08	1.78	0.1862
	Error	85	195.34		
	Total	107	1480.80		
Head Z Accel (G)	Cell	3	639.01	89.04	0.0001
	Experience	1	1.48	0.62	0.4344
	Gender	1	2.47	1.03	0.3121
	Subject (Experience*Gender)	10	51.60	2.16	0.0283
	Cell*Experience	3	6.05	0.84	0.4741
	Cell*Gender	3	5.97	0.83	0.4799
	Experience*Gender	1	0.25	0.10	0.7476
	Error	85	203.34		
	Total	107	1030.52		
Neck Z Force (lb)	Cell	3	79198.29	72.10	0.0001
	Experience	1	1279.46	3.49	0.0650
	Gender	1	2210.92	6.04	0.0160
	Subject (Experience*Gender)	10	12106.60	3.31	0.0012
	Cell*Experience	3	1440.49	1.31	0.2760
	Cell*Gender	3	163.06	0.15	0.9304
	Experience*Gender	1	108.27	0.30	0.5880
	Error	85	31121.39		
	Total	107	158650.72		

(**df** = degrees of freedom, **SS** = Sum of Squares, **F** = F-test, ***p*** = probability)

Test results indicate no significant interactions. The cell main effect was significant for all three dependent variables. A Bonferroni paired comparison procedure was used to compare the cell means with a family-wise error level of 0.05. For all three dependent variables, cells A, B, C, D were all significantly different from each other, with the exception of cells C and D. There was a significant main effect of experience for chest Z acceleration and a significant main effect of gender for chest Z acceleration and neck Z force. Least Squares Means were determined from the analyses of variance. These means use parameter estimates to determine estimated means (Table 22 and Figure 25).

For cell E, means were determined across replications for the five subjects with data. These means were then averaged across subjects (chest Z acceleration mean = 18.8, head Z acceleration mean = 16.2, neck Z force mean = 223). These cell E means are not comparable to those in Table 22 since they come from a subset of the subjects.

Table 22. Least-squares means from the analyses of variance

Factor	Level	Chest Z Accel (G)	Head Z Accel (G)	Neck Z Force (lb)
Cell	A	9.2	8.7	105
	B	12.9	12.3	148
	C	17.5	15.8	178
	D	17.3	15.7	191
Experience	No	13.9	13.0	152
	Yes	14.6	13.3	160
Gender	Male	13.8	13.0	161
	Female	14.7	13.3	150

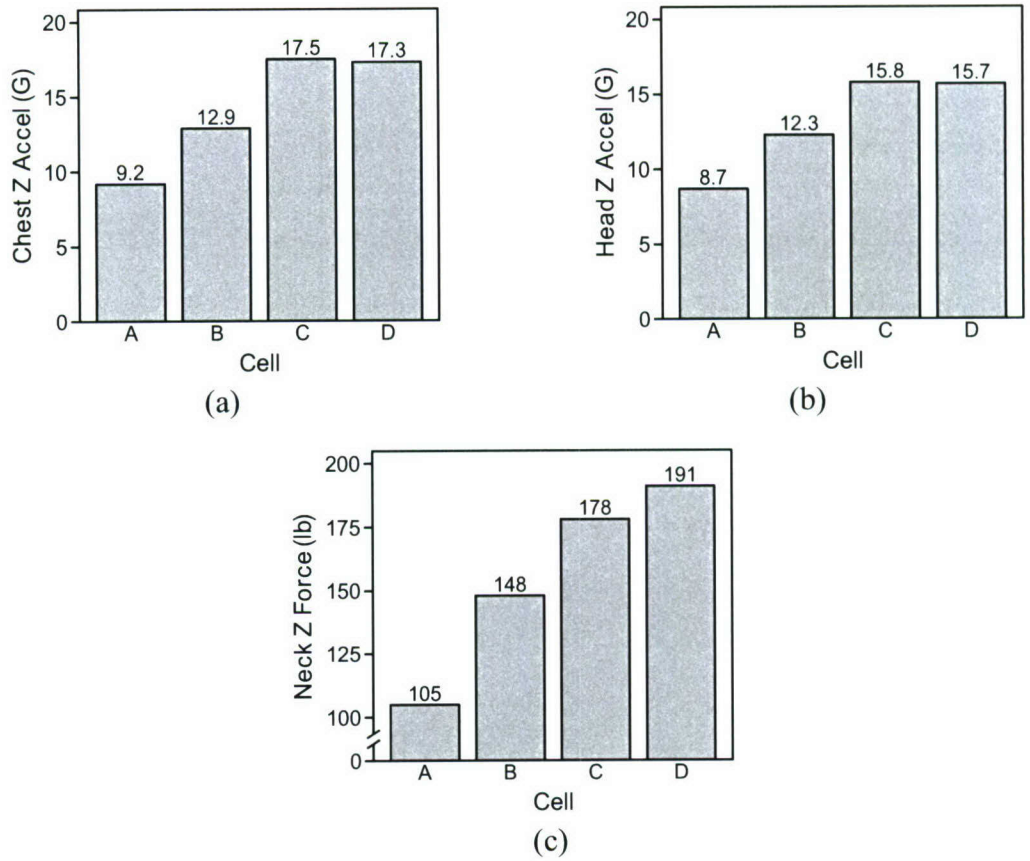

Figure 25. Least-squares means from the analyses of variance (a) chest Z acceleration, (b) head Z acceleration, (c) neck Z force

Approximately 95% of all pairs of replications from the same subject and cell (generated on different weeks) should differ in absolute value by less than the reproducibility limit (RL). Each combination of subject and cell that had at least two replications was used to determine the RL (Table 23). Due to the low sample size, a RL was not determined for each cell separately; however, the figures indicate that the variability of replications is similar across all cells. The RL was calculated by pooling the variance of replications and then multiplying the square root of this variance by 2.77. The mean was calculated by averaging across replications for each subject and cell used to determine the RL and then averaging these means across subject and cell. The procedure for determining the reproducibility limit is described in the American Society of Testing Materials (ASTM) designation: E 691-92 [29].

Table 23. Reproducibility Limits (RL) for each dependent variable

Dependent Variable	**Mean**	**RL**	**RL % of Mean**
Chest Z Accel (G)	15.1	4.7	31
Head Z Accel (G)	13.9	4.7	34
Neck Z Force (lb)	168.0	56.8	34

Subjective Data

After each test, the subjects were asked to rate the severity of impact and physical pain/discomfort based on a numeric scale. On a scale of 1 to 5 (1 being mild and 5 being severe), the average female response for impact severity was 2.04 and the average male response was 2.09. On a scale of 1 to 5 (1 being the most comfortable and 5 being the most uncomfortable), the average female response for physical discomfort/pain experienced was 1.61 and the average male response was 1.66. The average reported physical discomfort/pain for all subjects increased slightly with impact level (1.1, 1.7 and 1.9 consecutively) but did not show any trend across helmet weight. Subjects reported neck or back muscular strain or soreness after less than 10% of tests.

Three female subjects were exempt from cell E (10 G, 5.0-lb helmet) due to severe neck flexion during cell D (10 G, 4.0-lb helmet). Five male subjects (no females) completed cell E, none of which experienced neck or back discomfort. One cell D test was aborted due to subject anxiety immediately before the drop sequence. This subject (female) later successfully tested cell D without any problems. Two females and two males removed themselves from the study due to physical discomfort or anxiety.

One male subject was removed from the subject panel following a mild 10-15 percent anterior compression fracture of the T7 vertebral body. The injury occurred during cell C (10 G, 3.0-lb helmet). Detailed video and data analysis revealed very slight shoulder rotation during the drop, which may have been due to the subject taking a deep breath just prior to dropping. Otherwise, the bracing position appeared adequate. The harness and equipment were inspected and no abnormalities were found. At impact, there appeared to be a forward motion of the subject's torso which likely pushed his chest into the chest strap of the harness, resulting in the brief paralysis of his diaphragm and inability to breathe. This action resulted in an unfavorable subject position and undue strain on the thoracic spine. The subject was treated for his injury and fully recovered. To prevent future adverse events, the attachment points of the shoulder harness were re-designed to further restrict the subject's torso and prohibit forward motion of the subject's chest.

DISCUSSION

Acceleration Responses

Vertical (+Gz) accelerations increased proportionally with carriage accelerations. This was true for accelerations measured at the chest and head, although the average head Z acceleration was lower than the average chest Z acceleration. This was due to the rotation of the head coordinate system. When the head rotates forward in flexion, what was originally the Z axis in the mouth accelerometer package now picks up X acceleration as well (Figure 4). In the case of head rotation, the resultant head acceleration remains the same; however, the Z acceleration is reduced.

The weight added to the helmet had no apparent effect on the acceleration of the head during impact. Some subjects were able to maintain their head firmly against the headrest, resisting forward motion (X acceleration) of the head and flexion (angular Y acceleration) of the neck during a vertical impact. Other subjects experienced more forward motion, associated with neck flexion. The angular acceleration was obviously affected by G level (Figure 10). For cells A and B (6 and 8 G), females experienced a comparable percentage of neck flexion/extension as compared to their male counterparts (Figure 17). At the 10 G cells, however, females experienced significantly more flexion/extension of the neck: flexion or extension of the neck occurred in 55% of female cell C tests and 100% for cell D. Compare that to 32% and 16% for male subjects in cells C and D, respectively. The average neck circumference of the female subjects was 14.1 in., and 15.8 in. for the male subjects (Figure 3). This neck flexion/extension phenomenon at higher impact levels may indicate that subject strength and anthropometry play a significant role in the kinematic neck response during impact.

Neck Forces and Moments

Head accelerations were not statistically different across increasing helmet weight; however, the forces and moments incurred at the head/neck joint did have a statistically significant increase proportional with helmet weight. This correlation was expected as the mass added to the helmet made up a large percentage of the total head/helmet mass that is a key player in the forces generated at the OC. Although female subjects experienced slightly greater vertical head accelerations overall than their male counterparts, the lighter weight of the female heads led to an average female neck force that was lower than the male neck forces generated at the OC.

Using the 11-subject evaluation method to investigate the effect of helmet weight on neck forces and moments revealed higher neck moments across helmet weight. Of the five male subjects who completed cell E, four were considered to be experienced test subjects (having previous impact acceleration experience). Of the additional six subjects in the 11-subject evaluation method, only two were considered experienced. The average neck circumference of the five subjects is 15.9 in., which is 0.6 in. greater than the average circumference of the 11-subject population. Taking into account the experience and anthropometry statistics, the 5-subject evaluation had a larger percentage of subjects who were possibly better prepared to resist forward motion of the head during impact. This possibility would lead to the argument that the 5-subject evaluation method represents a more conservative representation of the effects of helmet weight on neck moments.

EMG

It was demonstrated that vertical impact stimulates the neck muscles to activate at levels much higher than during voluntary contraction; however, the magnitude of impact (between 6 and 10 G) and helmet weight (between 3.0 and 5.0 lbs) does not affect the force output of the muscle (Figures 19-22). The trapezius had a lower increase in amplitude than the SCM when comparing the bracing and impact periods. This observation is likely due to the physiological make-up of the muscles. During bracing the trapezius muscles are activated at relatively high levels because they are extenders and being activated in their mode of use during the brace. The EMG data support the conclusion that in this position the trapezius is

more easily stimulated voluntarily. The SCMs, however, acting as flexors and rotators, have the ability to involuntarily co-contract during impact to prevent rotation and hyperextension of the neck, thus having high peak amplitudes during impact.

From the EMG data there is no apparent effect of G level or helmet weight on neck muscle activity. This was true for both the bracing and impact period of the tests. Even though the trapezius %MVC showed a statistically significant difference between A and C in the bracing period and between A and B in the impact period, there were no significant differences in the EMG amplitudes from the trapezius muscles in either bracing or impact periods. The %MVC trends were therefore driven by the MVC collected before the tests. Considering the nature of the significant difference discovered in the trapezius %MVC, no conclusion on neck EMG trends can be drawn from this seemingly coincidental finding.

When examining the SCM RMS amplitude during impact (Appendix A), on average females had a lower peak activation; however, this difference was not statistically significant. There were no gender differences observed in impact or bracing EMG data for either neck muscle group.

The lack of significant difference in EMG data across helmet weight, impact level, and gender may indicate that at the lowest exposure, 6 G and 3.0-lb helmet, the neck muscles have already reached their physiological maximum exertion in response to an external, dynamic stimulus. This finding supports the argument that the muscles of the neck fully activate at lower G levels and helmet weights. When more weight is added and the impact becomes more severe, the muscles simply cannot exert any more force and the subject therefore experiences more neck motion, head acceleration, and subsequently increased neck loading, along with risk of injury. Neck kinematic observations from this study illustrate that the peak neck muscle activation was, on average, sufficient to resist head motion for subjects with a 3.0-lb helmet up to an impact level of 10 G (Figure 17). With 69% of male tests at cell E having neck flexion or extension, it is apparent that the muscle activity was not sufficient to resist motion with a 5.0-lb helmet during a 10 G vertical impact. Female subjects reached their maximum controlled weight limit earlier, at the 4.0-lb helmet weight, with 100% of all female tests at cell D exhibiting neck flexion or extension. Although the neck activation levels were the same across gender, anthropometric differences were noted as previously described. Due to these differences it may be possible that individuals with smaller neck anthropometry need higher levels of neck activation in order to properly support helmet mass.

Subject Reproducibility

The second modeled ANOVA test revealed a significant main effect of gender for neck Z force. There was also a significant main effect of experience and gender for the chest Z acceleration. Many factors may have influenced this effect, including: different subject body masses and proportions, seat cushion compression, and a change in the support strap system. Mid-way through this study, the restraint system was modified to decrease motion of the smaller subjects, many of whom were female (details of restraint modification can be found in Appendix C). A further investigation would be needed to analyze the differences between the old restraint system and the new.

The results of this portion of the study also revealed a high reproducibility limit. This RL could have been a result of uncontrollable factors when working with human subjects, such as: length of time between test days, personal training, motivation, different bracing technique, environmental factors, and natural body variations (weight, health). A data set created from a study done by Buhrman in 1999 contained 2-4 replications from each of 45 subjects for neck Z force of cell C (10 G, 3.0-lb helmet) [30]. The RL from these data was 41.6 with RL % of mean = 22. The difference in RL % of mean between the current data and the 1999 data is somewhat due to subjects in the current data having a relatively large range for his/her replications (example: subject H-28 in Figure 23). Considering results from both data sets, two replications of neck Z force from the same subject and cell, generated on different weeks, could differ by as much as 25-30%.

Subjective Data

Overall, the impacts were well tolerated. There was one adverse medical event during the duration of this study, but the injury did not occur in the cervical spine and was not related to helmet weight. There was no significant difference in the reported pain/discomfort across increasing helmet weight. There was also no significant difference in the reported incidence of pain/discomfort between males and females; however, females did not complete the same test conditions as males, i.e., 10 G, 5.0-lb helmet (cell E). Since some female subjects were excluded from cell E following extreme head motion and neck discomfort in cell D, it is likely that, had any female subjects completed the 5.0-lb configuration, increased pain/discomfort would have been reported.

Limitations

Neck muscle activity was reported in both actual mV (RMS) and %MVC. Caution should be employed when interpreting the %MVC data. It is recommended that MVCs be collected before every test and from each muscle separately [6]. Although the MVCs were collected from each subject before every test, due to time constraints the MVCs for all investigated neck muscles were taken simultaneously, during one bracing mechanism, as described in the Methods section. Due to the methodology employed, the trapezius muscles were utilized and therefore activated more than the SCMs during the MVC.

The method of neck force calculation may lose accuracy for individuals at extreme ends of the weight scale. To calculate neck force, Neckload3 first estimated the weight of the subject's head. To do this, the subject's body weight was used in a regression equation to estimate the head weight. Therefore, if the body weight increased, so did the estimated head weights, calculating a larger neck force. In this study, subject weight ranged from 104 lbs (female) to 291 lbs (male).

CONCLUSION

From analysis of the head acceleration and neck moment data, there appears to be a trend of higher accelerations and moments occurring in subjects of smaller anthropometry. This finding supports the argument that subjects with larger, stronger necks are less susceptible to injury. Further analysis is required to quantify this trend and determine which anthropometric measurements play a significant role in neck injury risk during vertical impact accelerations.

Training was not observed to have an affect on the subjects' biodynamic response during vertical impact accelerations. In general, two replications for the same subject and cell, generated on different weeks, could differ by as much as 25-30% for neck Z force. Further testing needs to be done with a larger subject population and with subjects completing all replications for a stronger conclusion to be reached on subject training and reproducibility. Future testing on the VDT should continue to test in a sequential manner (less severe first) given that there were no signs of an advantage to testing in a randomized manner. This will also secure the subjects' safety. Also there were no meaningful correlations per test condition for gender, experience, repeated exposures or neck flexion/extension.

No correlations were observed between neck muscle activity and helmet weight or impact G level. The findings from this study illustrate that the maximum physiological output was exerted in response to an impact of 6 G with a 3.0-lb helmet. Since this was the lowest test exposure of the study, the exact dynamic conditions at which the muscles exert their maximum output is unknown. Continued research is necessary to define the lower limit test conditions that solicit the maximum muscular response.

At the test conditions described, a peak neck muscle activation level was reached. The peak exertion was not sufficient to restrain the head during a 10 G vertical impact with weighted helmets. Male and female subjects reached their maximum restrained helmet weight at different levels, with male subjects able to adequately support more weight than their female counterparts. This finding begs the question: can those neck muscles be trained to increase their maximum activation in a dynamic environment, thus restricting head motion and better protecting crewmembers? More research is required to answer this and other questions to uncover the protective capabilities and limitations of the human neck.

The data from this study provide information on the amount of muscle activation present during vertical impact for a variety of G levels and helmet weights. The neck muscle activity collected during these tests will be applied to the development and validation of active musculature neck models. In addition, the EMG data will aid in the further development of injury risk curves by quantifying the muscle tone during neck compression, flexion and extension associated with vertical impact. Using these curves, muscle activity can be used to relate the risk of neck injury during impact. The information from this research will also be useful for developing models of a living crewmember for advanced simulations. This study provided methodology for collecting EMG in a vertical impact environment and could be transitioned to other dynamic environments to examine the effect of helmet weight on neck muscle activity during other phases of operational flight and ejection.

REFERENCES

1. Buhrman, J.R., E.J. Doczy, and S.E. Mosher. *The Effects of Variable Helmet Weight on Had Response and Neck Loading During Frontal -Gx Impact.* in *42nd Annual SAFE Symposium*. 2004.
2. Perry, C.E., et al., *Evaluation of the Effects of Variable Helmet Weight on Human Response During Lateral +Gy Impact*. 2003.
3. Van der Horst, M.J., et al., *The Influence of Muscle Activity on Head-Neck Response During Impact.* Stapp Car Crash Journal, 1997. **41**: p. 487-507.
4. Mertz, H.J., *Injury Risk Assessments Based on Dummy Responses.* Accidental Injury: Biomechanics and Prevention, 2002. **2**: p. 89-102.
5. Mertz, H.J. and P. Prasad, *Improved Neck Injury Risk Curves for Tension and Extension Moment Measurements of Crash Dummies.* Stapp Car Crash Journal, 2000. **44**: p. 59-75.
6. Konrad, P., *The ABC of EMG*. April 2005, Noraxon, Inc.
7. DelSys, *EMGworks Signal Acquisition and Analysis Software*. 2003: Boston, MA.
8. Wittek, A., et al., *Analysis and comparison of reflex times and electromyograms of cervical muscles under impact loading using surface and fine-wire electrodes.* IEEE Trans Biomed Eng, 2001. **48**(2): p. 143-53.
9. Jacobson, W.C., R.H. Gabel, and R.A. Brand, *Surface Vs. Fine-wire Electrode Ensemble-averaged Signals During Gait.* J Electromyogr and Kinesiol, 1995. **5**(1): p. 37-44.
10. Oberg, T., L. Sandsjo, and R. Kadefors, *Arm movement and EMG mean power frequency in the trapezius muscle: a comparison between surface and intramuscular recording techniques.* Electromyogr Clin Neurophysiol, 1992. **32**(1-2): p. 87-96.
11. Pease, W.S. and M.A. Elinski, *Surface and wire electromyographic. Recording during fatiguing exercise.* Electromyogr Clin Neurophysiol, 2003. **43**(5): p. 267-71.
12. Giroux, B. and M. Lamontagne, *Comparisons between surface electrodes and intramuscular wire electrodes in isometric and dynamic conditions.* Electromyogr Clin Neurophysiol, 1990. **30**(7): p. 397-405.
13. Enoka, R.M. and D.G. Stuart, *Neurobiology of muscle fatigue.* J Appl Physiol, 1992. **72**(5): p. 1631-48.
14. DeLuca, C.J., *The Use of Surface Electromyography in Biomechanics.* J Appl Biomech, 1997. **13**(2): p. 135-163.
15. Kleine, B.U., et al., *Surface EMG mapping of the human trapezius muscle: the topography of monopolar and bipolar surface EMG amplitude and spectrum parameters at varied forces and in fatigue.* Clin Neurophysiol, 2000. **111**(4): p. 686-93.
16. Hodgdon, J.A., et al., *Neck and Back Strain Profiles of Rotary-Wing Female Pilots*, in *Final Report for the U.S. Army Medical Research and Materiel Command*. 1997.
17. Phillips, C.A. and J.S. Petrofsky, *Quantitative electromyography: response of the neck muscles to conventional helmet loading.* Aviat Space Environ Med, 1983. **54**(5): p. 452-7.
18. Phillips, C.A. and J.S. Petrofsky, *Neck muscle loading and fatigue: systematic variation of headgear weight and center-of-gravity.* Aviat Space Environ Med, 1983. **54**(10): p. 901-5.
19. Falla, D., et al., *Myoelectric manifestations of sternocleidomastoid and anterior scalene muscle fatigue in chronic neck pain patients.* Clin Neurophysiol, 2003. **114**(3): p. 488-95.

20. Hamalainen, O. and H. Vanharanta, *Effect of Gz forces and head movements on cervical erector spinae muscle strain.* Aviat Space Environ Med, 1992. **63**(8): p. 709-16.
21. Getschow, K.R., et al., *Assessment of Neck Muscle Biodynamics during Impact*. 1993, AL/CF-SR-1995-0016.
22. Pellettiere, J.A., M.A. Sander, and E.J. Doczy. *Neck Muscle Activation Levels during Frontal Impacts*. in *42nd Annual SAFE Symposium*. 2004.
23. Drake, J.D. and J.P. Callaghan. *Elimination of ECG Contamination from EMG Signals: an Evaluation of Currently Used Removal Techniques*. in *ISB XXth Congress - ASB 29th Annual Meeting*. 2005. Cleveland, OH.
24. Hermens, H.J., et al., *Development of recommendations for SEMG sensors and sensor placement procedures.* J Electromyogr Kinesiol, 2000. **10**(5): p. 361-74.
25. Merletti, R. and L.R. Lo Conte, *Surface EMG signal processing during isometric contractions.* J Electromyogr Kinesiol, 1997. **7**(4): p. 241-250.
26. Dox, I.G., B.J. Melloni, and G.M. Eisner, *The Harper Collins Illustrated Medical Dictionary*. 1993, New York: HarperPerennial.
27. Nederhand, M.J., et al., *Chronic neck pain disability due to an acute whiplash injury.* Pain, 2003. **102**(1-2): p. 63-71.
28. Butler, B.P., *Helmeted Head and Neck Dynamics Under Whole-Body Vibrations*. 1992, The University of Michigan.
29. *Standard Practice for Conducting an Interlaboratory Study to Determine the Precision of a Test Method.* E 691-92. 1992, Philadelphia, PH: American Society for Testing and Materials.
30. Buhrman, J.R. and S.E. Mosher. *A Comparison of Male and Female Acceleration Responses During Laboratory +Gz Impact Tests*. in *37th Annual SAFE Symposium*. 1999.

APPENDIX A: EMG SUMMARY PLOTS

Cells A, B and C (Bracing):

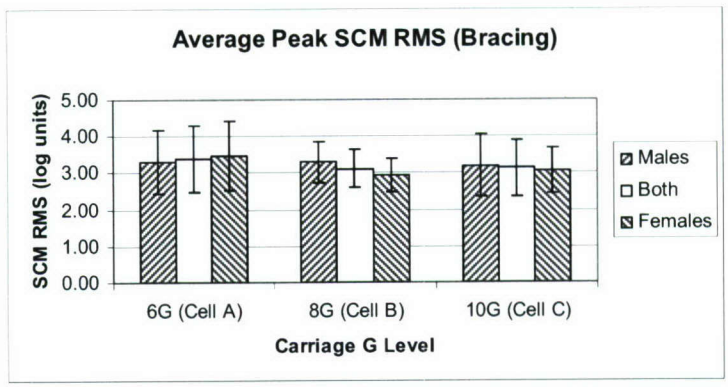

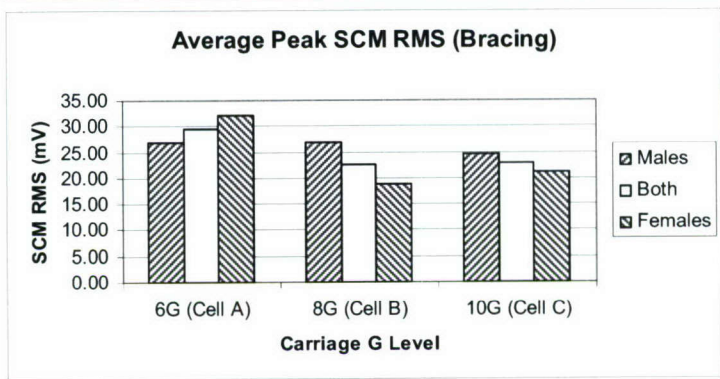

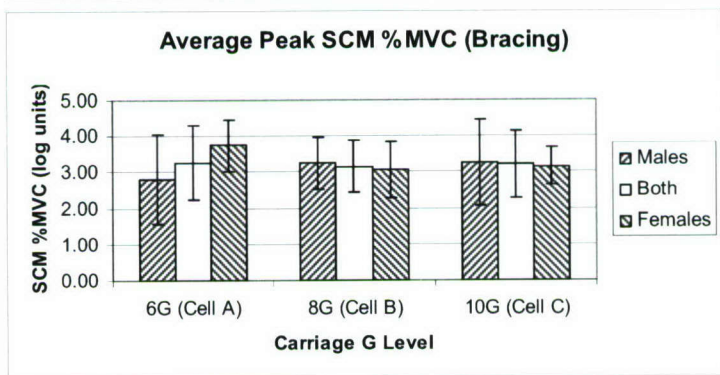

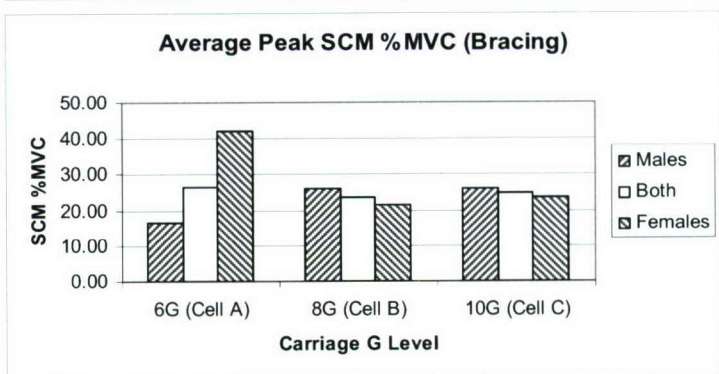

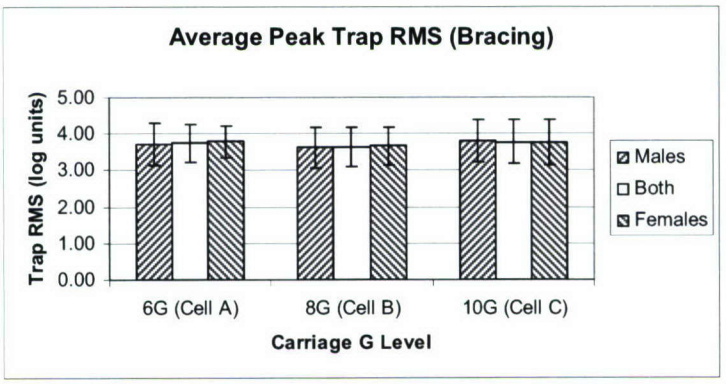
Average Peak Trap RMS (Bracing)
Trap RMS (log units)
5.00
4.00
3.00
2.00
1.00
0.00
6G (Cell A)
8G (Cell B)
10G (Cell C)
Carriage G Level
Males
Both
Females

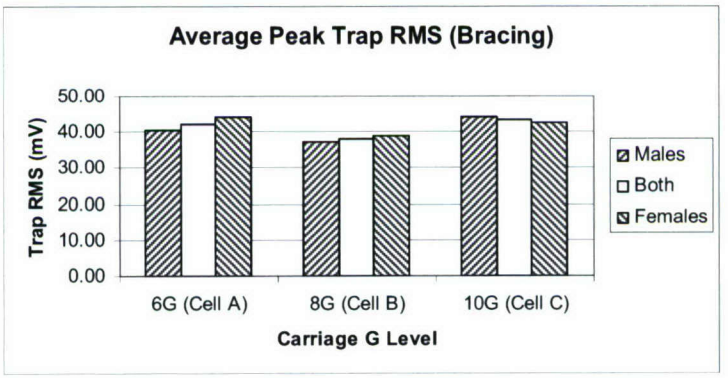
Average Peak Trap RMS (Bracing)
Trap RMS (mV)
50.00
40.00
30.00
20.00
10.00
0.00
6G (Cell A)
8G (Cell B)
10G (Cell C)
Carriage G Level
Males
Both
Females

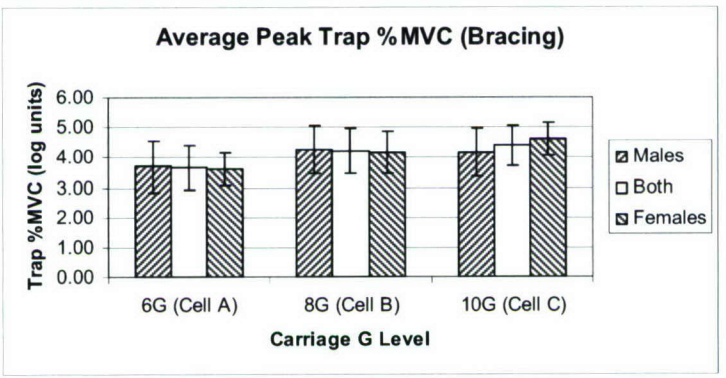
Average Peak Trap %MVC (Bracing)
Trap %MVC (log units)
6.00
5.00
4.00
3.00
2.00
1.00
0.00
6G (Cell A)
8G (Cell B)
10G (Cell C)
Carriage G Level
Males
Both
Females

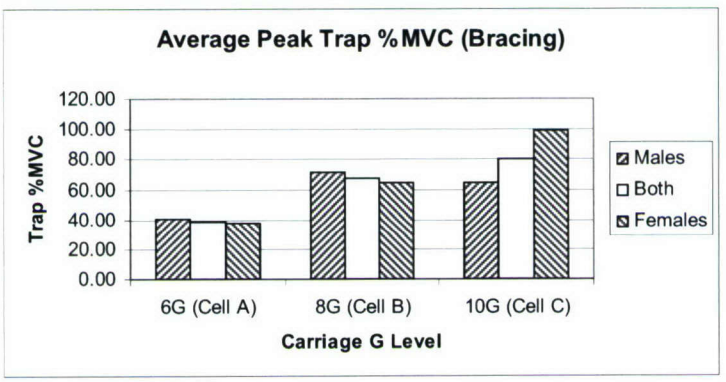
Average Peak Trap %MVC (Bracing)
Trap %MVC
120.00
100.00
80.00
60.00
40.00
20.00
0.00
6G (Cell A)
8G (Cell B)
10G (Cell C)
Carriage G Level
Males
Both
Females

Cells A, B and C (Impact):

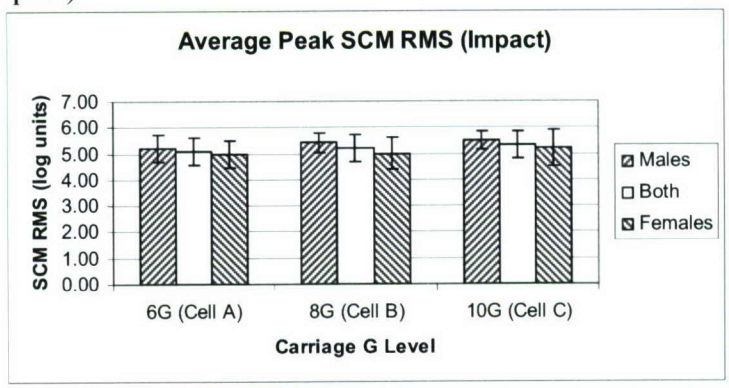

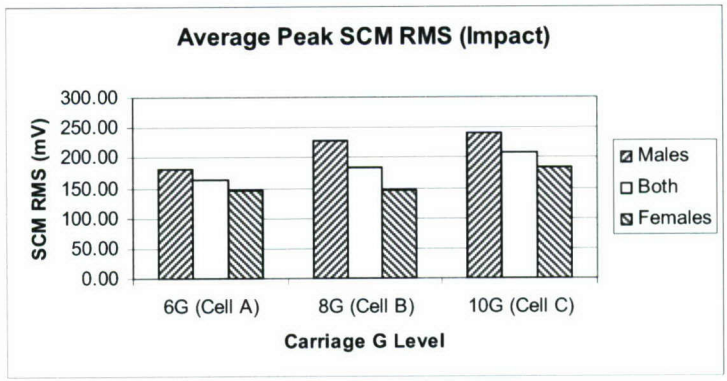

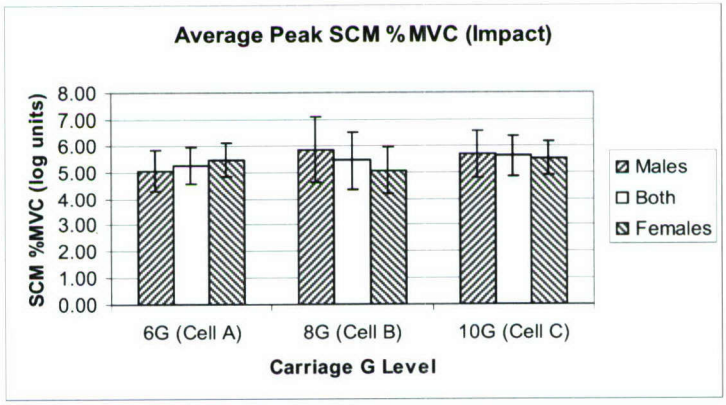

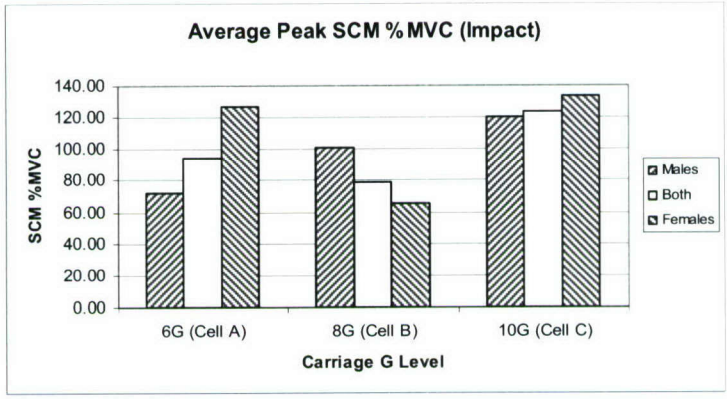

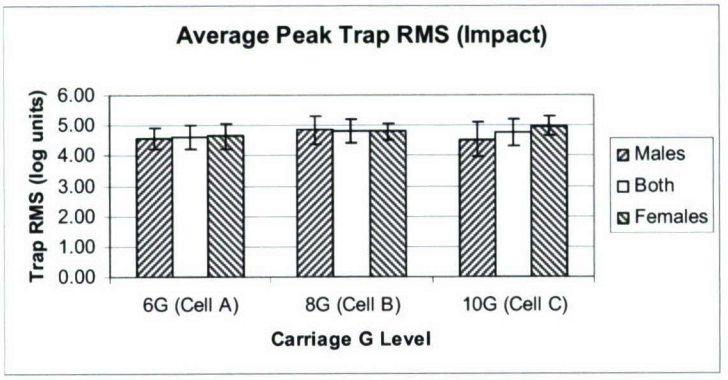
Average Peak Trap RMS (Impact)
Trap RMS (log units)
6.00
5.00
4.00
3.00
2.00
1.00
0.00
6G (Cell A)
8G (Cell B)
10G (Cell C)
Carriage G Level
Males
Both
Females

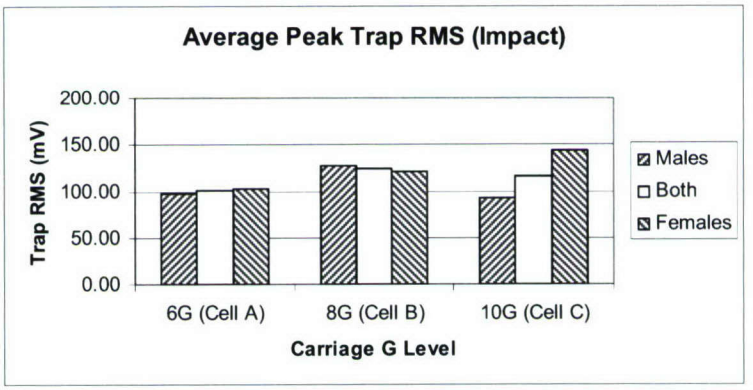
Average Peak Trap RMS (Impact)
Trap RMS (mV)
200.00
150.00
100.00
50.00
0.00
6G (Cell A)
8G (Cell B)
10G (Cell C)
Carriage G Level
Males
Both
Females

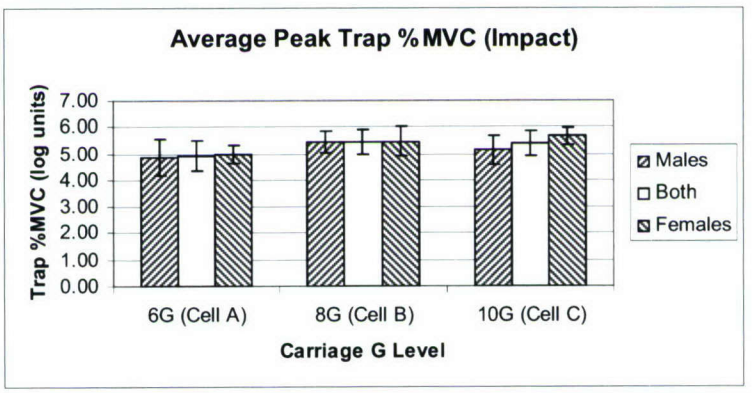
Average Peak Trap %MVC (Impact)
Trap %MVC (log units)
7.00
6.00
5.00
4.00
3.00
2.00
1.00
0.00
6G (Cell A)
8G (Cell B)
10G (Cell C)
Carriage G Level
Males
Both
Females

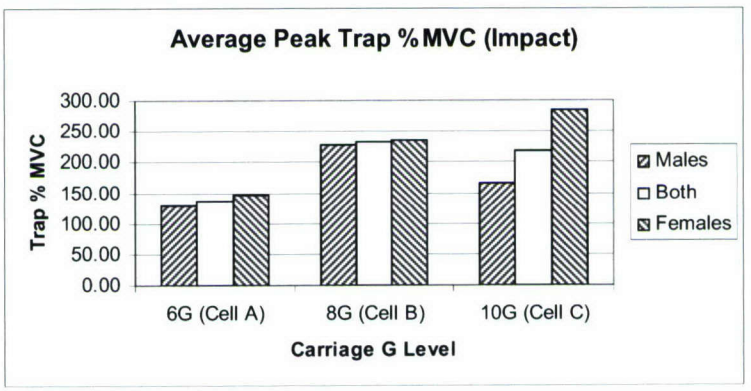
Average Peak Trap %MVC (Impact)
Trap % MVC
300.00
250.00
200.00
150.00
100.00
50.00
0.00
6G (Cell A)
8G (Cell B)
10G (Cell C)
Carriage G Level
Males
Both
Females

Cell C, D and E, 5-subject evaluation (bracing):

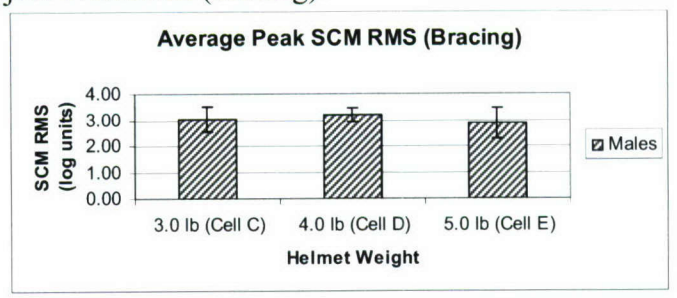

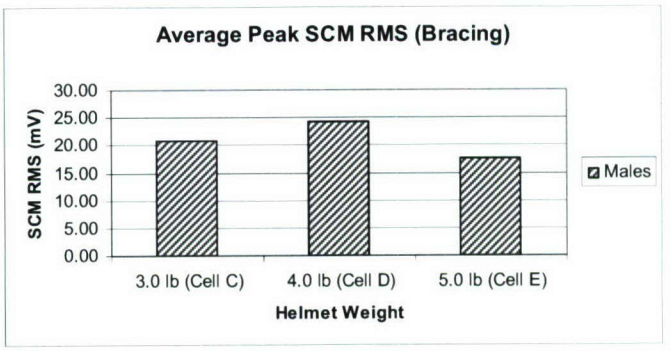

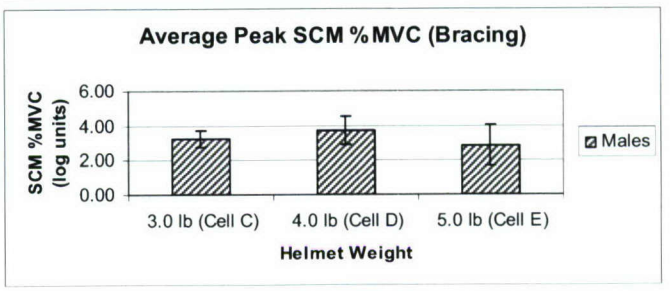

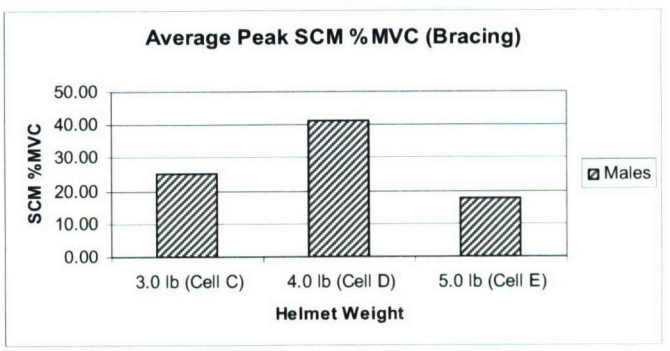

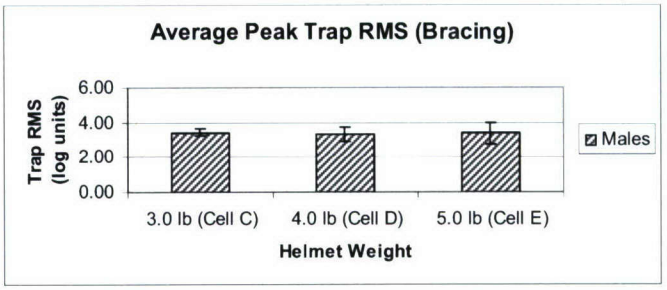
Average Peak Trap RMS (Bracing)
Trap RMS (log units)
6.00
4.00
2.00
0.00
3.0 lb (Cell C)
4.0 lb (Cell D)
5.0 lb (Cell E)
Helmet Weight
Males

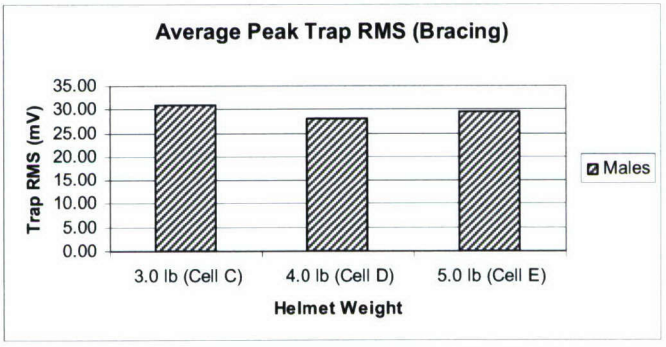
Average Peak Trap RMS (Bracing)
Trap RMS (mV)
35.00
30.00
25.00
20.00
15.00
10.00
5.00
0.00
3.0 lb (Cell C)
4.0 lb (Cell D)
5.0 lb (Cell E)
Helmet Weight
Males

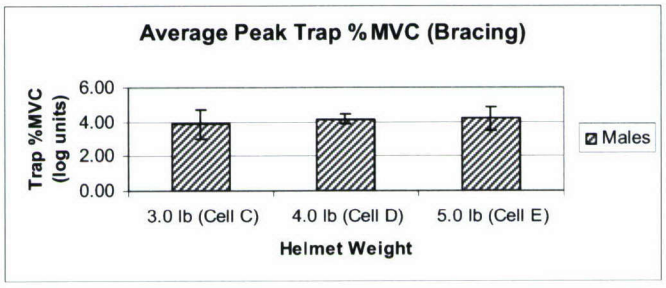
Average Peak Trap %MVC (Bracing)
Trap %MVC (log units)
6.00
4.00
2.00
0.00
3.0 lb (Cell C)
4.0 lb (Cell D)
5.0 lb (Cell E)
Helmet Weight
Males

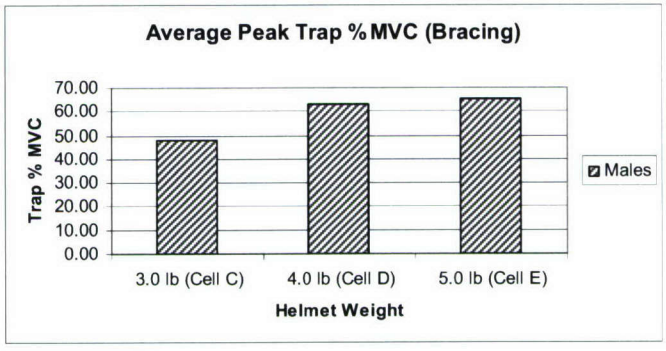
Average Peak Trap %MVC (Bracing)
Trap % MVC
70.00
60.00
50.00
40.00
30.00
20.00
10.00
0.00
3.0 lb (Cell C)
4.0 lb (Cell D)
5.0 lb (Cell E)
Helmet Weight
Males

Cell C, D and E, 5-subject evaluation (impact):

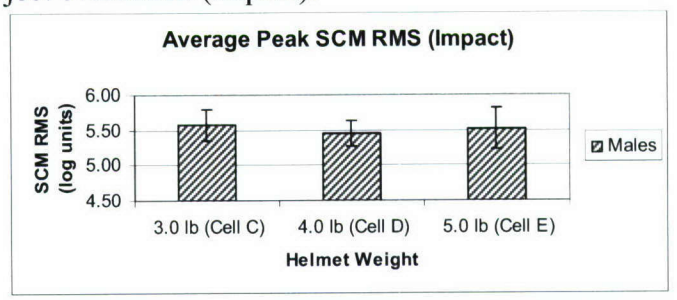

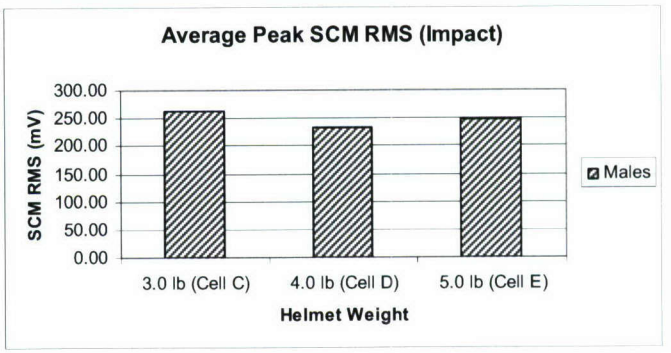

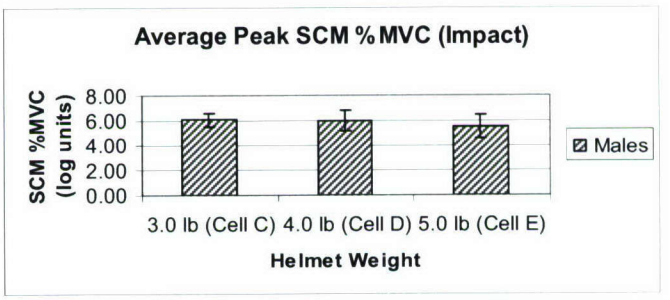

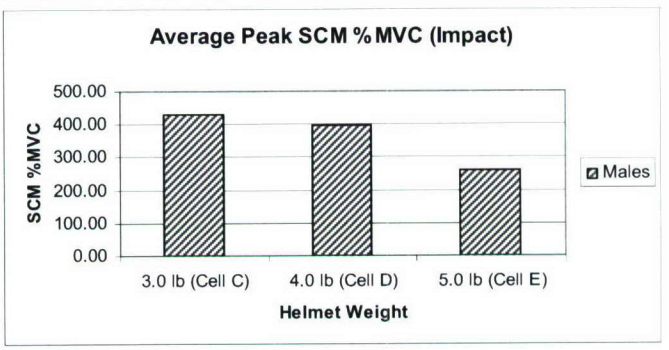

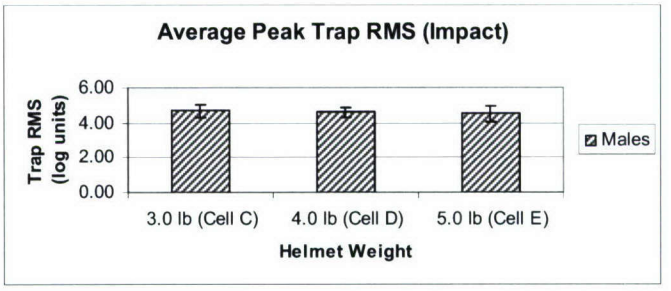
Average Peak Trap RMS (Impact)
Trap RMS (log units)
6.00
4.00
2.00
0.00
3.0 lb (Cell C)
4.0 lb (Cell D)
5.0 lb (Cell E)
Helmet Weight
Males

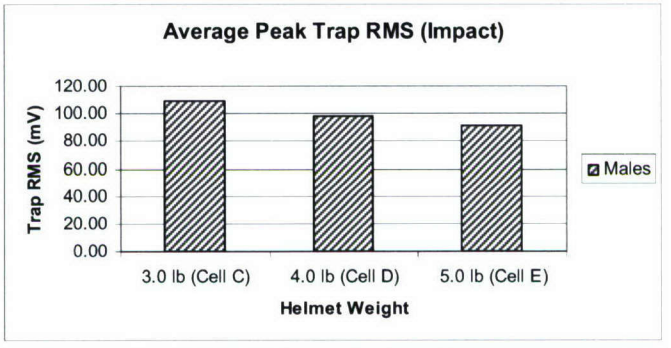
Average Peak Trap RMS (Impact)
Trap RMS (mV)
120.00
100.00
80.00
60.00
40.00
20.00
0.00
3.0 lb (Cell C)
4.0 lb (Cell D)
5.0 lb (Cell E)
Helmet Weight
Males

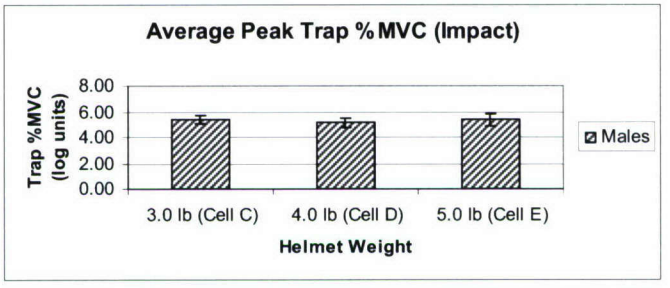
Average Peak Trap %MVC (Impact)
Trap %MVC (log units)
8.00
6.00
4.00
2.00
0.00
3.0 lb (Cell C)
4.0 lb (Cell D)
5.0 lb (Cell E)
Helmet Weight
Males

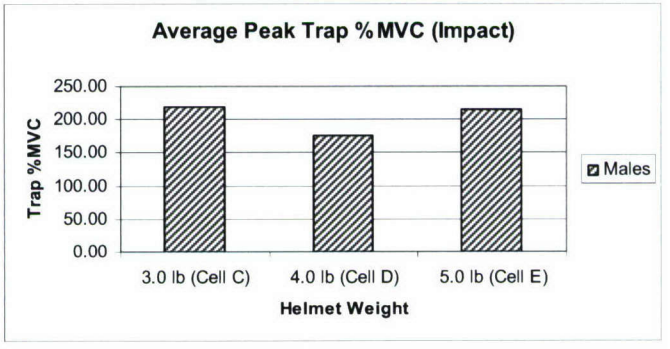
Average Peak Trap %MVC (Impact)
Trap %MVC
250.00
200.00
150.00
100.00
50.00
0.00
3.0 lb (Cell C)
4.0 lb (Cell D)
5.0 lb (Cell E)
Helmet Weight
Males

Cell C, D and E, 11-subject evaluation (bracing):

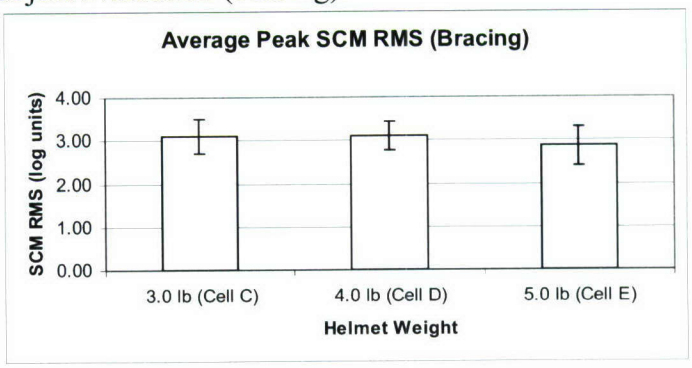

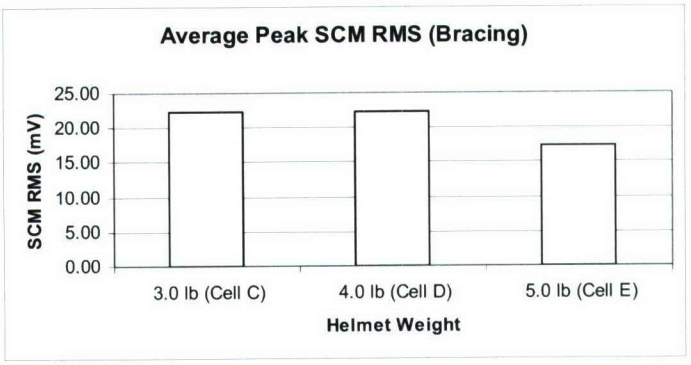

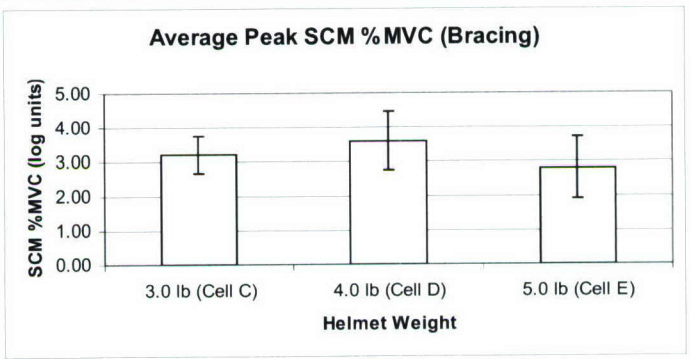

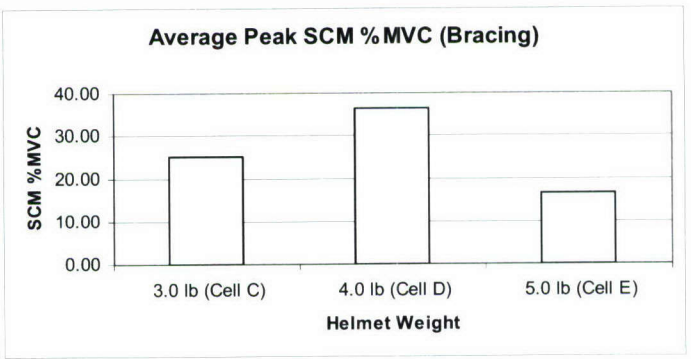

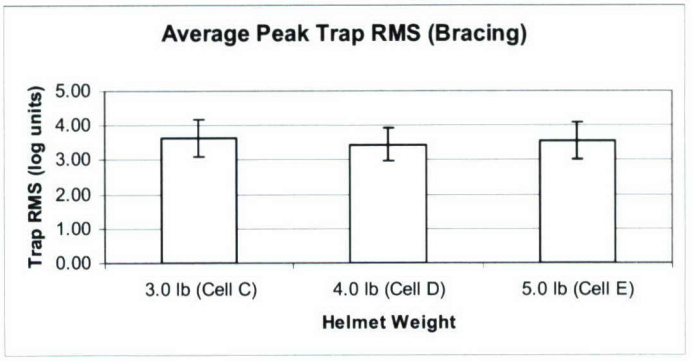
Average Peak Trap RMS (Bracing)
Trap RMS (log units)
5.00
4.00
3.00
2.00
1.00
0.00
3.0 lb (Cell C)
4.0 lb (Cell D)
5.0 lb (Cell E)
Helmet Weight

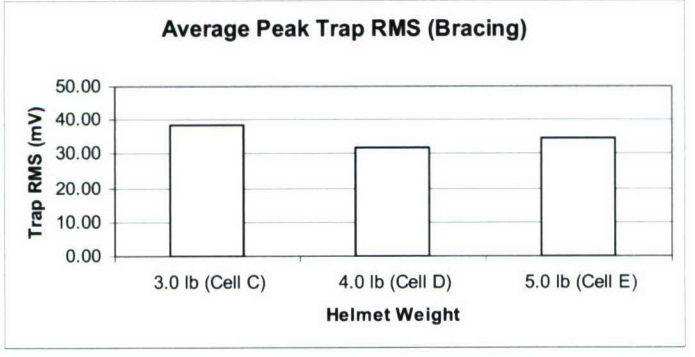
Average Peak Trap RMS (Bracing)
Trap RMS (mV)
50.00
40.00
30.00
20.00
10.00
0.00
3.0 lb (Cell C)
4.0 lb (Cell D)
5.0 lb (Cell E)
Helmet Weight

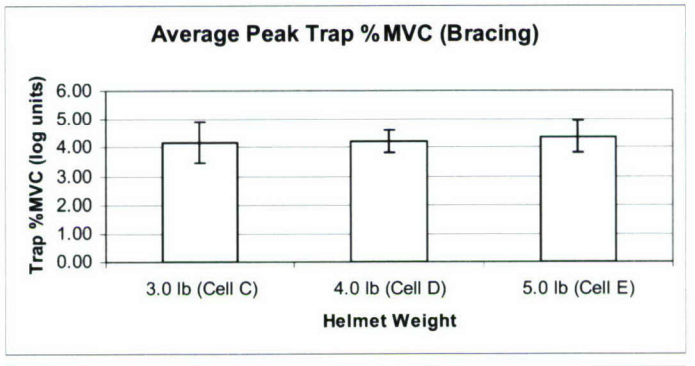
Average Peak Trap %MVC (Bracing)
Trap %MVC (log units)
6.00
5.00
4.00
3.00
2.00
1.00
0.00
3.0 lb (Cell C)
4.0 lb (Cell D)
5.0 lb (Cell E)
Helmet Weight

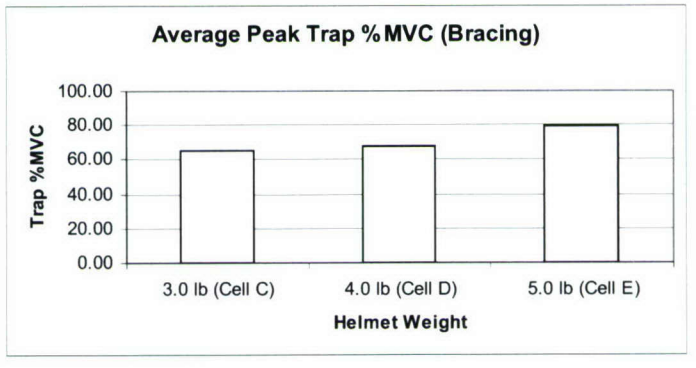
Average Peak Trap %MVC (Bracing)
Trap %MVC
100.00
80.00
60.00
40.00
20.00
0.00
3.0 lb (Cell C)
4.0 lb (Cell D)
5.0 lb (Cell E)
Helmet Weight

Cell C, D and E, 11-subject evaluation (impact):

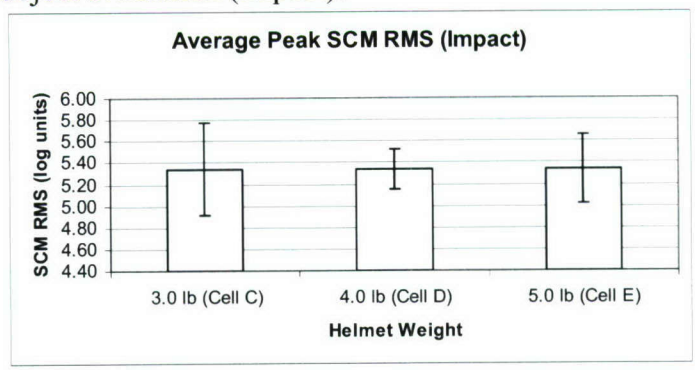

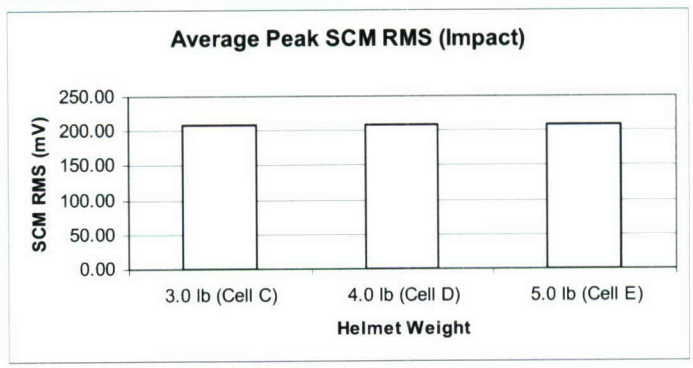

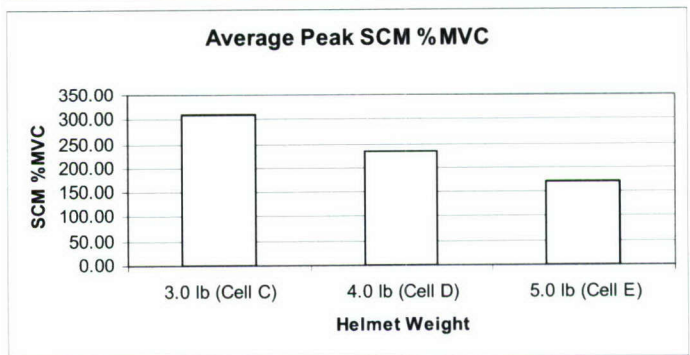

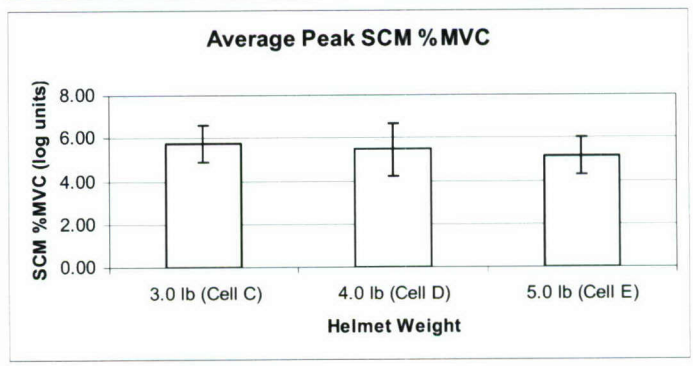

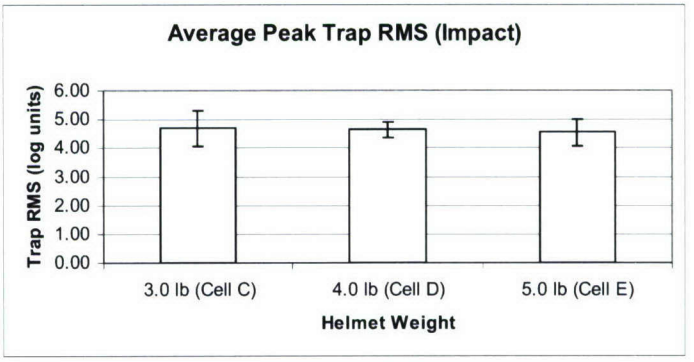
Average Peak Trap RMS (Impact)
Trap RMS (log units)
6.00
5.00
4.00
3.00
2.00
1.00
0.00
3.0 lb (Cell C)
4.0 lb (Cell D)
5.0 lb (Cell E)
Helmet Weight

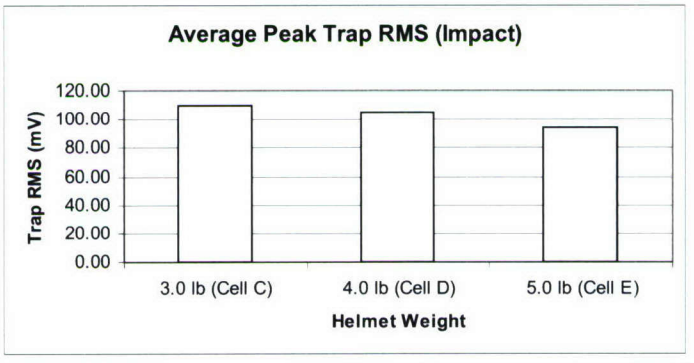
Average Peak Trap RMS (Impact)
Trap RMS (mV)
120.00
100.00
80.00
60.00
40.00
20.00
0.00
3.0 lb (Cell C)
4.0 lb (Cell D)
5.0 lb (Cell E)
Helmet Weight

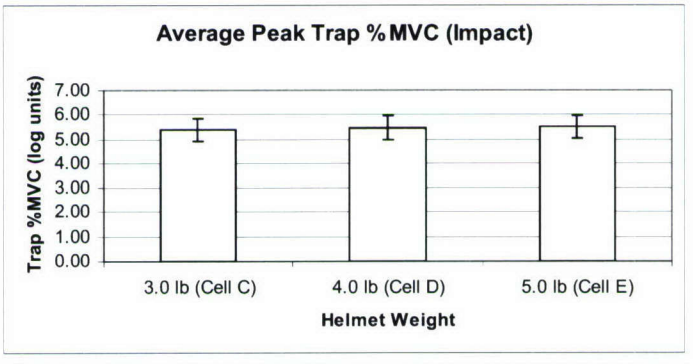
Average Peak Trap %MVC (Impact)
Trap %MVC (log units)
7.00
6.00
5.00
4.00
3.00
2.00
1.00
0.00
3.0 lb (Cell C)
4.0 lb (Cell D)
5.0 lb (Cell E)
Helmet Weight

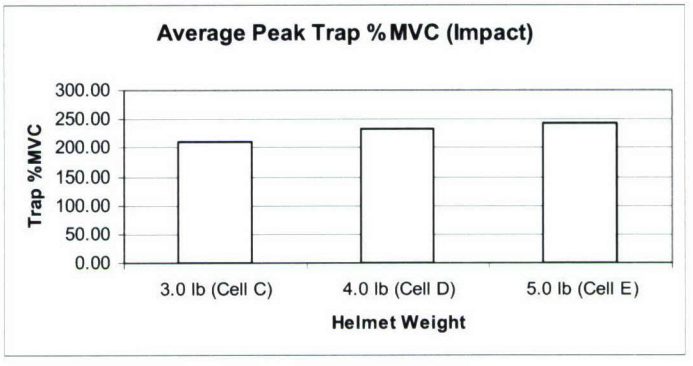
Average Peak Trap %MVC (Impact)
Trap %MVC
300.00
250.00
200.00
150.00
100.00
50.00
0.00
3.0 lb (Cell C)
4.0 lb (Cell D)
5.0 lb (Cell E)
Helmet Weight

APPENDIX B: HELMET INERTIAL PROPERTIES OF THE VWI HELMET

Nominal Weight	Size	Weight (lbs)	CGX (in.)	CGY (in.)	CGZ (in.)	MOIX (lb-in.^{2})	MOIY (lb-in.^{2})	MOIZ (lb-in.^{2})
3.0 lbs	**Medium**	2.80	-0.16	0.02	1.74	44.45	40.25	48.98
	Large	2.91	0.11	0.02	1.17	47.55	42.39	53.97
	X-Large	2.98	0.32	0.23	1.00	49.71	47.49	55.89
4.0 lbs	**Medium**	3.81	1.51	0.03	1.95	48.07	69.58	80.13
	Large	3.90	1.71	-0.03	1.52	52.08	74.67	84.08
	X-Large	3.99	1.93	0.30	1.44	53.97	79.60	90.82
5.0 lbs	**Medium**	4.81	2.46	0.10	1.69	66.76	75.87	104.21
	Large	4.87	2.57	0.12	1.59	73.68	77.37	108.74
	X-Large	4.96	2.51	0.00	1.64	73.62	84.69	113.33

Inertial properties measured with the following: Zeta Liner, MBU-12/P mask cut away, halo, and standard ear cups.

APPENDIX C: GENERAL DYNAMICS FACILTY REPORT

GENERAL DYNAMICS

Advanced Information Systems

NECK MUSCLE STRENGTH AND SUBJECT REPRODUCIBILITY DURING VERTICAL ACCELERATION WITH A VARIABLE WEIGHTED HELMET

Study Number 200403

Prepared under Contract FA8650-04-D-6472

OCTOBER 2005

Advanced Information Engineering Services
A General Dynamics Company
5200 Springfield Pike, Suite 200
Dayton, OH 45431

TABLE OF CONTENTS

LIST OF FIGURES

LIST OF TABLES

Test Report

Neck Muscle Strength and Subject Reproducibility during Vertical Impact Acceleration with a Variable Weighted Helmet (GzEMG)

Vertical Deceleration Tower (VDT) Tests

Introduction

General Dynamics has prepared this report for the Air Force Research Laboratory, Human Effectiveness Directorate, Biomechanics Branch under Air Force contract FA8650-04-D-6472. It describes the test facility, test configurations, data acquisition and analysis, and instrumentation procedures used for the Neck Muscle Strength and Subject Reproducibility during Vertical Acceleration with a Variable Weighted Helmet (GzEMG) Study (Study 200403). A series of impact tests were performed on the Vertical Deceleration Tower (VDT) located in Bldg 824 at Wright-Patterson AFB.

Test Facility

Vertical Deceleration Tower

The AFRL/HEPA VDT (Figure 1) was used for all of the tests. The facility consists of a 60-foot vertical steel tower with a dual guide rail system, an impact carriage and attached plunger, a hydraulic deceleration device, and a test control and safety system. The impact carriage can be raised to a maximum height of 39 feet prior to release. After release, the carriage free-falls until the plunger, attached to the undercarriage, enters a water-filled cylinder mounted at the base of the tower. The subject experiences a deceleration impulse as the plunger displaces water in the cylinder. The deceleration profile is determined by the free-fall distance, the carriage and occupant mass, the shape of the plunger, and the size of the water cylinder orifice. A rubber bumper is used to absorb the final impact as the carriage stops.

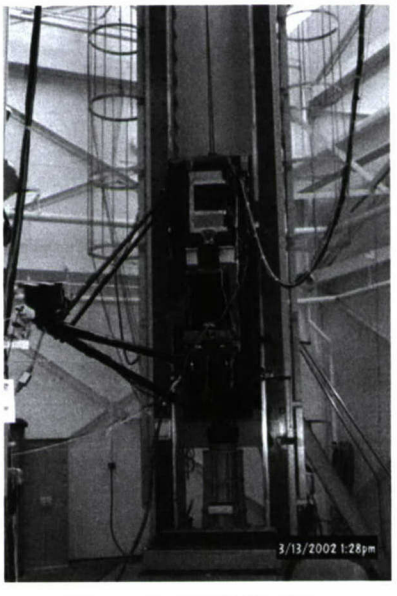

Figure 1. VDT Facility

For these tests, plunger #102 was mounted under the carriage. The drop height was adjusted to provide the desired input pulse. The nominal drop height for the 10G tests was 11 feet 7 inches. A total of 292 tests were completed on the VDT from 7 Jul 2004 to 29 Aug 2005. The 292 tests consisted of 143 human tests (91 male tests and 52 female tests) and 149 manikin tests. Before the human phase of this program began, 43 manikin tests were completed with an instrumented Large ADAM manikin (216 lbs). During the human phase of testing, the first test of each day was done with a Hybrid III 95th percentile automotive manikin (229 lbs.). This manikin test was done at that day's scheduled highest acceleration level and with the heaviest weighted helmet scheduled for that day. Other equipment and program documentation information is found in Table 1.

Table 1. Program Documentation Information

Equipment	ID
Facility	VDT
Pin Number	102
Seat Fixture	Modified ACES II F-16
Seat Cushions	ACES II - Oregon Aero
Harness	PCU-15/P or PCU-16/P
Helmet	Lightweight HGU-55/P – VWI, Integrated Chin Nape Strap (ICNS)
Inertia Reel	PSI straps
Lap Belt	Modified ACES II
Oxygen Mask	MBU-12/P – cut away
Headrest Positic	Vertical In-Line
Seat Pan Positic	Horizontal
Seat Back Positi	Vertical

Test Fixtures

Seat: A unique seat fixture was fabricated for the GzEMG study (Figure 2). The fixture was developed to incorporate the geometry of an F-16 ACES II ejection seat. The ACES II seat back was removed from the seat and mounted to the VDT carriage with the seat back tangent plane vertical. The ACES II seat pan was mounted to a horizontal surface of the VDT carriage. The seat pan was perpendicular to the seat back tangent plane. A contoured headrest was used for all tests, mounted parallel with the seat back plane.

Harness: The subjects were restrained to the seat using a PCU-15/P or PCU-16/P restraint harness. Prior to 28 October 2004, the parachute risers with standard inertia reel loops were secured to the subject's harness via standard Koch fittings. The inertia reel straps were routed through the inertia reel strap's hole (just below the headrest), secured to a single adjustable-length strap, around a pulley, and attached to a load cell mounted on the carriage. The two shoulder straps were tightened simultaneously by pulling on the single adjustable-length strap (Figure 3). Beginning 28 October 2004 the restraint system changed the harness configuration to incorporate two shoulder straps that were tightened separately. Each shoulder strap was attached to its own load cell. These modified, adjustable-length parachute riser straps went directly from the Koch fittings to the carriage-mounted load cells, as seen in Figure 4.

The modified ACES II lap belt consisted of east/west lap belt adjuster units mounted on each belt. Each belt (left and right) was attached to a tri-axial force load cell. These load cells were located on separate brackets mounted on the side of the seat frame on each side of the seat pan (Figure 5).

The pre-tension level of the restraint system (lap and shoulder belts) was 20 ± 5 lbs. Velcro ankle restraints were applied to limit ankle/leg flail, and Velcro straps were looped around the thighs to serve as handles to hold onto during human testing.

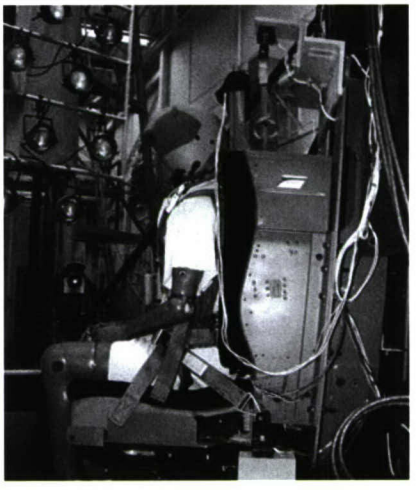

Figure 2. GzEMG ACES II Seat Fixture

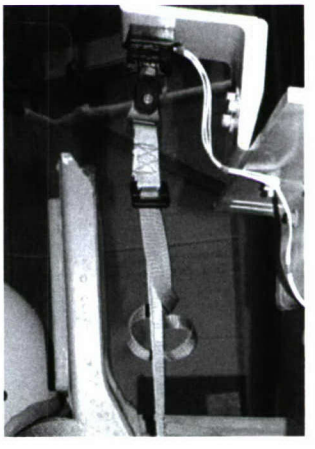

Figure 3. Shoulder Strap Configuration Prior to 28 October 2004

Figure 4. Shoulder Strap Configuration after 28 October 2004

Helmet: The variable weight impact (VWI) helmet consisted of a modified HGU-55/P flight helmet with additional weights placed on a "halo" that extended from the sides and front of the helmet. The weights were placed symmetrically about the sagittal plane of the helmet to maintain symmetry. Subjects were fitted with a medium, large or extra large helmet depending on their head length and breadth dimensions (Table 2). The center of gravity (CG) of the helmet with added mass was altered by adding these weights at specific locations to closely represent the weight and CG of current ANVIS F49/49 Night Vision Goggles (NVG) (4-lb configuration), and IPNVG (5-lb configuration). A modified MBU-12/P oxygen mask (cut away to allow for bite-bar instrumentation clearance) was used in conjunction with the helmet (Figure 6).

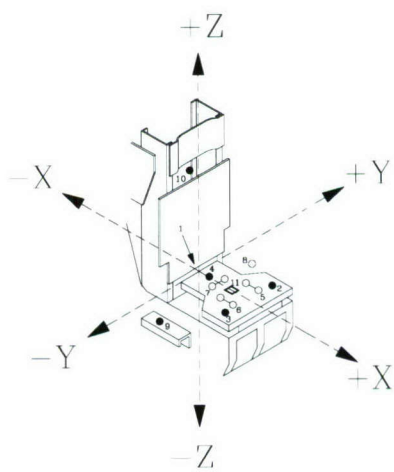

Figure 5. Coordinate System

Table 2. Sizing for the HGU-55/P

Head Length (cm)	Head Breadth (cm)	Helmet Size
18.3 – 19.8	Max = 15.7	Medium
19.5 - 21.0	Max = 16.5	Large
20.8 – 22.1	Max = 17.3	X-Large

Test Matrix

The subjects were exposed to a combination of varying helmet weights and +Gz impact levels (Table 3). The acceleration waveform for the VDT was an approximate half-sine wave with a peak of 6, 8, or 10 G and a time to peak of approximately 85 msec. Several parameter verification tests were completed prior to collection of human data. The subjects were tested in the seated posture.

Table 3. Test Matrix

	Total Head-Supported Weight		
Impact Level	3.0 lbs	4.0 lbs	5.0 lbs
6G	A		
8G	B		
10G	C	D	E

Instrumentation

Accelerometers and load cells were chosen to provide the optimum resolution over the expected test load range. Full-scale data ranges were chosen to provide the expected full-scale range plus 50% to assure the capture of peak signals. All transducer bridges were balanced for optimum output prior to the start of the program. The accelerometers were adjusted for the effect of gravity in software by adding the component of a 1 G vector in line with the force of gravity that lies along the accelerometer axis.

The accelerometer and load cell coordinate systems are shown in Figure 5. The seat coordinate system is right-handed with the z-axis parallel to the seat back and positive upward. The x-axis is perpendicular to the z-axis and positive eyes forward from the subject. The y-axis is perpendicular to the x- and z-axes according to the right-hand rule.

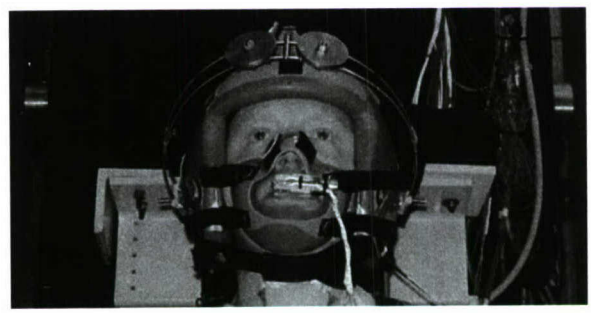

Figure 6. Variable Weight Impact (VWI) Helmet

For the transducer, fiducial, and camera location measurements listed in Table 4, the positive x-axis is defined as forward (from the subject's back to front). The positive z-axis is defined as upward (from the subject's feet to head). The positive y-axis is defined by the right-hand rule (to the subject's left). Measurements for the load cells were taken at the load contact point. Measurements for the belts were taken at the attachment point (interface between the belt and stationary load cell). The seat pan accelerometer was measured at the center of the attachment point to the mounting block. The origin of the coordinate system, or seat reference point (SRP), was measured at the midpoint of the lower edge of the bottom of the seat back. All vector components (for accelerations, angular accelerations, forces, moments, etc.) were positive when the vector component (x, y and z) was in the direction of the positive axis.

Table 4. Transducer, Fiducial, and Camera Location Measurements

Description	X (mm)	Y (mm)	Z (mm)
SRP	0.00	0.00	0.00
Shoulder	-23.85	-13.73	1002.72
Left Shoulder	-129.00	-170.00	690.25
Right Shoulder	-129.00	170.00	690.25
Left Lap	-24.80	242.79	-31.23
Right Lap	-20.15	-242.36	-43.93
Left Seat Pan X	206.35	149.96	-130.91
Right Seat Pan X	206.42	-152.86	-128.96
Seat Pan Y	85.82	47.81	-131.46
Left Seat Pan Z	307.42	124.64	-131.78
Right Seat Pan Z	308.52	-127.44	-128.86
Center Seat Pan Z	24.65	-1.41	-129.26
Seat Pan Accel ACES II Seat	210.39	31.00	-41.40
Upper Front Target	-134.36	-287.45	872.11
Upper Back Target	-438.70	-193.99	704.95
Lower Back Target	-441.85	-192.94	441.81
Lower Front Target	-120.80	-196.49	-26.48
Side Camera	255.12	-1509.54	280.09
Oblique Camera	1046.36	-1361.95	263.26

The linear accelerometers were wired to provide a positive output voltage when the acceleration experienced by the accelerometer was applied in the +x, +y and +z directions. The load cells and load links were wired to provide a positive output voltage when the force exerted by the load cell on the subject was applied in the +x, +y or +z direction. The angular Ry accelerometers were wired to provide a positive output voltage when the angular acceleration experienced by the angular accelerometer was applied in the +y direction according to the right-hand rule. The manikin lumbar load cells were wired to provide a positive output voltage when the force exerted by the load cell on the lumbar was applied in the +x, +y or +z direction. The manikin torque transducers were wired to provide a positive output voltage when the torque experienced by the transducer was applied in the +x, +y or +z direction. All transducers, except the carriage accelerometers were referenced to the seat coordinate system.

The seat pan accelerometer location was measured at the center of the attachment interface between the accelerometer block and accelerometer housing. The locations of the load cells that anchor the harness were measured at the point where the harness is attached to the load cell. The locations of the other loads cells were measured at the point on the load cell where the external force is applied.

Load Cell Transducers

Specific sensors are listed by channel in the Program Setup and Calibration Log (Table 5). The load parameters measured are indicated below:

Combined left and right shoulder x, y and z force (prior to 28 October 2004)
Left shoulder x, y and z force
Right shoulder belt x, y and z force
Seat pan x, y, and z force
Left lap belt x, y and z force
Right lap belt x, y and z force
Upper neck x, y and z force
Lumbar x, y and z force
Chin strap unidirectional force

The lap belt force tri-axial load cells were located on separate brackets mounted on the side of the seat frame on each side of the seat pan (Figure 7). Prior to 28 October 2004, the shoulder strap force tri-axial load cell was mounted to an angle bracket mounted behind the seat back and headrest (Figure 3). Post 28 October 2004, each shoulder strap was attached to its own tri-axial load cell (Figure 4). Left, right and center seat pan forces were measured using three load cells and three load links (Figures 8, 9). Strainsert Model FL2.5U-2SPKT load cells were used to measure seat pan loads. The three load links used Micro Measurement Model EA-06-062TJ-350 strain gages. All measurement devices were located under the seat pan support plate. The load links were used for measuring loads in the x and y directions, two in the x direction and one in the y direction. Each load link housed a swivel ball, which acted as a coupler between the seat pan and load cell mounting plate. The Strainsert load cells were used for measuring loads in the z direction.

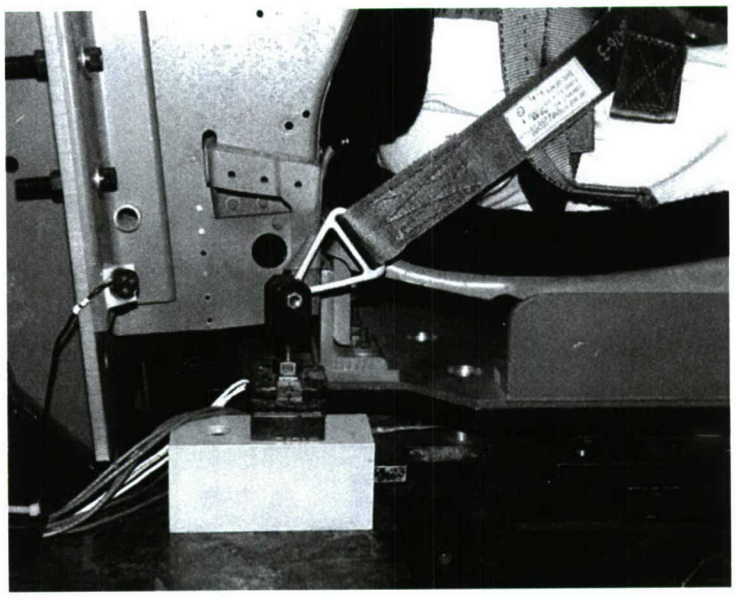

Figure 7. Lap Belt Load Cell

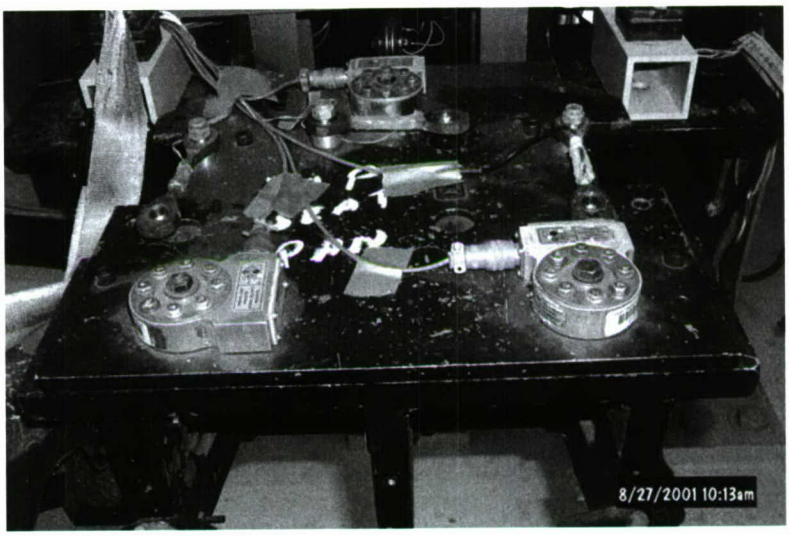

Figure 8. Seat Pan Load Cells and Load Links

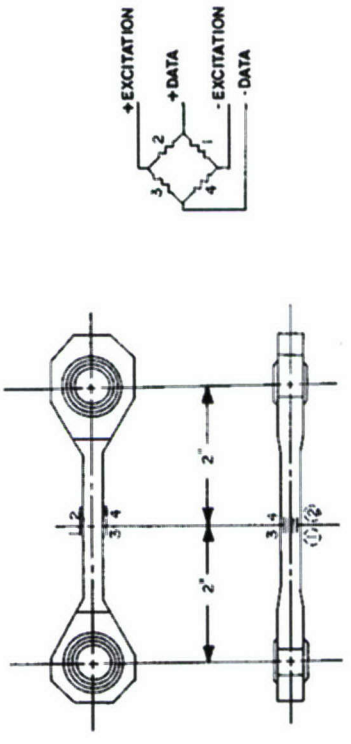

Figure 9. Load Links

Accelerometers

A bite block was fitted with three linear and one angular accelerometer that measured human subject head accelerations. One linear (z) accelerometer and one rate sensor (Ry) were also mounted on the humans' sternums. Manikin accelerometer packages included chest, head, sternum, and lumbar. They were arranged to measure linear acceleration of the chest, head, lumbar, and sternum in all three axes, and angular acceleration of the head and chest about all three axes. Angular rate was measured at the sternum.

A tri-axial accelerometer was mounted in a thin plastic disk and placed on top of the seat cushion for all tests. This accelerometer is commonly used in vibration studies, where it is referred to as a Ride Quality Meter (Figure 10). Carriage z acceleration was measured using one Endevco Model 2262A-200 linear accelerometer. The accelerometer was mounted on a small acrylic block and located behind the seat. An additional tri-axial accelerometer was used to measure acceleration at the seat pan. It was attached to an aluminum block and mounted on the seat pan just below the subject's spine (Figure 11).

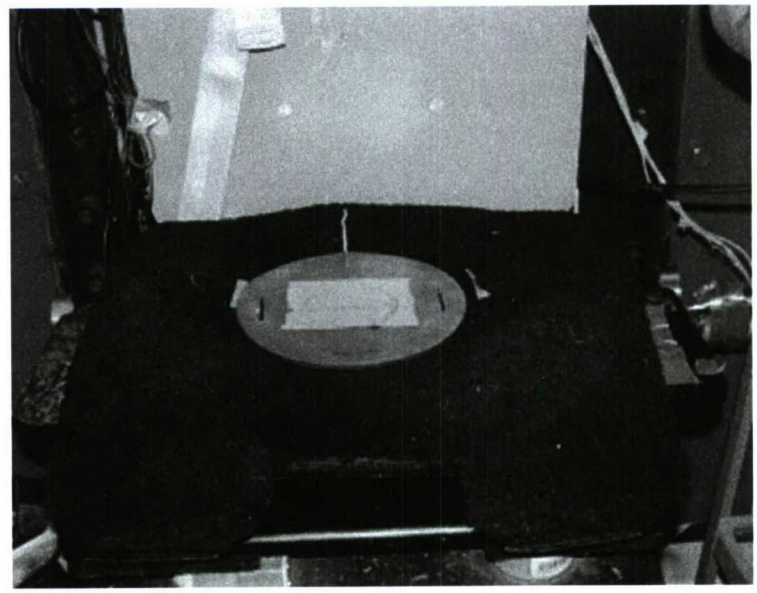

Figure 10. Ride Quality Meter

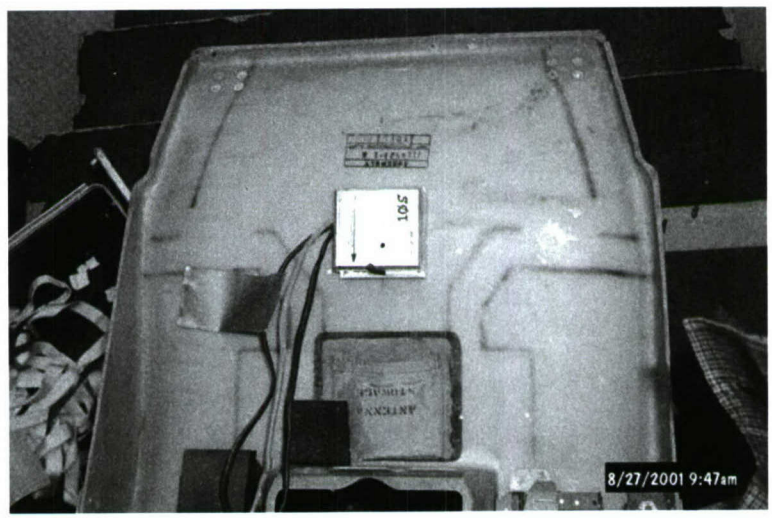

Figure 11. Seat Pan Accelerometer Block

The specific accelerometers used are listed by type and impact axis in the Program Setup and Calibration Logs. The logs also provide individual sensor serial numbers, model numbers, channel assignments and sensor sensitivities.

EMG Measurements

Electromyogram (EMG) measurements of the sternocleidomastoid and upper trapezius were recorded on the human subjects using a DelSys 8ch MyoMonitor (Figure 12). Four electrodes and one reference electrode were utilized to measure the two muscles of interest of both sides of the neck. The MyoMonitor Data Logger is based on a modified Jornada 720 Handheld Computer made by Hewlett Packard. After test number 4984 on 19 Oct 2004, the on-board TDAS was used to collected EMG data from the same DelSys sensors. The Delsys and TDAS

data acquisition systems had different sample rates; therefore, the number of points used for frequency and root mean square (RMS) calculations were adjusted to keep the time intervals consistent.

The DelSys acquisition system used a sample rate of 1024 Hz. The cutoff frequency was supplied by the 450 Hz filter built into the sensor. The DC offset was removed and the mean frequency was calculated using an FFT block size of 1024 points (1 second) with a 512-point overlap (0.5 second). No spectrum window was used. The RMS was calculated using a 64-point (0.0625 second) window. The TDAS sampled the EMG channels at 2000 Hz. The TDAS cutoff frequency was set at 500 Hz; however, the cutoff frequency of 450 Hz was still supplied by the EMG sensors' built-in filter. The DC offset was removed and the mean frequency was calculated using an FFT block size of 2000 points (1 second) with a 1000-point overlap (0.5 second). No spectrum window was used. The RMS was calculated using a 125-point (0.0625 second) window.

Figure 12. DelSys MyoMonitor

Transducer Calibration

Calibrations were performed before and after testing to confirm the accuracy and functional characteristics of the transducers. Pre-program and post-program calibrations are given in the Test Setup and Calibration Log. The Precision Measurement Equipment Laboratories (PMEL) at Wright-Patterson Air Force Base or General Dynamics personnel calibrated all Strainsert load cells.

The comparison method (Bouche, 1970) was used to calibrate the laboratory accelerometers. A laboratory standard accelerometer, calibrated on a yearly basis by Endevco with standards traceable to the National Bureau of Standards, and a test accelerometer were mounted on a shaker table. A random noise generator drove the shaker table and the accelerometer output was collected. The frequency response and phase shift of the test accelerometer were determined by using Fourier analysis on a PC. The natural frequency and the damping factor of the test accelerometer were determined, recorded and compared to previous calibration data for that test accelerometer. Sensitivities were calculated at 20 G and 100 Hertz. The sensitivity of the test accelerometer was determined by comparing its output to the output of the standard accelerometer.

General Dynamics calibrated the shoulder/lap tri-axial load cells and load links. These transducers were calibrated to a laboratory standard load cell in a special test fixture. The sensitivity and linearity of each test load cell were obtained by comparing the output of the test load cell to the output of the laboratory standard under identical loading conditions. The laboratory standard load cell is calibrated by PMEL on a regular basis.

The angular accelerometers are calibrated on a pre- and post-study basis by comparing their output to the output of two linear accelerometers. The angular sensors are mounted parallel to the axis of rotation of a Honeywell low inertia DC motor. The linear sensor is mounted perpendicular to the axis of rotation. An alternating current is supplied to the motor, which drives a constant sinusoidal angular acceleration of 100 Hz. The sensitivity of the angular accelerometer is calculated from the RMS output voltage to match the angular value computed from the linear standard.

Data Acquisition

The Master Instrumentation Control Unit in the Instrumentation Station controlled the data acquisition. Using a comparator, a test was initiated when the countdown clock reached zero. The comparator was set to start data collection at a pre-selected time. All data were collected at 1,000 samples per second and filtered at a 120 Hz cutoff frequency using an 8-pole Butterworth filter.

Prior to placing the manikin or human subject in the seat, data were recorded to establish a zero reference for all transducers. The reference data were stored separately from the test data and were used in the processing of the test data. A reference mark pulse was generated to mark the electronic data at a pre-selected time after test initiation to place the reference mark close to the impact point. The reference mark time was used as the start time for data processing of the electronic data.

TDAS PRO Data Acquisition System

The TDAS PRO Data Acquisition System (DAS), manufactured by Diversified Technical Systems (DTS), Inc., was used for this test program. The TDAS PRO is a ruggedized, DC powered, fully programmable signal conditioning and recording system for transducers and events. The TDAS PRO was designed to withstand a 100 G shock. The main unit was installed on top of the seat carriage as shown in Figure 13.

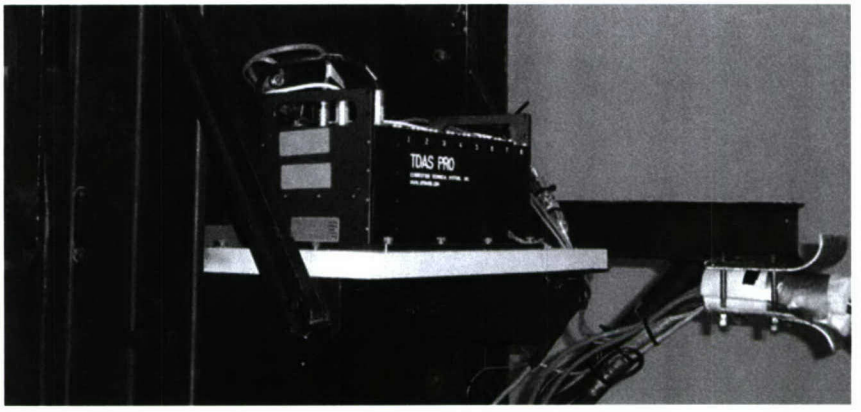

Figure 13. TDAS PRO

The TDAS PRO can accommodate up to 64 channels. The signal conditioning accepts a variety of transducers including full and partial bridges, voltage, and piezoresistive. Transducer signals are amplified, filtered, digitized and recorded in onboard solid-state memory.

The data acquisition system is controlled through an Ethernet interface using the Ethernet instruction language.

A desktop PC with an Ethernet board configures the TDAS PRO before testing and retrieves the data after each test. The PC stores the raw data and then passes it on to the RHEPFS001 computer for processing and output to permanent storage and printouts.

The DTS TDAS PRO program 'DTS_TDAS_PRO.EXE' on the PC controls the interface with the DAS. It includes options to compute and store zero reference voltage values; collect and store a binary zero reference data file; compute and display pre-load values; and collect and store binary test data. The program communicates over the GPIB interface.

Test data could be reviewed after conversion to digital format using the "quick look" SCAN_EME routine on the PC. SCAN_EME produced a plot of the data stored for each channel as a function of time. The routine determined the minimum and maximum values of each data plot. It also calculated the rise time, pulse duration, and carriage acceleration, and created a disk file containing significant test parameters.

Weinberger High-Speed Video

Two carriage-mounted Weinberger SpeedCam Visario cameras (Figure 14) were used to collect video and target motion data. One camera was mounted directly to the side of the carriage, while the other was mounted at an oblique angle to the carriage. The SpeedCam system is capable of data acquisition at up to 10,000 frames per second. The SpeedCam system is controlled via software specifically designed for Windows2000. The Control Unit allows for simultaneous operation of multiple cameras and controls the entire data management from system control, post processing and visualization to archiving of the completed image sequences.

The interface between cameras and the Control Unit occurs via LocalLinks. LocalLinks are system-specific cables, 5 and 15 meters in length, which carry all video and control data as well as the power for the connected camera heads.

The images for this study were collected at 500 frames/second. The video files were downloaded and converted to AVI format, and placed in the HEPA Biodynamic Data Bank.

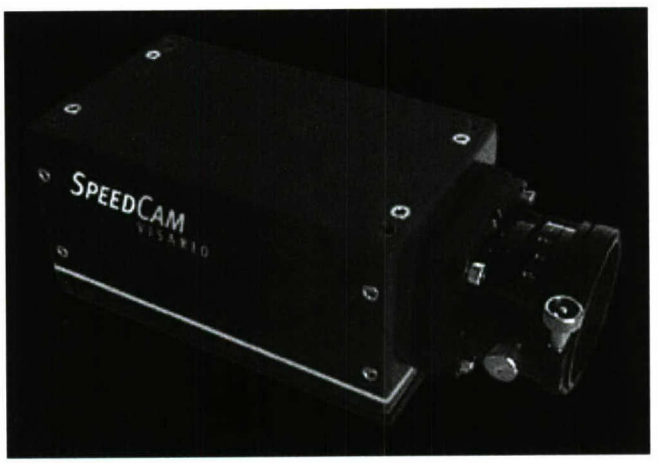

Figure 14. Weinberger SpeedCam Camera

Data Processing

The Excel 2000 Workbook GzEmgVdt_withEmg.xls is used to analyze the TDAS PRO test data from the GzEMG Study (VDT Facility). GzEmgVdt_withEmg.xls contains the Visual Basic module Module1 and the forms UserForm1 and UserForm2. Module1 contains one main subroutine that calls numerous other subroutines and functions. GzEmgVdt_withEmg.xls calls the DLL functions in the Dynamic Link Libraries ScanDll1, Mathdll and FortranMathDll. The shortcut ctrl+r can be used to execute the Visual Basic module. The Visual Basic module displays the two user forms.

UserForm1 requests the user to enter the system acronym, study description, impact channel number, magnitude of the impact start level, start time, processing time, T0 bit number and reference mark bit number. The user has the option to find the Weinberger start time, start at the reference mark time, and use the processing time as the impact window time. The user has the option to plot the channels, print the summary sheet, print the plots, update the Access database information for the Biodynamic Data Bank, and create an Excel time history workbook for the Biodynamic Data Bank. Default values are displayed based on the last test that was analyzed. The default values are stored in worksheet "Defaults" inside the workbook.

UserForm2 requests the user to enter the test number for each test to be processed. The default test parameters are retrieved from the test sensitivity file and displayed on the form. The user may specify new values for any of the displayed test parameters. The test parameters include the subject ID, weight, age, height and sitting height. Additional parameters include the cell type,

nominal g level, subject type (manikin or human), and belt pre-load status (computed or not computed), if used.
The workbook contains worksheets named "Channels," "Formulas," "Preloads," "Plots," "Time History File," "Plot Pages" and "Defaults." The "Channels" worksheet contains the channel number, channel name, database ID number, channel description, and summary sheet description for each channel. The "Formulas" worksheet contains Excel formulas and other data analysis functions. The "Preloads" worksheet contains the pre-load numbers and descriptions. The "Plots" worksheet contains the channel name, the plot description, and the plot vertical axis minimum, maximum and increment for each channel to be plotted. The "Time History File" worksheet defines the channel names for the time history files (the database time history files do not use this worksheet). The "Plot Pages" worksheet allows the user to print out selected plot pages (by default, all plot pages are printed). GzEmgVdt_withEmg.xls generates time histories for all channels, resultants, sums, and other calculated time histories.

Values for the pre-impact level and the extrema for each time history are stored in the Excel worksheet summary file and printed out as a summary sheet for each test. The time histories are also plotted with up to six plots per page. The user has the option to create test summary information and Excel workbooks containing the time histories for the Biodynamic Data Bank. GzEmgVdt_withEmg.xls automatically stores the test parameters, pre-loads and extrema values in an SQL Server database that contains the test data from ongoing test programs. This allows the test data to be viewed immediately following the test from an internal web site for ongoing test programs.

Table 5. Program Set-Up and Calibration Log

DATA POINT	TRANSDUCER S/N, MFG. & MODEL	PRE-CAL		POST-CAL		% D	DAS SENSITIVITY	FULL SCALE	NOTES
		DATE	SENS	DATE	SENS				
CARRIAGE X ACCEL (G)	CC99H ENDEVCO 7264-200	26-May-04	3.0260 mv/g at 10V exc.	15-Sep-05	2.9991 mv/g at 10V exc.	-0.9	.30260 mv/v/g	15 G	Used on all tests.
CARRIAGE Y ACCEL (G)	CC86H ENDEVCO 7264-200	26-May-04	2.8365 mv/g at 10V exc.	15-Sep-05	2.8110 mv/g at 10V exc.	-0.9	.28365 mv/v/g	15 G	½ Bridge Used on all tests.
CARRIAGE Z ACCEL (G)	MH82 ENDEVCO 2262A-200	26-May-04	2.0701 mv/g at 10V exc.	15-Sep-05	2.0489 mv/g at 10V exc	-1	.20701 mv/v/g	25 G	Used on all tests.
SEAT CUSHION X ACCEL (G)	96J96J15 TB01 ENTRAN EGV3-F-250 (X)	21-Apr-04	.8215 mv/g at 10V exc.	15-Sep-05	.8130 mv/g at 10V exc.	-1	.08215 mv/v/g	15 G	Used on tests 4845 thru 4851, 4855 thru 5196.
SEAT CUSHION Y ACCEL (G)	96J96J15 TB01 ENTRAN EGV3-F-250 (Y)	21-Apr-04	-.8060 mv/g at 10V exc.	15-Sep-05	.7904 mv/g at 10V exc.	-1.9	.0806 mv/v/g	15 G	Use Negative Sensitivity. Used on tests 4845 thru 4851, 4855 thru 5196.
SEAT CUSHION Z ACCEL (G)	96J96J15 TB01 ENTRAN EGV3-F-250 (Z)	21-Apr-04	.7961 mv/g at 10V exc.	15-Sep-05	.7933 mv/g at 10 V exc.	-0.4	.07961 mv/v/g	25 G	Used on tests 4845 thru 4851, 4855 thru 5196.
SEAT PAN X ACCEL (G)	97C97C20 TB04 ENTRAN EGV3-F-250	23-Apr-04	1.0322 mv/g at 10V exc.	15-Sep-05	1.0421 mv/g at 10V exc.	1	1.0322 mv/v/g	15 G	Used on tests 4845 thru 4851, 4855 thru 5196.

SEAT PAN Y ACCEL (G)	97C97C20 TB04 ENTRAN EGV3-F-250	23-Apr-04	-1.0252 mv/g at 10V exc.	15-Sep-05	1.0153 mv/g at 10V exc.	-1	.10252 mv/v/g	15 G	Use Negative Sensitivity. Used on tests 4845 thru 4851, 4855 thru 5196.
SEAT PAN Z ACCEL (G)	97C97C20 TB04 ENTRAN EGV3-F-250	23-Apr-04	.9884 mv/g at 10V exc.	15-Sep-05	.9813 mv/g at 10V exc.	-0.7	.09884 mv/v/g	25 G	Used on tests 4845 thru 4851, 4855 thru 5196.
HEAD X ACCEL (G)	92D92D13 TF01 ENTRAN EGV3-F-250	23-Apr-04	.6646 mv/g at 10V exc.	NA	NA	NA	.06646 mv/v/g	15 G	Used on tests 4890 and 4891. Used on tests 4900 thru 4933. Broke on test 4933.
HEAD X ACCEL (G)	97C97C27 TB05 ENTRAN EGV3-F-250	27-Jul-04	.9573 mv/g at 10V exc.	NA	NA	NA	.09573 mv/v/g	15 G	Used on tests 4934 thru 4936. Broke on test 4936.
HEAD X ACCEL (G)	94G94G30TB02 ENTRAN EGV3-F-250	28-Sep-04	.8880 mv/g at 10V exc.	15-Sep-05	.8710 mv/g at 10V exc.	-1.9	.08880 mv/v/g	15 G	Used on tests 4937 thru 5196.
HEAD Y ACCEL (G)	92D92D13 TF01 ENTRAN EGV3-F-250	23-Apr-04	.6377 mv/g at 10V exc.	NA	NA	NA	.06377 mv/v/g	15 G	Used on tests 4890 and 4891. Used on tests 4900 thru 4933. Broke on test 4933.
HEAD Y ACCEL (G)	97C97C27 TB05 ENTRAN EGV3-F-250	27-Jul-04	.9177 mv/g at 10V exc.	NA	NA	NA	.09177 mv/v/g	15 G	Used on tests 4934 thru 4936. Broke on test 4936.
HEAD Y ACCEL (G)	94G94G30 TB02 ENTRAN EGV3-F-250	28-Sep-04	.8993 mv/g at 10V exc.	15-Sep-05	.8922 mv/g at 10V exc.	-0.8	.08993 mv/v/g	15 G	Used on tests 4937 thru 5196.
HEAD Z ACCEL (G)	92D92D13 TF01 ENTRAN EGV3-F-250	23-Apr-04	.6773 mv/g at 10V exc.	NA	NA	NA	.06773 mv/v/g	25 G	Used on tests 4890 and 4891. Used on tests 4900 thru 4933. Broke on test 4933.
HEAD Z ACCEL (G)	97C97C27 TB05 ENTRAN EGV3-F-250	27-Jul-04	.9629 mv/g at 10V exc.	NA	NA	NA	.09629 mv/v/g	25 G	Used on tests 4934 thru 4936. Broke on test 4936.
HEAD Z ACCEL (G)	94G94G30 TB02 ENTRAN EGV3-F-250	28-Sep-04	.8880 mv/g at 10V exc.	15-Sep-05	.8767 mv/g at 10V exc.	-1.3	.08880 mv/v/g	25 G	Used on tests 4937 thru 5196.
HEAD Ry ANG ACCEL (RAD/SEC2)	10203 ENDEVCO 7302B	27-Apr-04	3.73 uv/rad/sec2 at 10V exc.	15-Sep-05	3.75 uv/rad/sec2 at 10V exc.	0.5	.000373 mv/v/rad/sec2	5000 RAD/SEC2	Used on tests 4890 and 4891. Used on tests 4900 thru 5196.
STERNUM Z ACCEL (G)	BH76H ENDEVCO 7264-200	23-Apr-04	3.2381 mv/g at 10V exc.	15-Sep-05	3.1914 mv/g at 10V exc.	-1.4	.0003281 mv/v/rad/sec2	25 G	½ Bridge Used on tests 4890 and 4891. Used on tests 4900 thru 5196.
STERNUM Ry ANG VELOCITY (RAD/SEC)	IR 1 MURATA GYROSTAR ENC-03J	27-Apr-04	-38.53 mv/rad/sec at 5V exc.	15-Sep-05	38.9 mv/rad/sec at 5V exc.	1	7.706 mv/v/rad/sec	100 RAD/SEC	Use Negative Sensitivity. Used on tests 4890 and 4891. Used on tests 4900 thru 5196.
LEFT LAP X FORCE (LB)	1 MICH-SCI 4000	28-May-04	-14.17 uv/lb at 10V exc.	19-Sep-05	13.19 uv/lb at 10V exc.	-2	.001417 mv/v/lb	1000 LB	Use Negative Sensitivity. Broke during maintenance. Used on tests 4846 thru 4984.
LEFT LAP X FORCE (LB)	3 MICH-SCI 4000	25-Jun-04	-14.39 uv/lb at 10V exc.	19-Sep-05	14.05 uv/lb at 10V exc.	-2.6	.001439 mv/v/lb	1000 LB	Use Negative Sensitivity. Used on tests 4985 thru 5196.
LEFT LAP Y FORCE (LB)	1 MICH-SCI 4000	28-May-04	-13.91 uv/lb at 10V exc.	19-Sep-05	13.84 uv/lb at 10V exc.	-0.5	.001391 mv/v/lb	1000 LB	Use Negative Sensitivity. Broke during maintenance. Used on tests 4846 thru 4984.

LEFT LAP Y FORCE (LB)	3 MICH-SCI 4000	25-Jun-04	-13.68 uv/lb at 10V exc.	19-Sep-05	13.26 uv/lb at 10V exc.	-3	.001368 mv/v/lb	1000 LB	Use Negative Sensitivity. Used on tests 4985 thru 5196.
LEFT LAP Z FORCE (LB)	1 MICH-SCI 4000	28-May-04	13.47 uv/lb at 10V exc.	19-Sep-05	13.19 uv/lb at 10V exc.	-2.1	.001347 mv/v/lb	1000 LB	Broke during maintenance. Used on tests 4846 thru 4984.
LEFT LAP Z FORCE (LB)	3 MICH-SCI 4000	25-Jun-04	-13.57 uv/lb at 10V exc.	19-Sep-05	13.22 uv/lb at 10V exc.	-2.6	.001357 mv/v/lb	1000 LB	Used on tests 4985 thru 5196.
RIGHT LAP X FORCE (LB)	2 MICH-SCI 4000	28-May-04	-14.49 uv/lb at 10V exc.	19-Sep-05	14.42 uv/lb at 10V exc.	-0.5	.001449 mv/v/lb	1000 LB	Use Negative Sensitivity. Used on all tests.
RIGHT LAP Y FORCE (LB)	2 MICH-SCI 4000	28-May-04	-13.88 uv/lb at 10V exc.	19-Sep-05	13.88 uv/lb at 10V exc.	0	.001388 mv/v/lb	1000 LB	Use Negative Sensitivity. Used on all tests.
RIGHT LAP Z FORCE (LB)	2 MICH-SCI 4000	28-May-04	13.89 uv/lb at 10V exc.	19-Sep-05	13.99 uv/lb at 10V exc.	0.7	.001369 mv/v/lb	1000 LB	Used on all tests.
SHOULDER X FORCE (LB)	5 MICH-SCI 4000	28-May-04	-13.51 uv/lb at 10V exc.	NA	NA	NA	.001351 mv/v/lb	1000 LB	Use Negative Sensitivity. Broke during maintenance. Used on tests 4846 thru 4984.
SHOULDER X FORCE (LB)	4 MICH-SCI 4000	25-Jun-04	-13.24 uv/lb at10V exc.	19-Sep-05	13.23 uv/lb at 10V exc.	-0.1	.001324 mv/v/lb	1000 LB	Use Negative Sensitivity. Used on tests 4985 thru 4989.
LEFT SHOULDER X FORCE (LB)	4 MICH-SCI 4000	25-Jun-04	13.65 uv/lb at10V exc.	19-Sep-05	13.35 uv/lb at 10V exc.	-2.2	.001365 mv/v/lb	1000 LB	Changed to Left Shoulder X on test 4990. Used on tests 4990 thru 5196.
SHOULDER Y FORCE (LB)	5 MICH-SCI 4000	28-May-04	-13.96 uv/lb at 10V exc.	NA	NA	NA	.001396 mv/v/lb	1000 LB	Use Negative Sensitivity. Broke during maintenance. Used on tests 4846 thru 4984.
SHOULDER Y FORCE (LB)	4 MICH-SCI 4000	25-Jun-04	-13.65 uv/lb at 10V exc.	19-Sep-05	13.54 uv/lb at 10V exc.	-0.8	.001365 mv/v/lb	1000 LB	Use Negative Sensitivity. Used on tests 4985 thru 4989.
LEFT SHOULDER Y FORCE (LB)	4 MICH-SCI 4000	25-Jun-04	13.65 uv/lb at 10V exc.	19-Sep-05	13.54 uv/lb at 10V exc.	-0.8	.001365 mv/v/lb	1000 LB	Changed to Left Shoulder Y on test 4990. Used on tests 4990 thru 5196.
SHOULDER Z FORCE (LB)	5 MICH-SCI 4000	28-May-04	-13.22 uv/lb at 10V exc.	NA	NA	NA	.001322 mv/v/lb	1000 LB	Use Negative Sensitivity. Broke during maintenance. Used on tests 4846 thru 4984.
SHOULDER Z FORCE (LB)	4 MICH-SCI 4000	25-Jun-04	-13.65 uv/lb at 10V exc.	19-Sep-05	13.35 uv/lb at 10V exc.	-2.2	.001365 mv/v/lb	1000 LB	Use Negative Sensitivity. Used on tests 4985 thru 4989.
LEFT SHOULDER Z FORCE (LB)	4 MICH-SCI 4000	25-Jun-04	-13.24 uv/lb at 10V exc.	19-Sep-05	13.23 uv/lb at 10V exc.	-0.1	.001324 mv/v/lb	1000 LB	Changed to Left Shoulder Z on test 4990. Use Negative Sensitivity. Used on tests 4990 thru 5196.
LEFT SEAT PAN X FORCE (LB)	1 AAMRL / DYN LOADLINK	22-Apr-04	10.72 uv/lb at 10V exc.	16-Sep-05	10.74 uv/lb at 10V exc.	0.2	.001072 mv/v/lb	500 LB	Used on all tests.
RIGHT SEAT PAN X FORCE (LB)	10 AAMRL / DYN LOADLINK	22-Apr-04	10.25 uv/lb at 10V exc.	16-Sep-05	10.16 uv/lb at 10V exc.	-0.9	.001025 mv/v/lb	500 LB	Used on all tests.

SEAT PAN Y FORCE (LB)	8 AAMRL / DYN LOADLINK	22-Apr-04	-10.69 uv/lb at 10V exc.	16-Sep-05	10.66 uv/lb at 10V exc.	-0.3	.001069 mv/v/lb	500 LB	Use Negative Sensitivity. Used on all tests.
LEFT SEAT PAN Z FORCE (LB)	Q-3294-4 STRANSERT FLU2.5-2SPKT	22-Apr-04	-7.87 uv/lb at 10V exc.	19-Sep-05	7.96 uv/lb at 10V exc.	1.1	.000787 mv/v/lb	1500 LB	Use Negative Sensitivity. Used on all tests.
RIGHT SEAT PAN Z FORCE (LB)	Q-3294-5 STRANSERT FLU2.5-2SPKT	22-Apr-04	-7.76 uv/lb at 10V exc.	19-Sep-05	7.78 uv/lb at 10V exc.	0.3	.000776 mv/v/lb	1500 LB	Use Negative Sensitivity. Used on all tests.
CENTER SEAT PAN Z FORCE (LB)	Q-3294-6 STRANSERT FLU2.5-2SPKT	22-Apr-04	-7.78 uv/lb at 10V exc.	19-Sep-05	7.95 uv/lb at 10V exc.	2.2	.000778 mv/v/lb	1500 LB	Use Negative Sensitivity. Used on all tests.
LEFT CHIN STRAP LOAD FORCE (LB)	7 GD-AIS / AFRL/HEPA	26-May-04	46 uv/lb at 10V exc.	NA	NA	NA	.0046 mv/v/lb	200 LB	Broke on test 4928.
LEFT CHIN STRAP LOAD FORCE (LB)	6 GD-AIS / AFRL/HEPA	12-Aug-04	58.44 uv/lb at 10V exc.	9-Dec-04	61.95 uv/lb at 10 V exc.	**6**	.005844 mv/v/lb	200 LB	Used on tests 4929 thru 5006. Broke on test 5006.
LEFT CHIN STRAP LOAD FORCE (LB)	2 GD-AIS / AFRL/HEPA	13-Aug-04	55.43 uv/lb at 10V exc.	28-Sep-05	49.39 uv/lb at 10V exc.	**-10.9**	.005543 mv/v/lb	200 LB	Used on tests 5006 thru 5196.
INT HEAD X ACCEL (G)	95H95H14-A07 ENTRAN EGE-72-200	20-Apr-04	-2.6102 mv/g at 10V exc.	10-Sep-04	2.6286 mv/g at 10V exc.	0.7	.26102 mv/v/g	100 G	Use Negative Sensitivity. Used on tests 4845 thru 4889, 4892 thru 4898.
RIGHT SHOULDER X FORCE (LB)	1 MICH-SCI 4000	28-May-04	13.47 uv/lb at 10V exc.	19-Sep-05	13.19 uv/lb at 10V exc.	-2.1	.001347 mv/v/lb	1000 LB	Used on tests 4990 thru 5196.
INT HEAD X ACCEL (G)	CA53H ENDEVCO 7264-200	28-Sep-04	-2.6739 mv/g at 10V exc.	11-Oct-04	2.6866 mv/g at 10V exc.	0.5	.26739 mv/v/g	100 G	Use Negative Sensitivity. Used for GzEMG_NVG tests 4947 thru 4975.
RIGHT SHOULDER Y FORCE (LB)	1 MICH-SCI 4000	28-May-04	-13.91 uv/lb at 10V exc.	19-Sep-05	13.84 uv/lb at 10V exc.	-0.5	.001391 mv/v/lb	1000 LB	Use Negative Sensitivity. Used on tests 4990 thru 5196.
INT HEAD Y ACCEL (G)	01G01G13-N10 ENTRAN EGE-72-200	20-Apr-04	-2.0842 mv/g at 10V exc.	10-Sep-04	2.0786 mv/g at 10V exc.	-0.3	.20842 mv/v/g	100 G	Use Negative Sensitivity. Used on tests 4845 thru 4889, 4892 thru 4898.
INT HEAD Y ACCEL (G)	CL83H ENDEVCO 7264-200	28-Sep-04	-2.9623 mv/g at 10V exc.	11-Oct-04	2.9581 mv/g at 10V exc.	-0.1	.29623 mv/v/g	100 G	Use Negative Sensitivity. Used for GzEMG_NVG tests 4947 thru 4975.
RIGHT SHOULDER Z FORCE (LB)	1 MICH-SCI 4000	28-May-04	-14.17 uv/lb at 10V exc.	19-Sep-05	13.19 uv/lb at 10V exc.	-2	.001417 mv/v/lb	1000 LB	Use Negative Sensitivity. Used on tests 4990 thru 5196.
INT HEAD Z ACCEL (G)	95I95I06-D02 ENTRAN EGE-72-200	20-Apr-04	2.7121 mv/g at 10V exc.	10-Sep-04	2.7135 mv/g at 10V exc.	0.1	.27121 mv/v/g	100 G	Used on tests 4845 thru 4889, 4892 thru 4898.
INT HEAD Z ACCEL (G)	J14785 ENDEVCO 7264-200	21-Apr-04	4.3847 mv/g at 10V exc.	11-Oct-04	4.4032 mv/g at 10V exc.	0.4	.43847 mv/v/g	100 G	Used for GzEMG_NVG tests 4947 thru 4975.
LEFT TRAPEZIUS	DELSYS INC DE-2.3	NA	1 mv/v	NA	NA	NA	.1 mv/v/v		Used on tests 4990 thru 5196

INT HEAD Rx ANG ACCEL (RAD/SEC2)	10206 ENDEVCO 7302B	20-Apr-04	-4.54 uv/rad/sec2 at 10V exc.	13-Sep-04	4.46 uv/rad/sec2 at 10V exc.	-0.2	.000454 mv/v/rad/sec2	5000 RAD/SEC2	Use Negative Sensitivity. Used on tests 4845 thru 4889, 4892 thru 4898.
INT HEAD Ry ANG ACCEL (RAD/SEC2)	10214 ENDEVCO 7302B	13-Sep-04	-3.63 uv/rad/sec2	11-Oct-04	3.67 uv/rad/sec2 at 10V exc.	1.1	.000363 mv/v/rad/sec2	5000 RAD/SEC2	Use Negative Sensitivity. Used for GzEMG_NVG tests 4947 thru 4975.
INT LUMBAR X FORCE (LB)	390 DENTON 1914A	1-Apr-05	6.75 uv/lb at 10V exc.	3-Oct-05	6.73 uv/lb at 10V exc.	-0.3	.000675 mv/v/lb	2500 LB	Used on tests 5197 thru 5212.
RIGHT TRAPEZIUS	DELSYS INC DE-2.3	NA	1 mv/v	NA	NA	NA	.1 mv/v/v		Used on tests 4990 thru 5196
INT HEAD Ry ANG ACCEL (RAD/SEC2)	10229 ENDEVCO 7302B	20-Apr-04	-3.57 uv/rad/sec2 at 10V exc.	13-Sep-04	3.48 uv/rad/sec2 at 10V exc.	-2.5	.000357 mv/v/rad/sec2	5000 RAD/SEC2	Use Negative Sensitivity. Used on tests 4845 thru 4889, 4892 thru 4898.
INT NECK X FORCE (LB)	820 DENTON 1716	30-Jun-04	-8.20 uv/lb at 10V exc.	12-Oct-04	8.20 uv/lb at 10V exc.	0	.00082 mv/v/lb	2500 LB	Use Negative Sensitivity. Used for GzEMG_NVG tests 4947 thru 4975.
INT LUMBAR Y FORCE (LB)	390 DENTON 1914A	1-Apr-05	6.72 uv/lb at 10V exc.	3-Oct-05	6.73 uv/lb at 10V exc.	0.1	.000672 mv/v/lb	2500 LB	Used on tests 5197 thru 5212.
LEFT STERNOCLEIDO MASTOID	DELSYS INC DE-2.3	NA	1 mv/v	NA	NA	NA	.1 mv/v/v		Used on tests 4990 thru 5196.
INT HEAD Rz ANG ACCEL (RAD/SEC2)	10214 ENDEVCO 7302B	20-Apr-04	3.66 uv/rad/sec2 at 10V exc.	13-Sep-04	3.63 uv/rad/sec2 at 10V exc.	-0.8	.000366 mv/v/rad/sec	5000 RAD/SEC2	Used on tests 4845 thru 4889, 4892 thru 4898.
INT NECK Y FORCE (LB)	820 DENTON 1716	30-Jun-04	-8.37 uv/lb at 10V exc.	12-Oct-04	8.31 uv/lb at 10V exc.	-0.7	.000837 mv/v/lb	2500 LB	Use Negative Sensitivity. Used for GzEMG_NVG tests 4947 thru 4975.
INT LUMBAR Z FORCE (LB)	390 DENTON 1914A	1-Apr-05	2.78 uv/lb at 10V exc.	3-Oct-05	2.77 uv/lb at 10V exc	-0.4	.000278 mv/v/lb	2500 LB	Used on tests 5197 thru 5212.
INT NECK X FORCE (LB)	624 DENTON 1716	23-Sep-03	-8.23 uv/lb at 10V exc.	10-Aug-04	8.23 uv/lb at 10V exc.	0	.000823 mv/v/lb	2500 LB	Use Negative Sensitivity. Used on tests 4845 thru 4889, 4892 thru 4898.
INT NECK Z FORCE (LB)	820 DENTON 1716	30-Jun-04	-4.51 uv/lb at 10V exc.	12-Oct-04	4.51 uv/lb at 10V exc.	0	.000451 mv/v/lb	2500 LB	Use Negative Sensitivity. Used for GzEMG_NVG tests 4947 thru 4975.
RIGHT STERNOCLEIDO MASTOID	DELSYS INC DE-2.3	NA	1 mv/v	NA	NA	NA	.1 mv/v/v		Used on tests 4990 thru 5196.
INT LUMBAR Mx TORQUE (IN-LB)	390 DENTON 1914A	1-Apr-05	5.24 uv/in-lb at 10V exc.	3-Oct-05	5.22 uv/in-lb at 10V exc	-0.4	.000524 mv/v/in-lb	2500 LB	Used on tests 5197 thru 5212.
INT NECK Y FORCE (LB)	624 DENTON 1716	23-Sep-03	-8.31 uv/lb at 10V exc.	10-Aug-04	8.42 uv/lb at 10V exc.	1.3	.000831 mv/v/lb	2500 LB	Use Negative Sensitivity. Used on tests 4845 thru 4889, 4892 thru 4898.
INT NECK Mx TORQUE (IN-LB)	820 DENTON 1716	30-Jun-04	6.79 uv/in-lb at 10V exc.	12-Oct-04	6.79 uv/in-lb at 10V exc.	0	.000679 mv/v/in-lb	2500 IN-LB	Used for GzEMG_NVG tests 4947 thru 4975.

INT HEAD X ACCEL (G)	CL83H ENDEVCO 7264-200	11-Oct-04	-2.9581 mv/g at 10V exc.	11-Jan-05	2.9524 mv/g at 10V exc.	-0.2	.29581 mv/v/g	100 G	Use Negative Sensitivity. Used on tests 5036 thru 5043.
INT LUMBAR My TORQUE (IN-LB)	390 DENTON 1914A	1-Apr-05	5.29 uv/in-lb at 10V exc.	3-Oct-05	5.22 uv/in-lb at 10V exc	-1.3	.000529 mv/v/lb	2500 LB	Used on tests 5197 thru 5212.
INT NECK Z FORCE (LB)	624 DENTON 1716	23-Sep-03	-4.08 uv/lb at 10V exc.	10-Aug-04	4.08 uv/lb at 10V exc.	0	.000408 mv/v/lb	2500 LB	Use Negative Sensitivity. Used on tests 4845 thru 4889, 4892 thru 4898.
INT NECK My TORQUE (IN-LB)	820 DENTON 1716	30-Jun-04	6.83 uv/in-lb at 10V exc.	12-Oct-04	6.79 uv/in-lb at 10V exc.	-0.6	.000683 mv/v/in-lb	2500 IN-LB	Used for GzEMG_NVG tests 4947 thru 4975.
INT HEAD Y ACCEL (G)	J14785 ENDEVCO 7264-200	11-Oct-04	-4.4032 mv/g at 10V exc.	11-Jan-05	4.3792 mv/g at 10V exc.	-0.5	.44032 mv/v/g	100 G	Use Negative Sensitivity. Used on tests 5036 thru 5043.
INT LUMBAR Mz TORQUE (IN-LB)	390 DENTON 1914A	1-Apr-05	8.85 uv/in-lb at 10V exc.	3-Oct-05	8.94 uv/in-lb at 10V exc.	1	.000885 mv/v/iv-lb	2500 LB	Used on tests 5197 thru 5212.
INT NECK Mx TORQUE (IN-LB)	624 DENTON 1716	23-Sep-03	6.89 uv/in-lb at 10V exc.	10-Aug-04	6.91 uv/in-lb at 10V exc.	0.3	.000689 mv/v/in-lb	2500 IN-LB	Used on tests 4845 thru 4889, 4892 thru 4898.
INT NECK Mz TORQUE (IN-LB)	820 DENTON 1716	30-Jun-04	9.24 uv/in-lb at 10V exc.	12-Oct-04	9.24 uv/in-lb at 10V exc.	0	.000924 mv/v/in-lb	2500 IN-LB	Used for GzEMG_NVG tests 4947 thru 4975.
INT HEAD Z ACCEL (G)	CA53H ENDEVCO 7264-200	11-Oct-04	2.6866 mv/g at 10V exc.	11-Jan-05	2.6725 mv/g at 10V exc.	-0.5	.26866 mv/v/g	100 G	Used on tests 5036 thru 5043.
INT NECK My TORQUE (IN-LB)	624 DENTON 1716	23-Sep-03	6.90 uv/in-lb at 10V exc.	10-Aug-04	6.91 uv/in-lb at 10V exc.	0.1	.00069 mv/v/in-lb	2500 IN-LB	Used on tests 4845 thru 4889, 4892 thru 4898.
INT HEAD Ry ANG ACCEL (RAD/SEC2)	10206 ENDEVCO 7302B	13-Sep-04	-4.46 uv/rad/sec2 at 10V exc.	11-Jan-05	4.47 uv/rad/sec2 at 10V exc.	0.7	.000446 mv/v/rad/sec2	5000 RAD/SEC2	Use Negative Sensitivity. Used on tests 5036 thru 5043.
INT NECK Mz TORQUE (IN-LB)	624 DENTON 1716	23-Sep-03	9.35 uv/in-lb at 10V exc.	10-Aug-04	9.31 uv/in-lb at 10V exc.	-0.4	.000935 mv/v/in-lb	2500 IN-LB	Used on tests 4845 thru 4889, 4892 thru 4898.
INT NECK X FORCE (LB)	820 DENTON 1716A	12-Oct-04	8.2 uv/lb at 10V exc.	17-Feb-05	8.17 uv/lb at 10V exc.	-0.3	.00082 mv/v/lb	2500 LB	Use Negative Sensitivity. Used on tests 5036 thru 5043.
INT CHEST X ACCEL (G)	CL83H ENDEVCO 7264-200	19-Apr-04	2.9482 mv/g at 10V exc.	10-Sep-04	2.9553 mv/g at 10V exc.	0.2	.29482 mv/v/g	50 G	Used on tests 4845 thru 4889, 4892 thru 4898.
INT NECK Y FORCE (LB)	820 DENTON 1716A	12-Oct-04	8.31 uv/lb at 10V exc.	17-Feb-05	8.27 uv/lb at 10V exc.	-0.5	.000831 mv/v/lb	2500 LB	Use Negative Sensitivity. Used on tests 5036 thru 5043.
INT CHEST Y ACCEL (G)	CA53H ENDEVCO 7264-200	19-Apr-04	-2.6668 mv/g at 10V exc.	10-Sep-04	2.6753 mv/g at 10V exc.	0.3	.26668 mv/v/g	50 G	Use Negative Sensitivity. Used on tests 4845 thru 4889, 4892 thru 4898.
INT NECK Z FORCE (LB)	820 DENTON 1716A	12-Oct-04	4.51 uv/lb at 10V exc.	17-Feb-05	4.49 uv/lb at 10V exc.	-0.4	.000451 mv/v/lb	2500 LB	Use Negative Sensitivity. Used on tests 5036 thru 5043.
INT CHEST Z ACCEL (G)	02E02D26-N02 ENTRAN EGE-73B-200	19-Apr-04	1.8297 mv/g at 10V exc.	10-Sep-04	1.8142 mv/g at 10V exc.	-0.8	.18297 mv/v/g	50 G	Used on tests 4845 thru 4889, 4892 thru 4898.

INT NECK Mx TORQUE (IN-LB)	820 DENTON 1716A	12-Oct-04	6.79 uv/in-lb at 10V exc.	17-Feb-05	6.63 uv/in-lb at 10V exc.	-2.4	.000679 mv/v/in-lb	2500 IN-LB	Used on tests 5036 thru 5043.
INT CHEST Ry ANG ACCEL (RAD/SEC2)	10200 ENDEVCO 7302B	19-Apr-04	3.18 uv/rad/sec2 at 10V exc.	13-Sep-04	3.20 uv/rad/sec2 at 10V exc.	0.7	.000318 mv/v/rad/sec2	5000 RAD/SEC2	Used on tests 4845 thru 4889, 4892 thru 4898.
INT NECK My TORQUE (IN-LB)	820 DENTON 1716A	12-Oct-04	6.79 uv/in-lb at 10V exc.	17-Feb-05	6.68 uv/in-lb at 10V exc.	-1.6	.000668 mv/v/in-lb	2500 IN-LB	Used on tests 5036 thru 5043.
INT LUMBAR X ACCEL (G)	8XTB02 (Z) ENTRAN EGV3-F-250	12-May-04	.7735 mv/g at 10V exc.	10-Sep-04	.7862 mv/g at 10V exc.	1.6	.07735 mv/v/g	50 G	Used on tests 4845 thru 4889, 4892 thru 4898.
INT NECK Mz TORQUE (IN-LB)	820 DENTON 1716A	12-Oct-04	9.24 uv/in-lb at 10V exc.	17-Feb-05	9.08 uv/in-lb at 10V exc.	-1.7	.000924 mv/v/in-lb	2500 IN-LB	Used on tests 5036 thru 5043.
INT LUMBAR Y ACCEL (G)	8XTB02 (Y) ENTRAN EGV3-F-250	12-May-04	-.7650 mv/g at 10V exc.	10-Sep-04	.7636 mv/g at 10V exc.	-0.2	.07650 mv/v/g	50 G	Use Negative Sensitivity. Used on tests 4845 thru 4889, 4892 thru 4898.
INT LUMBAR Z ACCEL (G)	8XTB02 (X) ENTRAN EGV3-F-250	12-May-04	-.7438 mv/g at 10V exc.	10-Sep-04	.7423 mv/g at 10V exc.	-0.2	.07438 mv/v/g	50 G	Use Negative Sensitivity. Used on tests 4845 thru 4889, 4892 thru 4898.
INT LUMBAR X FORCE (LB)	154 DENTON 1914A	6-Oct-03	-6.58 uv/lb at 10V exc.	11-Aug-04	6.59 uv/lb at 10V exc.	0.2	.000658 mv/v/lb	2500 LB	Use Negative Sensitivity. Used on tests 4845 thru 4889, 4892 thru 4898.
INT LUMBAR Y FORCE (LB)	154 DENTON 1914A	6-Oct-03	-6.56 uv/lb at 10V exc.	11-Aug-04	6.57 uv/lb at 10V exc.	0.2	.000656 mv/v/lb	2500 LB	Use Negative Sensitivity. Used on tests 4845 thru 4889, 4892 thru 4898.
INT LUMBAR Z FORCE (LB)	154 DENTON 1914A	6-Oct-03	-2.73 uv/lb at 10V exc.	11-Aug-04	2.73 uv/lb at 10V exc.	0	.000273 mv/v/lb	2500 LB	Use Negative Sensitivity. Used on tests 4845 thru 4889, 4892 thru 4898.
INT LUMBAR Mx TORQUE (IN-LB)	154 DENTON 1914A	6-Oct-03	5.16 uv/in-lb at 10V exc.	11-Aug-04	5.14 uv/in-lb at 10V exc.	-0.4	.000516 mv/v/in-lb	2500 IN-LB	Used on tests 4845 thru 4889, 4892 thru 4898.
INT LUMBAR My TORQUE (IN-LB)	154 DENTON 1914A	6-Oct-03	5.16 uv/in-lb at 10V exc.	11-Aug-04	5.15 uv/in-lb at 10V exc.	-0.2	.000515 mv/v/in-lb	2500 IN-LB	Used on tests 4845 thru 4889, 4892 thru 4898.
INT LUMBAR Mz TORQUE (IN-LB)	154 DENTON 1914A	6-Oct-03	8.94 uv/in-lb at 10V exc.	11-Aug-04	8.78 uv/in-lb at 10V exc.	-1.8	.000878 mv/v/in-lb	2500 IN-LB	Used on tests 4845 thru 4889, 4892 thru 4898.

Reference

1. Bouche, R.R. (1970) High Frequency Shaker for Accurate Accelerometer Calibrations. The Journal of Environmental Sciences, May/June.